Journal of Medicinal Chemistry

Article

Aniline-based inhibitors of influenza H1N1 virus acting on hemagglutinin-mediated fusion

Rosana Leiva, Marta Barniol-Xicota, Sandra Codony, Tiziana Ginex, Evelien Vanderlinden, Marta Montes, Michael Caffrey, F. Javier Luque, Lieve Naesens, and Santiago Vazquez

J. Med. Chem., **Just Accepted Manuscript** • DOI: 10.1021/acs.jmedchem.7b00908 • Publication Date (Web): 08 Dec 2017

ACS Publications

Journal of Medicinal Chemistry is published by the American Chemical Society. 1155 Sixteenth Street N.W., Washington, DC 20036

Aniline-based inhibitors of influenza H1N1 virus acting on hemagglutinin-mediated fusion

Rosana Leiva,[∫] Marta Barniol-Xicota,[∫,ǁ] Sandra Codony,[∫,ǁ] Tiziana Ginex,[#,ǁ] Evelien Vanderlinden,[§] Marta Montes,[∫] Michael Caffrey,[†] F. Javier Luque,[#] Lieve Naesens,[§] and Santiago Vázquez*[∫]*

[∫]Laboratori de Química Farmacèutica (Unitat Associada al CSIC), Facultat de Farmàcia i Ciències de l'Alimentació, and Institute of Biomedicine (IBUB), Universitat de Barcelona, Av. Joan XXIII, 27-31, Barcelona, E-08028, Spain

[#]Department of Nutrition, Food Science and Gastronomy, Faculty of Pharmacy and Food Sciences, and Institute of Biomedicine (IBUB), Universitat de Barcelona, Av. Prat de la Riba 171, Santa Coloma de Gramanet, E-08921, Spain

[§]Rega Institute for Medical Research, KU Leuven, B-3000 Leuven, Belgium

[†]Department of Biochemistry & Molecular Genetics, University of Illinois at Chicago, 900 South Ashland Avenue, Chicago, Illinois 60607, United States

KEYWORDS. Influenza A virus, antiviral drug, hemagglutinin, fusion, molecular dynamics.

ABSTRACT. Two series of easily accessible anilines were identified as inhibitors of influenza A virus subtype H1N1, and extensive chemical synthesis and analysis of the structure-activity relationship were performed. The compounds were shown to interfere with low pH-induced membrane fusion mediated by the H1 and H5 (group 1) hemagglutinin (HA) subtypes. A combination of virus resistance, HA interaction and molecular dynamics simulation studies elucidated the binding site of these aniline-based influenza fusion inhibitors, which significantly overlaps with the pocket occupied by some H3 HA-specific inhibitors, indicating the high relevance of this cavity for drug design.

Introduction

Influenza A and B viruses are highly contagious respiratory pathogens and the cause of annual epidemics with high medical and economic burden.[1] Besides, influenza A causes occasional pandemics due to gene reassortment between human and zoonotic viruses. The notorious 1918 Spanish influenza infected one third of the world population with >40 million deaths.[2] The recent pandemic of 2009 was caused by a swine-origin H1N1 virus that killed ~300,000 people within only 18 months, particularly in younger populations.[3] Hence, cost-effective antiviral strategies must be developed for preventing and eradicating emerging influenza pandemics.

Influenza therapy currently relies on two classes of antiviral drugs: the M2 proton channel blockers (restricted to influenza A) and neuraminidase inhibitors (NAIs).[4] The currently approved M2 inhibitors suffer from global virus resistance, making it necessary to develop new chemical scaffolds.[5] Resistance is also a growing issue for the NAIs, particularly oseltamivir.[6] Hence, there is an urgent need for new drugs having superior efficacy, high barrier for resistance, and eventually targeting other proteins

relevant for the viral life cycle.[7-10] The most extensively studied targets are the influenza hemagglutinin (HA)[11], RNA polymerase complex,[12] and NS1 protein.[13]

The homotrimeric HA, abundantly present on the viral envelope, has a crucial and dual role in virus entry into the host cell.[14] First, the HA globular head mediates virus binding *via* its receptor-binding site for sialylated cell surface glycans. The second function lies in the HA stem domain. After endosomal uptake, this domain undergoes low pH-induced and drastic refolding, which leads to release of the hydrophobic fusion peptide and fusion of the viral envelope with the endosomal membrane.[15] Once the viral genome segments are released into the cytoplasm and transferred into the cell nucleus, viral RNA replication begins.[12]

One notable difficulty in targeting HA is related to its sequence diversity. The eighteen HA subtypes of influenza A fall into two phylogenetic groups, for instance H1 and H5 belong to group 1 whereas H3 and H7 are in group 2. In the last years, several broadly neutralizing antibodies against HA group 1, 2, or both, have advanced towards clinical trials.[16] They target conserved head or stem epitopes which were revealed by cocrystallographic analyses.[17] In contrast, broadly-acting small molecule inhibitors of HA are challenging since the only example is arbidol (umifenovir, Chart 1), which is commercially available in Russia and in clinical trials elsewhere.[18] Besides other antiviral mechanisms of action, arbidol was shown to prevent fusion by inhibiting the conformational change of HA at low pH.[19] Only recently, cocrystallization of arbidol with H3 and H7 HAs (PDB codes: 5T6N and 5T6S, respectively) revealed that it binds in a hydrophobic cavity within the HA trimer stem, clamping the protomers together.[20] This site partially overlaps with that of *tert*-butylhydroquinone (TBHQ),[21] another influenza fusion inhibitor for which HA cocrystallization data are available (PDB codes: 3EYK and 3EYM).[22] The structure-activity relationship (SAR) of TBHQ derivatives

was recently revisited.[23] In addition, the literature contains many molecules (some of which are shown in Chart 1) which, based on mechanistic and virus resistance data, classify as HA stem-binding fusion inhibitors.[9] Although the HA subtype-dependent antiviral activity of these molecules forms an obstacle for clinical development, they are suitable scaffolds to design inhibitors that potentially cover a broader range of HA subtypes.

Chart 1. Structures of some reported inhibitors of influenza A HA-mediated fusion.

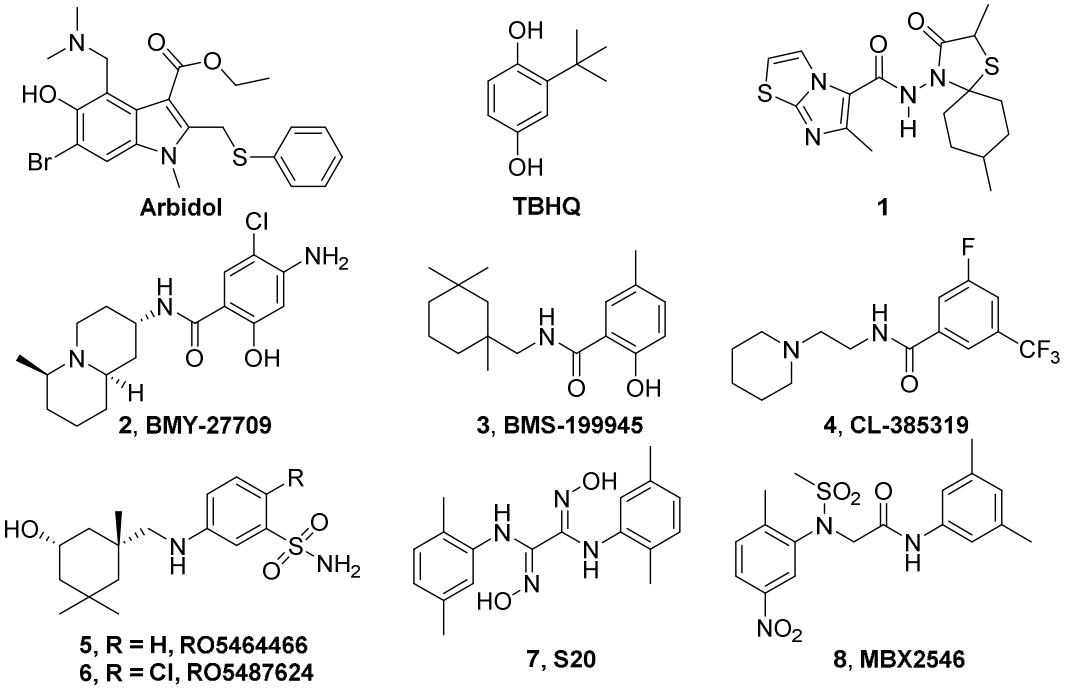

TBHQ and a substituted azaspiro compound, **1**,[24] which were predicted to target the same HA stem pocket, are restricted towards H3 (a group 2) HA. The structurally related compounds **2** (BMY-27709),[25-27] **3** (BMS-199945),[28] and **4** (CL385319)[29-31] (Chart 1) proved limited to HA subtypes H1, H2 and/or H5 (group 1). The latter activity spectrum was also reported for **5** (RO5464466) and its 2-chloro derivative, **6** (RO5487624),[32-33] and the entirely different inhibitors **7** (S20)[34] and **8** (MBX2546).[35-36]

All these HA fusion inhibitors potently suppress replication of some influenza A virus subtypes in cell-based assays, and for **6** activity was confirmed in a lethal mouse model with influenza H1N1.[33]

We here describe the synthesis, antiviral activity and mechanism of action of two series of novel aniline derivatives and related compounds of general structures **I** and **II** (Scheme 1). Considering that the benzamide group of **3** could be replaced by an aniline group as in **5** and **6**, we reasoned that, starting from **4**, compounds of general structure **I** may also display anti-influenza activity. On the other hand, the similar physicochemical properties between the 1,3,3-trimethylcyclohex-1-yl moiety present in **3** and the adamantyl unit, suggest that they may behave as bioisosteric groups (see Table S1 in Supporting Information). This inspired us to take advantage of the well-known antiviral activity of adamantane derivatives,[37] and the large experience of our group in the synthesis of adamantane-containing and adamantane-related polycyclic compounds,[38-43] to explore compounds in which the cyclohexyl moiety of **5** is replaced by a bulkier adamantane. Specifically, we developed a series of analogs to investigate: a) the optimal substitution for the aromatic moiety in series **I** and **II**; b) the effects of the heteroatom in the linker of **I**; and c) the size of the hydrophobic moiety. Anti-influenza A activity was evaluated in cell-based assays with H1N1 and H3N2 strains. The fusion inhibiting effect was demonstrated in an influenza polykaryon assay, and resistant virus was selected and characterized. Finally, NMR experiments and molecular dynamics simulations were conducted to predict the plausible binding site of the lead compounds within the HA protein.

Scheme 1. General structures of the newly designed HA inhibitors. Y = NH, O, S; m = 1 or 2; n = 0, 1 or 2; Z = H or CH_3.

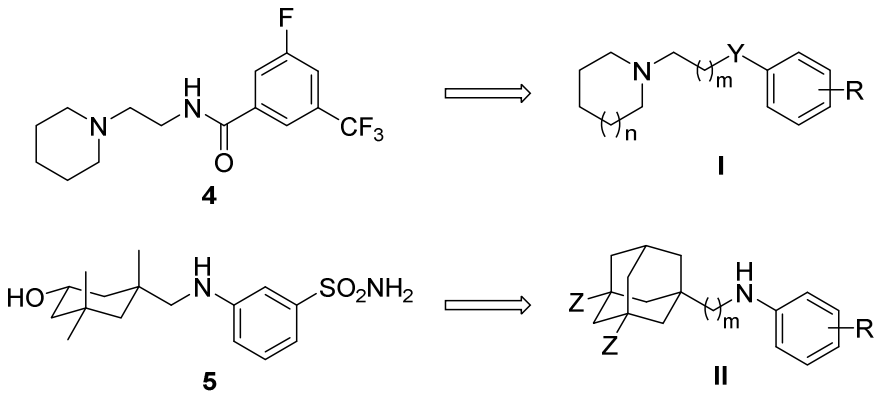

Results and discussion

Chemistry. The synthesis of piperidines with general structure **I** (n = 1) and related ring-expanded (n = 2) and ring-contracted (n = 0) analogs is shown in Scheme 2. These compounds could be accessed in just one facile synthetic step from commercially available starting materials. Anilines, phenols or thiophenols bearing the desired substitution were used for the aromatic moiety, as well as a range of diverse chloroalkyl compounds. The attack of the nucleophilic group in the aromatic moiety to the chloroalkyl derivative upon heating furnished the desired products in low (for the less reactive anilines) to very good (for the phenols and thiophenols) yields. While a few of the alkylated anilines were obtained in high yields (ca 80%) by heating a neat mixture of the aniline and *N*-(2-chloroethyl)piperidine hydrochloride at 120 ºC overnight,[44] the less reactive anilines (e.g. bearing electron-withdrawing groups) needed the addition of base, either K_2CO_3 or NaH, KI catalyst and extended (30 hours) heating, furnishing the products in only low to moderate yields. The corresponding alkylation of phenols and thiophenols proceeded in medium to very high yields by using NaOH in refluxing ethanol.

A different synthetic strategy was undertaken for the preparation of the (adamantylmethyl)anilines of general structure **II** (Scheme 3). Compounds of structure **19** were prepared *via* a three-step route, starting from the commercially available 1-adamantanecarboxylic acid, **16a**. Using thionyl chloride, the corresponding acyl chloride was readily obtained and added to a solution of the corresponding aniline in dry acetone. Upon continuous heating, the desired amides **18a-w** did precipitate in good yields. Without further purification, this precipitate was treated with sodium bis-(2-methoxyethoxy)aluminum hydride to furnish the corresponding anilines in moderate to good yields. Aniline **19x** was synthesized in a similar way, starting from commercially available 3,5-dimethyl-1-adamantanecarboxylic acid, **16b**.

The preparation of the 3-hydroxyadamantane derivatives **22a-b** was first envisaged as a direct step, through the direct low-temperature hydroxylation with HNO_3/H_2SO_4 of anilines **19**. Unfortunately, this procedure led to complex mixtures of products, probably arising from competitive oxidation of the aniline. Alternatively, derivatives **22a-b** were accessed from 3-hydroxyadamantanecarboxylic acid, **20**,[45] which reacted with the required aniline using EDC as a coupling agent to furnish amides **21a-b**, and finally to products **22a-b** after reduction with sodium bis-(2-methoxyethoxy)aluminum hydride. Finally, aniline **25**, featuring an additional methylene unit in the linker, was prepared in an analogous manner to the **19** series (Scheme 3).

Scheme 2. Synthesis of the general scaffold **I** derivatives **9**-**15**.[a]

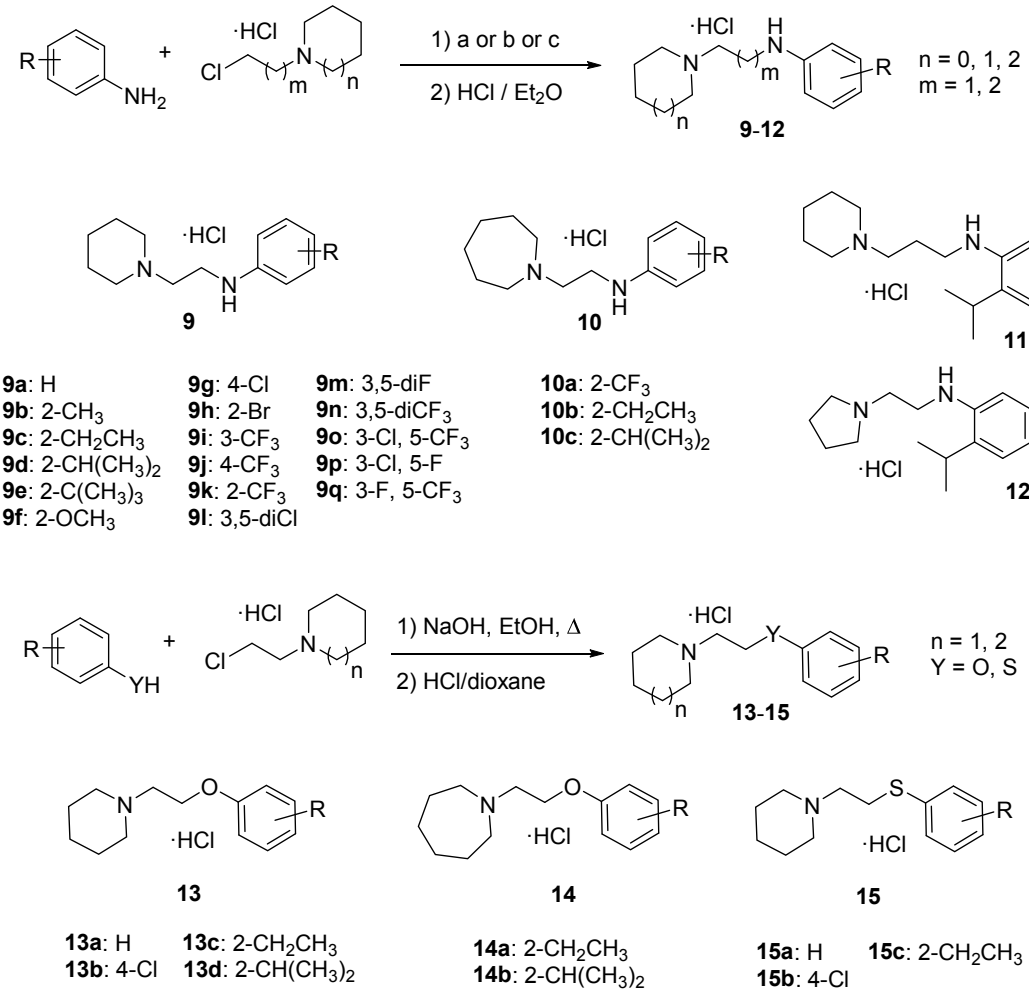

[a]Reagents and conditions: (a) K_2CO_3, KI, DMF, heat; (b) heat; (c) NaH, KI, dry DMF, heat. See experimental for further details.

Scheme 3. Synthesis of anilines **19a-x**, **22a-b** and **25**.[a]

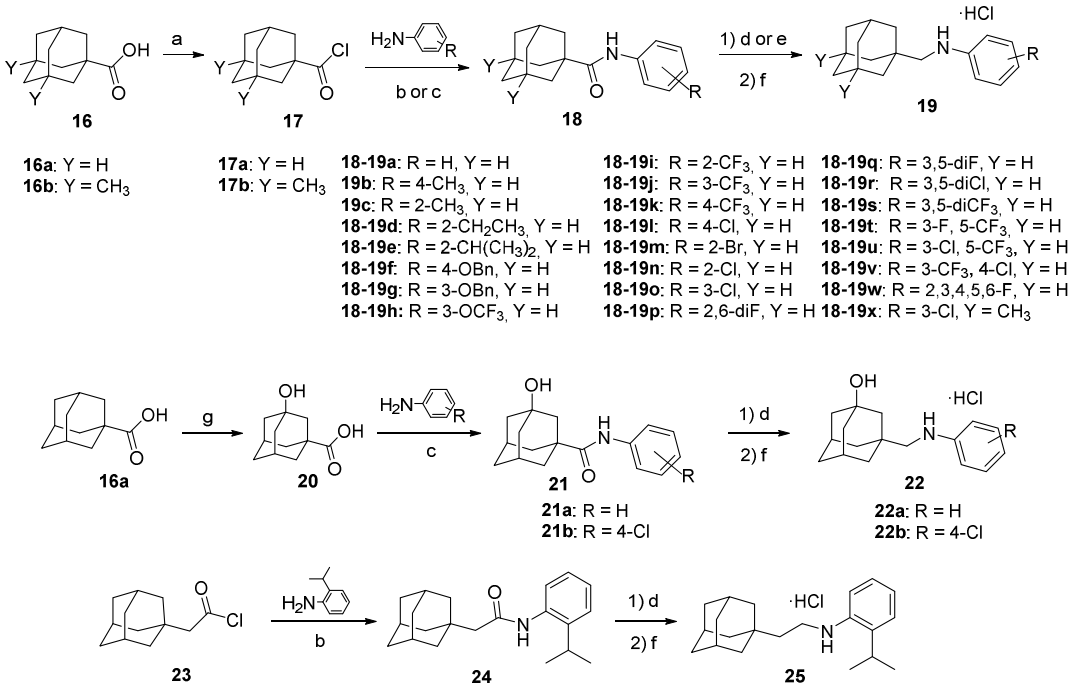

[a]Reagents and conditions: (a) $SOCl_2$, 80 ºC, 2 h; (b) Et_3N, acetone, reflux, 3 h; (c) EDC·HCl, DMAP, dichloromethane, rt, overnight; (d) $NaAlH_2(OCH_2CH_2OCH_3)_2$, toluene, 95 ºC, 24 h; (e) BH_3·THF, 0ºC to rt, 24 h; (f) HCl/Et_2O; (g) HNO_3, H_2SO_4, rt, overnight, 95%. See experimental and Supporting Information for further details.

Of note, while the reduction of **18j**, featuring a trifluoromethyl group in the *meta* position, proceeded as expected to furnish aniline **19j**, the reduction of its *ortho* and *para* isomers, **18i** and **18k**, did not furnish the expected anilines, but **19c** and **19b**, respectively (Scheme 4). The formation of **19b** and **19c** can be easily explained taking into account the strong basicity of the hydride reagent, which triggers a dehalogenation reaction that competes with the reduction process. In order to avoid this problem, we switched from the hydride to borane, an electrophilic reductor agent that smoothly furnished anilines **19i** and **19k**.

Scheme 4. Reduction of amides **18i-k** with sodium bis-(2-methoxyethoxy)aluminum hydride.[a]

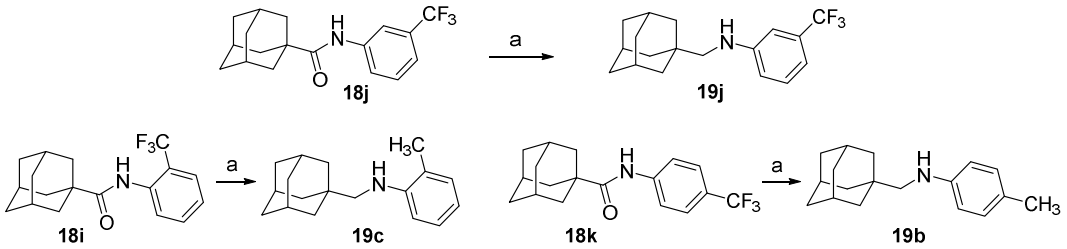

[a]Reagents and conditions: (a) $NaAlH_2(OCH_2CH_2OCH_3)_2$, toluene, 95 ºC, 24 h. See experimental for further details.

Overall, from the aforementioned synthetic work, fifty eight new amines were synthesized, fully characterized as the corresponding hydrochloride derivatives and subsequently tested for antiviral activity.

Anti-influenza virus activity and cytotoxicity in cell culture. The novel compounds were tested in MDCK cells using three influenza A strains [A/Hong Kong/7/87 (H3N2 subtype); A/PR/8/34 (H1N1 subtype); and A/Virginia/ATCC3/2009 (H1N1 subtype)] as well as an influenza B strain (B/Hong Kong/5/1972). The A/Hong Kong/7/87 strain carries an amantadine-sensitive wild-type M2 channel, while the other influenza A strains carry mutations in M2 that confer resistance to amantadine, i.e. V27T plus S31N in A/PR/8/34 and S31N in A/Virginia/ATCC3/2009. The inhibitory effect of the compounds on virus replication as well as their cytotoxicity, were monitored by microscopic examination of the viral cytopathic effect (CPE) at three days post infection, and confirmed by the colorimetric MTS cell viability assay (Table 1).[24]

All compounds were found to be inactive against influenza A/H3N2 and influenza B (results not shown). On the other hand, several ones displayed favorable activity against

the influenza A/H1N1 strains revealing some interesting SAR trends. Regarding the aromatic moiety, ring-substitution is required for activity, as the unsubstituted **9a**, **13a**, **15a** and **19a** were inactive (data not shown). Moreover, the *ortho* position is the most appropriate substitution site for anti-influenza activity, whereas *para*-, *meta*- or full ring substitution patterns, e.g. **9g**, **9i**, **19w** respectively, were deleterious. More specifically, the isopropyl group in *ortho* position yielded very potent compounds (**9d**, **13d** and **19e**). Of note, compounds **9l-q**, featuring two electron withdrawing groups in the *meta* positions, were inactive, in sharp contrast with **4** and several analogs of **6** that feature one or two electron withdrawing groups in the *meta* positions (Chart 1).[29,32] Within the series of 2-alkyl-*N*-[2-(piperidin-1-yl)ethyl]anilines **9a-d**, progressive chain increase from hydrogen (**9a)**, methyl (**9b)**, ethyl (**9c)**, to isopropyl (**9d**), increased the antiviral activity against both A/H1N1 strains. In addition, the drop in activity for the *tert*-butyl-substituted compound **9e**, sets the length limit for this structural part.

Regarding the linker between the aromatic ring and the piperidine, a length of three atoms was found to be optimal for the inhibitory activity (e.g. **9d** *vs* **11**). Concerning the nature of the linker's heteroatom, a nitrogen was similar or slightly better than oxygen (compare **9c** *vs* **13c**, **9d** *vs* **13d**, **10b** *vs* **14a** and **10c** *vs* **14b**), while the sulfur analogs were always inactive (**15a-c**).

Focusing our attention on the heterocyclic ring, piperidine seemed to give the best activity. Ring-contraction from piperidine to pyrrolidine reduced the antiviral activity for both A/H1N1 strains (e.g. **9d** *vs* **12**). Ring-expansion from piperidine to the azepane ring was deleterious for the activity against the A/PR/8/34 strain and also increased the cytotoxicity (e.g. **9c** *vs* **10b**).

Table 1. Antiviral activity in influenza virus H1N1-infected MDCK[a] cells. For the sake of clarity, only active compounds are shown.

Compound	Antiviral EC_{50} (μM)[b,c] Influenza A/H1N1				Cytotoxicity (μM)	
	A/PR/8/34		A/Virginia/ATCC3/2009		CC_{50}[d]	MCC[e]
	CPE	MTS	CPE	MTS		
9c	21	21	13	9.6	>100	100
9d	4.6	5.5	1.7	1.5	>100	100
9e	29	32	36	26	>100	>100
9f	>100	>100	32	8.3	>100	>100
9h	45	48	45	47	>100	>100
9k	15	10	5.4	2.6	61	100
10a	>100	>100	≤0.8	<0.8	11	20
10b	>100	>100	1.7	1.5	14	20
10c	8.4	8.9	1.6	1.3	52	100
11	>100	>100	18	7.9	74	60
12	23	39	17	8.0	>100	>100
13c	8.9	11	8.0	5.7	>100	100
13d	30	15	0.89	1.0	>100	≥100
14a	>100	>100	4.0	<0.8	11	20
14b	>100	>100	2.6	2.0	26	20
18f	>100	>100	52	39	>100	>100
19d	>100	>100	0.19	0.15	0.87	2.0
19e	>100	>100	0.8	<0.8	3.4	4.0
19q	>100	>100	0.21	0.12	1.9	2.0
22a	5.6	5.2	>100	>100	23	20
25	>100	>100	<0.8	<0.8	1.6	4
Amantadine	85	178	>500	>500	>500	>500
Ribavirin	16	45	12	9.8	>100	≥100

[a]MDCK: Madin-Darby canine kidney cells. [b]50% Effective concentration, or concentration producing 50% inhibition of viral cytopathicity, as determined by microscopic scoring of the cytopathic effect (CPE) or by measuring the cell viability with the colorimetric formazan-based MTS assay. [c]All compounds were inactive (highest tested concentration: 100 μM) against influenza A/H3N2 (A/HK/7/87) and influenza B (B/HongKong/5/1972). [d]50% Cytotoxic concentration, as determined by measuring the cell viability with the colorimetric formazan-based MTS assay. [e]Minimum compound concentration that causes a microscopically detectable alteration of normal cell morphology. Values shown are the mean of 2 or 3 determinations.

Remarkably, **18f** and **22a** seemed not to follow the previous activity trends. The amide **18f** displayed antiviral activity against A/Virginia/ATCC3/2009 and stood out for two reasons: it is the only amide from series **18a-x** endowed with anti-influenza activity, and it bears a *para*-benzyloxy group in the aromatic moiety, being the only active compound with an electron donating group. Interestingly, **22a**, which bears a hydroxyl group in the adamantane moiety, is not only the sole active analog with an unsubstituted aromatic moiety, but also the only one to inhibit A/PR/8/34 but not A/Virginia/ATCC3/2009. Taking into account the unique antiviral profile of adamantanol-containing compound, **22a**, and that **5** and **6** also feature a hydroxyl group, further derivatives of **22a** should be explored.

Activity in the influenza polykaryon assay. While this work was in progress, Basu *et al*. reported that compound **14a** (MBX-2329 in their paper) inhibits influenza HA-mediated membrane fusion, as demonstrated in a hemolysis assay with influenza A/PR/8/34.[35] Hence, we determined the inhibitory activity of **9d** and **14a** in the polykaryon assay which is based on cell-cell fusion when HA-transfected cells are exposed to low pH.[24] We included not only H1 HA (from A/PR/8/34), but also H5 HA (derived from the avian H5N1 virus A/duck/Hunan/795/2002) and H3 HA (from the A/X31 virus). As shown in Figure 1, compounds **9d** and **14a**, at a concentration of 100 μM, provided 100% inhibition of H1 and H5 HA-mediated polykaryon formation. The two compounds were equipotent for H1 HA (EC_{50}: 10.1 and 9.6 μM for **9d** and **14a**, respectively), whereas for H5 HA, **14a** was two-fold more active than **9d** (EC_{50}: 16.7 and 39.6 μM, respectively). This means that **14a** produces a similar effect on H1 HA as **9d**. The lack of activity of **14a** in the CPE reduction assay with A/PR/8/34 thus appears related to its relatively high cytotoxicity, which most likely obscures an antiviral effect. No inhibition of H3 HA-induced polykaryon formation was observed (data not shown),

consistent with the lack of antiviral activity of **9d** and **14a** against H3N2 virus. Finally, the possibility was excluded that the different activity against the H1N1 and H3N2 viruses could be related to an action of these molecules on the neuraminidase component, since **9d** and **14a** produced no inhibition in an enzymatic neuraminidase assay with A/PR/8/34 virus (IC_{50} values of **9d** and **14a** and zanamivir: >100 μM; 100 μM and 1.4 nM, respectively; method adapted from reference 46).

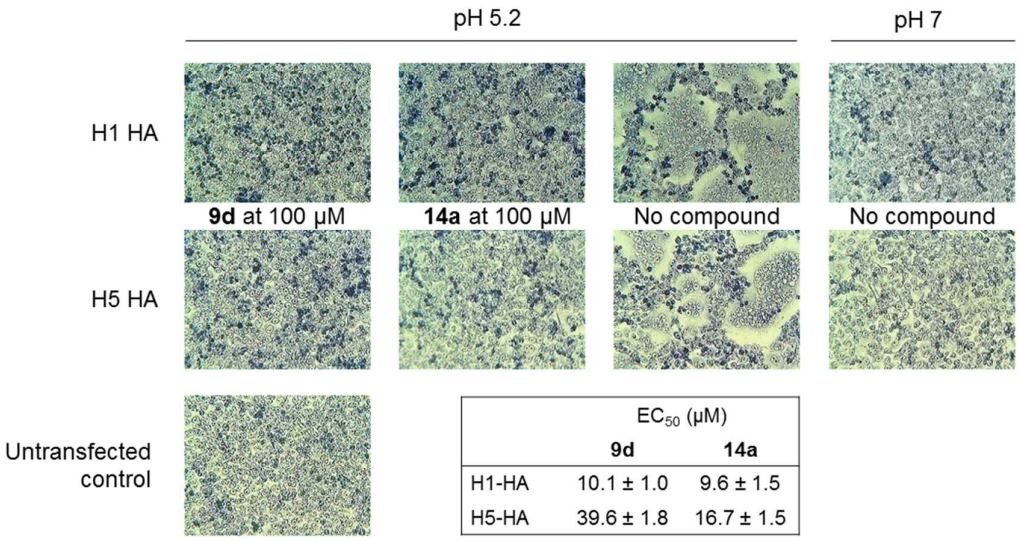

	EC_{50} (μM)	
	9d	**14a**
H1-HA	10.1 ± 1.0	9.6 ± 1.5
H5-HA	39.6 ± 1.8	16.7 ± 1.5

Figure 1. Inhibition of HA-induced polykaryon formation at low pH. HeLa cells expressing HA subtype H1 (top row) or H5 (middle row) were treated with trypsin to render the HA fusion-competent. After pre-incubation with compound **9d** or **14a** at 100 μM, the cells were briefly exposed to pH 5.2 to induce membrane fusion, then incubated with medium during 3 h to allow polykaryon formation. The panels on the right show HA-transfected controls exposed to pH 7, and the bottom row are untransfected control cells. Representative fields are shown (original magnification x200). The table summarizes the EC_{50} values (mean ± SEM; n = 3), defined as the compound concentration at which the number of polykaryons was 50% compared to the no compound control.

Selection and characterization of 9d-resistant virus mutants. Having confirmed that **9d** represents a class of influenza fusion inhibitors with group 1 specificity, we next characterized its binding interaction with the HA protein. First, we selected resistant mutants by serial virus passaging under compound **9d**. As shown in Table 2, virus clones obtained after three passages under up to 50 μM of compound **9d** were resistant to **9d** and its ring-expanded analogue **10c**, whereas the control virus passaged in the absence of compound was equally sensitive as the parent A/PR/8/34 virus used at the start. Sequencing revealed that both **9d-**resistant virus clones contained four substitutions in HA (Table 2). The changes $S186_1P$ and $I10_2V$ were considered less relevant since they were linked to cell culture adaptation in a previous A/PR/8/34 passage study.[39] The two remaining HA changes are both located in the HA stem, with $T107_2I$ lying at a more membrane-distal site than $R153_2I$. The resistance to **9d** was not related to an increase in the viral fusion pH (which indicates that the HA has become less stable allowing its refolding at less acidic pH), since the pH to achieve 50% hemolysis was 5.4 for the virus passaged under **9d** compared to 5.3 for the virus passaged in the absence of compound (data not shown).

We thus concluded that either $Thr107_2$ or $Arg153_2$ lies at or close to the region involved in inhibitor binding. Support for the relevance of $Thr107_2$ comes from the finding that an azide analogue of **3** localized to this region in HA_2 in photoaffinity labelling experiments.[28] Also, substitution of $Phe110_2$ was observed in H1N1 influenza viruses with resistance to **2**.[26]

Table 2. Phenotypic and genotypic characterization of H1N1 virus that was passaged under **9d**.[a]

Compound	**9d^{res}-cl1**	**9d^{res}-cl2**	**No cpd-cl1**	**Parent virus**	Cytotoxicity (μM)	
	Substitutions in HA[b]					
	$T107_2I$ $R153_2I$	$T107_2I$ $R153_2I$	$T54_2A$	-		
	Antiviral EC_{50} (μM)[c]				CC_{50}[d]	MCC[e]
9d	>100	>100	2.3	4.6	>100	100
10c	>100	>100	1.5	8.4	52	100
Ribavirin	11	11	15	16	>100	100

[a]A/PR/8/34 virus was passaged three times under compound **9d** (at 12.5, 25 and 50 μM, successively); a control was included that was passaged in the absence of compound. The harvested viruses were plaque-purified (cl1 and cl2: clone 1 and 2, respectively) prior to HA sequencing. The parent virus means the virus stock that was used to start passage #1. [b]The residues are numbered per HA polypeptide part, i.e. HA_1 and HA_2. Clones 1d^{res}-cl1 and 1d^{res}-cl2 contained the indicated substitutions besides two additional changes ($S186_1P$ and $I10_2V$) previously associated to cell-culture adaptation.[39] [c]50% Effective concentration determined by cytopathic effect (CPE) assay; similar EC_{50} values were obtained by MTS assay (data not shown). [d]50% Cytotoxic concentration, as determined by measuring the cell viability with the colorimetric formazan-based MTS assay. [e]Minimum compound concentration that causes a microscopically detectable alteration of normal cell morphology. Values shown are the mean of 2 or 3 determinations.

NMR experiments. The saturation transfer difference (STD) NMR experiment has been shown to be useful to characterize the interaction between small molecules and large protein targets, including interactions between an inhibitor and influenza hemagglutinin.[23,47] In this experiment, the ^{1}H atoms of the protein are selectively saturated and the observation of magnetization transfer from the protein ^{1}H to the ligand ^{1}H is observed, which enables identification of ligand ^{1}H in closest proximity to the protein surface.[48] Taking into account that the sequence identity between H1 and H5 HA in the HA2 region is very high (see Table S2 and Figure S1 in the Supporting Information), we assayed the binding of **9d** and **10c** to recombinant H5 HA, a group 1 HA, by STD NMR. As shown in Figure 2A, the signals of **9d** and **10c** clearly suggest

binding to H5 HA. Interestingly, in matched experiments, **10c** exhibited significantly stronger STD signals than **9d**, which suggests a better interaction with ^{1}H in closer proximity to the H5 HA surface. As shown in Figure 2B, quantitation of the individual STD signals suggests that the aromatic moiety of both molecules is in closest relative contact to the H5 HA surface and that the piperidine and azepane moieties of **9d** and **10c**, respectively, are more distant. In addition, the isopropyl group of **9d** appears to make better relative contact with the H5 HA surface.

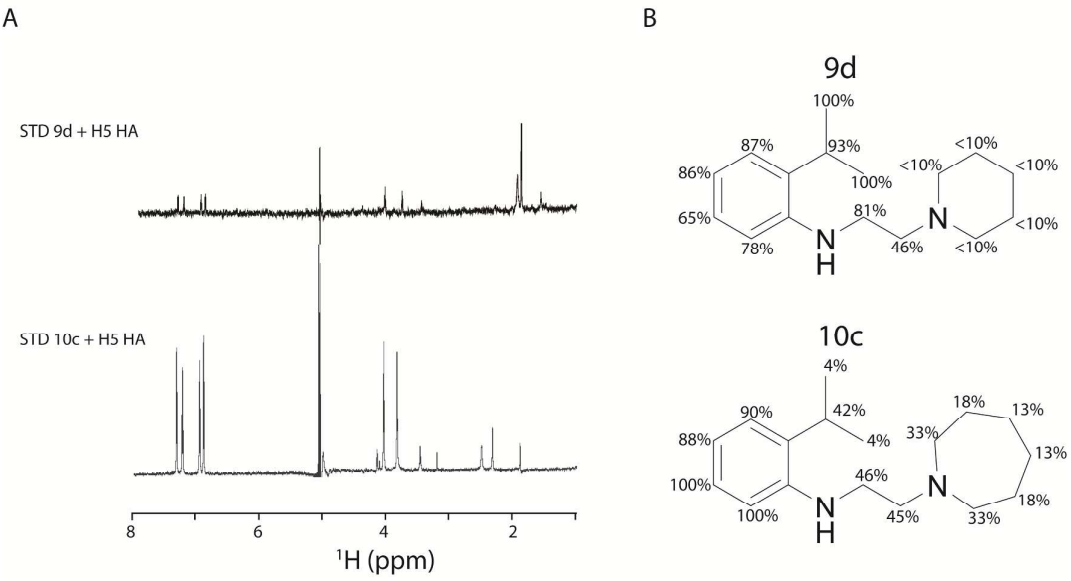

Figure 2. STD NMR experiments (A) and relative STD signals (B) of compounds **9d** and **10c** in the presence of recombinant H5 HA. The experimental conditions were 100 μM compound and 1 μM H5 HA in 20 mM PO_4/pH 7.5, 150 mM NaCl, and 100% $^{2}H_2O$ performed on a Bruker 900 MHz Avance spectrometer equipped with a cryoprobe at 25˚C.

Molecular modeling studies.

Homology modeling. A 3D model of H1 HA in the open form was built up from the X-ray crystal structure of TBHQ bound to X31 HA (see Experimental Section and Figure S2 in the Supporting Information). Although the residues that shape the TBHQ pocket

in H3 HA appeared to be generally conserved in the H1 protein, two important differences were noted. First, $Arg54_2$ in H3 HA, which forms a salt bridge with $Glu97_2$ in the X-ray structure, is replaced by Ser in A/PR/8/34, and by Thr in A/Virginia/ATCC3/2009, respectively. Second, the electrostatic potential in the binding pocket shows a more pronounced negative potential in H1 HA compared to the H3 protein (Figure 3), which can stabilize positively charged ligands such as **9d**, whereas in H3 HA the site is less polar, and hence better suited to accommodate hydrophobic ligands.

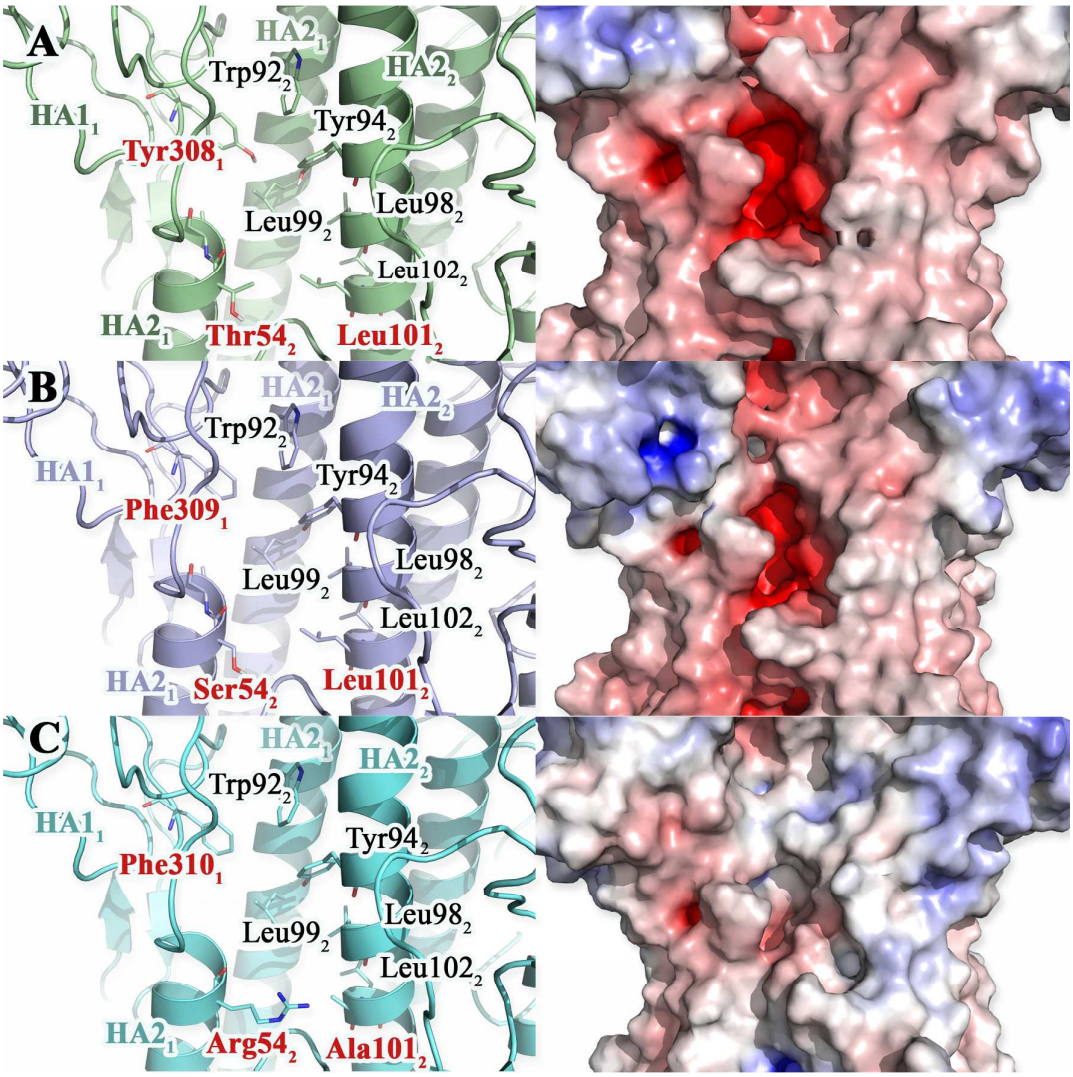

Figure 3. Comparison of (*left*) the binding sites for the H1 HA subtypes (A) A/PR/8/34 and (B) A/Virginia/ATCC3/2009, and (C) the H3 HA subtype A/HK/7/87 obtained by homology modelling. HA2 residues that differ among the three strains are shown in red font. (*Right*) Representation of the solvent-screened electrostatic potential for (A) A/PR/8/34, (B) A/Virginia/ATCC3/2009, and (C) A/HK/7/87. The isosurface corresponds to electrostatic potential values ranging from -9 (red) to +3 (blue) kcal/mol.

Docking and Molecular Dynamics calculations. Choice of the starting structures of the ligand-protein complexes used in MD simulations relied on the analysis of both docking score and population of poses, as well as on the comparison with the available X-ray structural information, specifically regarding the binding mode of THBQ.[21] Clusterization was performed to identify poses with similar arrangement in the binding pocket (poses were grouped into a single cluster if the RMSD was less than 2 Å). This process led to two and four major binding poses in the binding cavity of A/PR/8/34 and A/Virginia/ATCC3/2009, respectively (see Figure S3 in the Supporting Information).

With regard to A/PR/8/34, the most populated pose of compound **9d** revealed that the backbone oxygens of $Lys58_2$ and $Thr54_2$ act as hydrogen-bond acceptors of the protonated piperidine and aniline nitrogen atoms (see Figure S3 in the Supporting Information for the docking scores). In the second cluster, the protonated piperidine interacts with the backbone of $Val55_2$. A solution pertaining to the first, best-scored cluster was selected for MD simulations (see below). With regard to A/Virginia/ATCC3/2009, clusters 1 and 4 show a similar orientation of compound **9d** in the binding pocket, which is reversed in clusters 2 and 3. Keeping in mind the docking scores reported in Figure S3, and the resemblance with the position occupied by TBHQ in the X-ray structure, clusters 1 and 4 were considered for subsequent MD simulations. However, only the simulation starting from cluster 4 led to a stable complex along the

trajectory (see below). We note that the representative poses of cluster 1 in A/PR/8/34 and cluster 4 in A/Virginia/ATCC3/2009 adopt a similar arrangement in the binding pocket (see Figure S3 in the Supporting Information). Finally, attempts to dock compound **9d** within the TBHQ binding site of H3 HA (A/HK/7/87) models were unsuccessful, likely due to the reduced accessibility caused by the $Arg54_2$ side chain and the electrostatic repulsion with the positive charge of **9d**, in agreement with its H1 selectivity in biological experiments.

Next, the structural integrity of the selected poses of compound **9d** bound to A/PR/8/34 and A/Virginia/ATCC3/2009 was examined by MD simulations. In both cases a stable accommodation of the ligand in the binding pocket was found after the first 25 ns of simulation (see Figure S4 in the Supporting Information). The 2-isopropylaniline moiety is placed in a subpocket delimited by $Leu98_2$, $Leu99_2$, and $Leu101_2$, matching most of the region filled by TBHQ in H3 HA, whereas the piperidine ring would occupy the inner part of the cavity, facing $Tyr308_1$ in A/PR/8/34 and $Phe309_1$ in A/Virginia/ATCC3/2009 (Figure 4). According to this arrangement, it can be expected that relatively small hydrophobic substituents bound to the aniline moiety, such as ethyl (**9c**), *t*-butyl (**9e**) and bromine (**9h**), would be tolerated, while substitutions in *meta* (**9i** and **9l-q**) or *para* (**9g**, **9j**, **13b** or **15b**) may be expected to cause steric clashes with residues in the binding pocket, thus explaining the reduced antiviral activity. On the other hand, binding of **9d** would be assisted by stable hydrogen-bonding interactions between the piperidine and aniline nitrogen atoms with the backbone carbonyl groups of $Glu57_2$ and $Thr54_2$ in A/PR/8/34, and of $Val55_2$ and $Ser54_2$ in A/Virginia/ATCC3/2009 (Figure 4). Among the two hydrogen-bond interactions, the former can be expected to be more stabilizing, since it involves a positively charged hydrogen-bond donor (i.e., the protonated piperidine). This is

reflected in average distances close to 2.8 Å (piperidine N) and 3.5 Å (aniline N), and O···H-N angles in the range of 130°-160°. It was further quantified by means of QM calculations performed at the M062X/6-311++G(d,p) level for model systems composed of formaldehyde and either protonated trimethylamine or methylaniline (see Table S3 in the Supporting Information). These calculations were performed for two distinct orientations, which correspond to a linear hydrogen-bond arrangement and a geometry shifted 45º from linearity (chosen according to the range of O···H-N angles sampled in simulations; see above). The results indicate that the interaction of the protonated piperidine with the carbonyl group of $Glu57_2$ (in A/PR/8/34) / $Val55_2$ (in A/Virginia/ATCC3/2009) is intrinsically around 13 kcal/mol more stabilizing than the interaction formed by the aniline nitrogen atom. Hence, it can be concluded that the hydrogen bond formed by the aniline moiety is less stabilizing for the binding of compound **9d**.

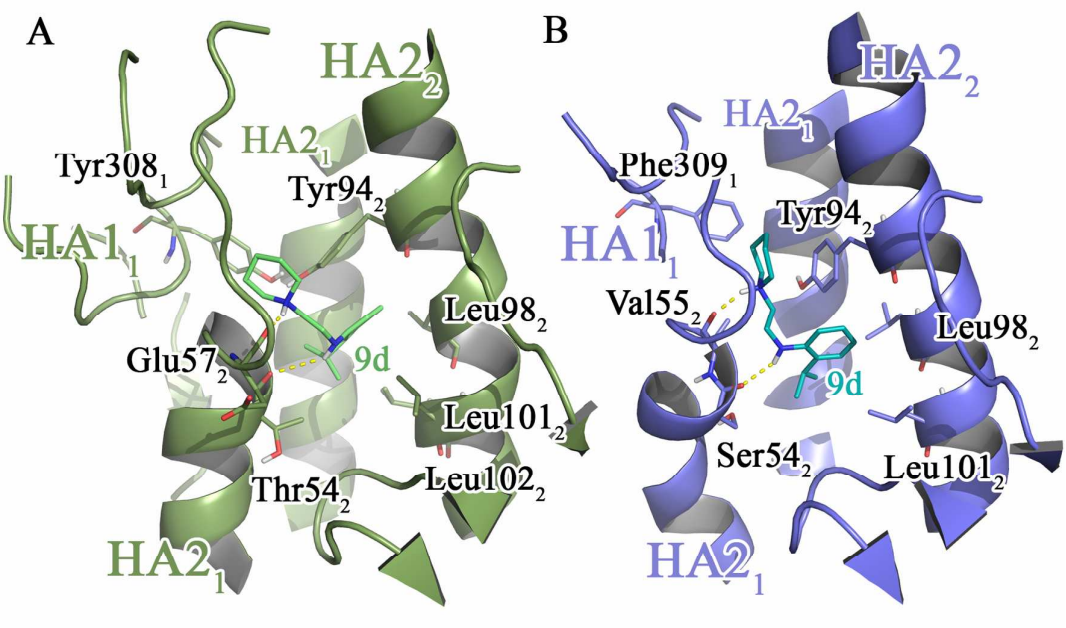

Figure 4. Protein-inhibitor complexes for compound **9d** within the HA2 polypeptide of (A) A/PR/8/34 and (B) A/Virginia/ATCC3/2009, obtained after 50 ns of MD simulations.

Hence, along the MD simulations, we observed a stable interaction pattern that resulted from ligand anchoring due to hydrogen bonding, especially involving the piperidine moiety (see Figure S4 in the Supporting Information). Nevertheless, from a wider perspective, MM/PBSA calculations performed for the set of snapshots collected along the last 15 ns of MD trajectories, showed that the calculated HA binding affinity of compound **9d** for A/Virginia/ATCC3/2009 exceeds that of A/PR/8/34 by around 3.5 kcal/mol (see Table S4 in the Supporting Information). This preference can be mainly ascribed to the non-polar contribution (-16.0 and -19.5 kcal/mol, respectively for A/PR/8/34 and A/Virginia/ATCC3/2009). In this context, we noted that non-electrostatic interactions were identified to have a major contribution in the binding of **14a** to HA.[49] Taking together the lower impact of the hydrogen bond formed by the aniline moiety on the interaction energy, and the significant contribution of the non-electrostatic terms, it can be expected that the replacement of the aniline moiety (in **9d**) by a phenoxy- group (in **13d**) should not be a critical modification in terms of binding affinity, since loss of the weaker hydrogen-bond may be counterbalanced by non-electrostatic interactions in the binding pocket.

The arrangement of compound **9d** in the binding pocket shows a significant overlap with both TBHQ and arbidol (see Figure S5 in the Supporting Information). Moreover, this pocket is also close to the residues ($Glu103_2$, $Asn104_2$, and $Glu105_2$) in HA2 that were primarily implicated in an A/PR/8/34 HA photoaffinity labelling study with an azide analog of fusion inhibitor **3** (see Figure S5 in the Supporting Information).[28] Very recently, this HA binding pocket of A/PR/8/34 was proposed to accommodate the fusion inhibitor **8**.[36]

*Impact of **9d**-resistance mutation T107$_2$I*. As explained above, serial passaging of A/PR/8/34 in the presence of compound **9d** resulted in a resistant virus carrying a Thr107→Ile change in HA2 (Table 2). Residue Thr107$_2$ is located near the fusion peptide portion and helps to stabilize the orientation of the three α-helices that form the "TBHQ pocket" (Figure 5) through a water-assisted network of polar interactions involving Thr107$_2$, Arg106$_2$, Glu103$_2$, Lys51$_2$ and Thr54$_2$. The Thr107→Ile change could destabilize these interactions, particularly the electrostatic interaction between Lys51$_2$ and Glu103$_2$, which in turn interact with Arg106$_2$ and water molecules below the ligand binding site. Such a destabilization could weaken the binding affinity for **9d**, thus explaining why the mutant virus is insensitive to **9d**.

Finally, we noted that most of the resistance mutations obtained under the fusion inhibitors **7**[34] and **8**[36] co-localize with the position of Thr107$_2$, which is placed close to the proposed binding pocket for compound **9d** (see Figure S6 in the Supporting Information).

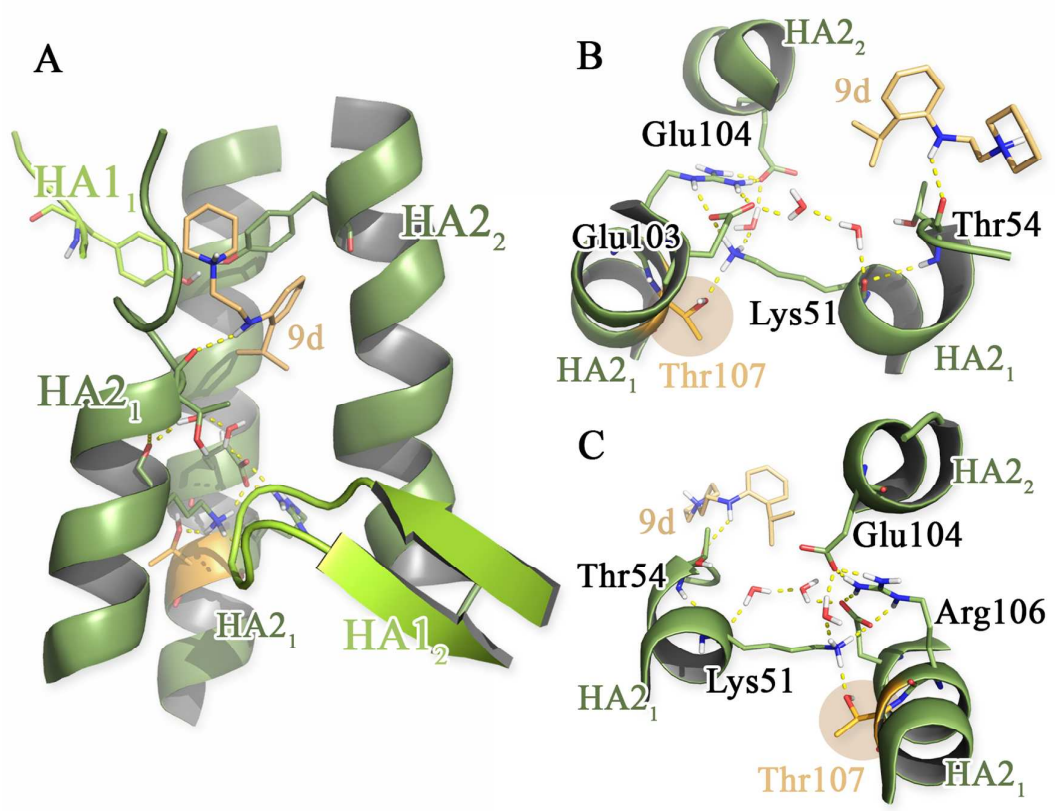

Figure 5. (**A**) Putative effects of the **9d**-associated Thr107→Ile mutation on water-assisted polar network among residues pertaining to $HA2_1$ and $HA2_2$ helices in A/PR/8/34 HA. Detailed view of specific interactions in (**B**) $HA2_1$, and (**C**) $HA2_1$ and $HA2_2$ helices. The Thr107→Ile change not only would break the interaction between the hydroxyl group of $Thr107_2$ and $Lys51_2$, but would also destabilize the electrostatic interaction between $Lys51_2$ and $Glu103_2$, which in turn interacts with $Arg106_2$ and water molecules below the ligand binding site.

Binding mode for the adamantane analogues. To evaluate the effect of substitution of the piperidine by the adamantane moiety, the docking and MD simulations protocol described for compound **9d** was also performed for compound **25**, which contains aniline and adamantane moieties linked by two methylene units. This compound was found to be potent against the A/Virginia/ATCC3/2009 strain, yet poorly active against A/PR/8/34.

The different activity profile of compound **25** can be explained by its distinct accommodation in the binding site (see Figure 6). Compound **25** nicely fills the binding site of A/Virginia/ATCC3/2009, where the adamantane moiety occupies the hydrophobic cavity formed by $Trp92_2$, $Tyr94_2$, $Phe309_1$ and $Pro308_1$, forming van der Waals interactions with these residues (see Figure 6C). On the opposite site of the binding pocket, the aniline nitrogen atom is engaged in a hydrogen bond with the backbone oxygen of $Ser54_2$, while the aromatic ring fills the hydrophobic region occupied by TBHQ in the reference structure 3EYM.

The worse binding of compound **25** to A/PR/8/34 is reflected in the shift of the adamantane unit toward the entrance of the cavity, where it is surrounded by polar residues ($Asp90_2$, $Lys321_1$, $Asn60_2$, and $Arg324_1$) and becoming more exposed to the aqueous solvent (see Figure 6A). This agrees with the worse fit of the adamantane unit in the interior of the cavity, as the presence of $Tyr308_1$ in A/PR/8/34 (replaced by $Phe309_1$ in A/Virginia/ATCC3/2009) tends to reduce the hydrophobicity of the pocket, but possibly more importantly changes the shape of the inner pocket in A/Virginia/ATCC3/2009 due to the hydrogen bond formed by $Tyr308_1$ with $Tyr94_2$ in A/PR/8/34 (see Figure 6B, D).

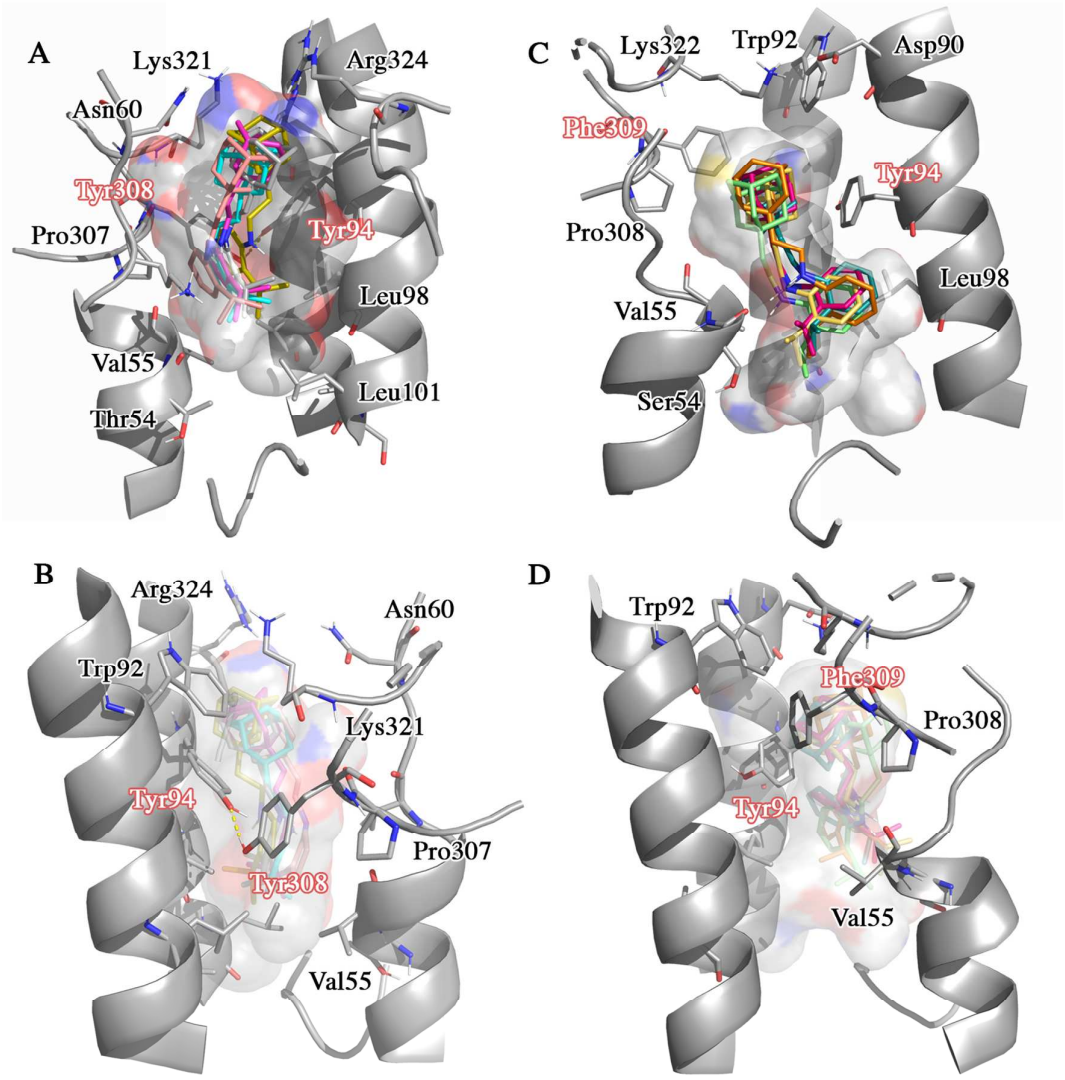

Figure 6. Front (A, C) and back (B, D) view of the MD-derived protein-ligand complex for compound **25** in the HAs from A/PR/8/34 (A, B) and A/Virginia/ATCC3/2009 (C, D). Key residues in the binding site are shown in red. Solid contours reflect the shape of the binding site. Note the distinct shape of the pockets due to the replacement of Tyr308 in A/PR/8/34 by $Phe309_1$ in A/Virginia/ATCC3/2009, which breaks the hydrogen bond formed between $Tyr94_2$ and $Tyr308_1$ in the former.

Evaluation against other viruses. In addition to influenza virus testing, all compounds underwent broad evaluation in CPE reduction assays with a panel of DNA and RNA viruses, i.e. herpes simplex virus type 1 and type 2; vaccinia virus; feline coronavirus;

feline herpesvirus; vesicular stomatitis virus (VSV); Coxsackie B4 virus; respiratory syncytium virus; para-influenza-3 virus; reovirus-1; Sindbis virus; and Punta Toro virus.[50] Three derivatives carrying the adamantyl scaffold proved active against the veterinary virus VSV, with antiviral EC_{50} values of 45 μM (**14b**); 12 μM (**19t**) and 12 μM (**19u**) (data not shown). Compound **19i** was a potent inhibitor of parainfluenza-3 virus (EC_{50}: 9 μM) whereas **19f** displayed activity against Coxsackie B4 virus (EC_{50}: 8.9 μM). Based on these results, the general scaffolds **I** and **II** appear relevant for the design of novel antiviral compounds against diverse viruses with medical importance.

Conclusions

Two series of novel anilines have been synthesized, characterized and evaluated as antiviral compounds. Several ones displayed activity against A/H1N1 influenza with EC_{50} values in the low micromolar range. Influenza fusion, virus resistance as well as NMR experiments with the lead molecule **9d** demonstrated that it interferes with HA-mediated fusion by binding to the HA stem and preventing its refolding at low pH. MD simulations suggest that ligand **9d** is able to fill the "TBHQ pocket" in the HAs of A/PR/8/34 and A/Virginia/ATCC3/2009. This implies that the "TBHQ pocket" represents a common and particularly relevant site for small-molecule HA fusion inhibitors, although distinct chemotypes are required to address the different polarity of this cavity in group-1 *versus* group-2 HA subtypes.

Experimental Section

Chemical Synthesis. General Methods. Melting points were determined in open capillary tubes with a MFB 595010M Gallenkamp. 400 MHz ^{1}H/100.6 MHz ^{13}C NMR spectra, and 500 MHz ^{1}H NMR spectra were recorded on Varian Mercury 400, and

Varian Inova 500 spectrometers, respectively. The chemical shifts are reported in ppm (δ scale) relative to internal tetramethylsilane, and coupling constants are reported in Hertz (Hz). Assignments given for the NMR spectra of the new compounds have been carried out on the basis of DEPT, COSY $^{1}H/^{1}H$ (standard procedures), and COSY $^{1}H/^{13}C$ (gHSQC and gHMBC sequences) experiments. IR spectra were run on Perkin-Elmer Spectrum RX I spectrophotometer. Absorption values are expressed as wave-numbers (cm^{-1}); only significant absorption bands are given. High-resolution mass spectrometry (HRMS) analyses were performed with an LC/MSD TOF Agilent Technologies spectrometer. The elemental analyses were carried out in a Flash 1112 series Thermofinnigan elemental microanalyzator (A5) to determine C, H and N. Column chromatography was performed on silica gel 60 AC.C (35−70 mesh, SDS, ref 2000027). Thin-layer chromatography was performed with aluminum-backed sheets with silica gel 60 F_{254} (Merck, ref 1.05554), and spots were visualized with UV light and 1% aqueous solution of $KMnO_4$. The analytical samples of all of the new compounds which were subjected to pharmacological evaluation possessed purity ≥95% as evidenced by their elemental analyses.

General Procedure A. To a solution of the required aniline (2 eq) in dry DMF at room temperature, the chloroalkyl derivative (1 eq), K_2CO_3 (2 eq) and KI (0.1 eq) were sequentially added. The reaction mixture was stirred and heated at 90 ºC during 30 h. After cooling down to room temperature, the resulting crude material was dissolved in DCM. The solution was washed with water, dried over anh. Na_2SO_4, filtered and concentrated *in vacuo* to obtain the desired product and some recovered starting materials. Column chromatography (Hexane/Ethyl acetate mixtures) gave the expected product. An analytical sample of its hydrochloride salt was prepared by adding an

excess of HCl either in diethyl ether or 1,4-dioxane to a solution of the base in ethyl acetate.

General Procedure B. A solution of the required aniline (2 eq) and 1-(2-chloroethyl)piperidine hydrochloride (1 eq) was stirred and heated at 120 ºC overnight. After cooling down to room temperature, the resulting mixture was dissolved in water and solid sodium acetate was added to obtain pH 5.5. The excess of aniline was extracted with diethyl ether. The aqueous layer was alkalized with 2 N NaOH aqueous solution and extracted with diethyl ether. The combined organic layers were dried over anh. Na_2SO_4, filtered and concentrated *in vacuo* to obtain the desired product. An analytical sample of its hydrochloride salt was prepared by adding an excess of HCl either in diethyl ether or 1,4-dioxane to a solution of the base in ethyl acetate.

General Procedure C. Sodium hydroxide (0.800 g, 20 mmol, 2 eq) was refluxed in ethanol (150 mL) for 30 min. To the resulting solution was added the corresponding phenol or tiophenol (10 mmol, 1 eq) and further refluxed for 1 h. A solution in ethanol (35 mL) of either 1-(2-chloroethyl)piperidine hydrochloride or 1-(2-chloroethyl)azepane hydrochloride (10 mmol, 1 eq) was added to the basic solution and the reaction mixture refluxed for further 3 h. After pouring into cold water (125 mL), the product was extracted with DCM (4 x 125 mL) and the joined extracts were washed with water (4 x 150 mL), dried over anh. Na_2SO_4, filtered and concentrated *in vacuo* to obtain the desired product. Its hydrochloride salt was prepared by adding an excess of HCl either in diethyl ether or 1,4-dioxane to a solution of the base in ethyl acetate.

***N*-[2-(piperidin-1-yl)ethyl]aniline hydrochloride, 9a**.[51] Following general procedure B, aniline (1.82 mL, 20 mmol) and 1-(2-chloroethyl)piperidine hydrochloride (1.83 g, 10 mmol) gave the product as an orange oil (2.06 g, 86% yield), that formed its hydrochloride salt as a white solid (904 mg). The analytical sample was obtained by

crystallization from EtOAc/Pentane, mp = 185-186 ºC. IR (ATR) ν: 691, 747, 830, 851, 871, 902, 949, 988, 1013, 1027, 1075, 1125, 1155, 1178, 1194, 1243, 1268, 1290, 1324, 1356, 1405, 1433, 1472, 1497, 1534, 1602, 2575, 2537, 2639, 2848, 2948, 3026, 3273 cm^{-1}. ^{1}H-NMR (400 MHz, CD_3OD) δ: 1.60-1.78 (complex signal, 2 H, 11-H_2), 1.80-1.94 [complex signal, 4 H, 10(12)-H_2], 3.15-3.34 [complex signal, 4 H, 9(13)-H_2], 3.27 (t, *J* = 6.4 Hz, 2 H, 8-H_2), 3.53 (t, *J* = 6.4 Hz, 2 H, 7-H_2), 6.68 (m, 1 H, 4-H), 6.70 [m, 2 H, 2(4)-H], 7.15 [m, 2 H, 3(5)-H]. ^{13}C-NMR (100.5 MHz, CD_3OD) δ: 22.8 (CH_2, C11), 24.2 [CH_2, C10(12)], 39.5 (CH_2, C7), 54.7 [CH_2, C9(13)], 57.1 (CH_2, C8), 114.1 [CH, C2(6)], 119.0 (CH, C4), 130.3 [CH, C3(5)], 149.1 (C, C1).

2-methyl-*N*-[2-(piperidin-1-yl)ethyl]aniline hydrochloride, 9b. Following the general procedure A, 2-methylaniline (1.07 mL, 10 mmol), 1-(2-chloroethyl)piperidine hydrochloride (920 mg, 5 mmol), K_2CO_3 (1.38 g, 10 mmol) and KI (83 mg, 0.5 mmol) in dry DMF (2 mL) were mixed to obtain a yellowish oil (1.38 g). After column chromatography, the product was obtained as a colourless oil (557 mg, 51% yield) that formed its hydrochloride salt as a white solid (600 mg), mp = 182-183 ºC. IR (ATR) ν: 665, 708, 753, 771, 804, 854, 930, 948, 963, 988, 1008, 1049, 1079, 1117, 1132, 1170, 1196, 1226, 1261, 1292, 1330, 1405, 1451, 1479, 1514, 1582, 1600, 1648, 2400, 2526, 2612, 2936, 3321 cm^{-1}. ^{1}H-NMR (400 MHz, CD_3OD) δ: 1.55 (m, 1 H, 11-H_{ax}), 1.76-2.00 [complex signal, 5 H, 11-H_{eq} and 10(12)-H_2], 2.30 (s, 3 H, CH_3), 3.04 [m, 2 H, 9(13)-H_{ax}], 3.45 (t, *J* = 6.8 Hz, 2H, 8-H_2), 3.62 (m, 2 H, 9(13)-H_{eq}), 3.72 (t, *J* = 6.8 Hz, 2 H, 7-H_2), 6.89 (dd, *J* = *J'* = 7.8 Hz, 1 H, 4-H), 6.97 (d, *J* = 7.8 Hz, 1 H, 6-H), 7.15 (d, *J* = 7.8 Hz, 1 H, 3-H), 7.18 (ddd, *J* = *J'* = 7.8 Hz, J'' = 1.2 Hz, 1 H, 5-H). ^{13}C-NMR (100.5 MHz, CD_3OD) δ: 17.8 (CH_3), 22.6 (CH_2, C11), 24.1 [CH_2, C10(12)], 41.2 (CH_2, C7), 54.8 [CH_2, C9(13)], 55.8 (CH_2, C8), 114.9 (CH, C6), 122.7 (CH, C4), 127.1 (CH,

C5), 128.4 (CH, C3), 132.1 (C, C2), 142.9 (C, C1). HRMS-ESI+ m/z $[M+H]^+$ calcd for $[C_{14}H_{22}N_2+H]^+$: 219.1856, found: 219.1858.

2-Ethyl-*N*-[2-(piperidin-1-yl)ethyl]aniline hydrochloride, 9c. Following general procedure B, 2-ethylaniline (2.47 mL, 20 mmol) and 1-(2-chloroethyl)piperidine hydrochloride (1.83 g, 10 mmol) gave the product as a yellow oil (1.93 g, 83%), that formed its hydrochloride salt as a pale brown solid (818 mg), mp = 173-174 ºC. IR (ATR) ν: 728, 745, 799, 833, 902, 925, 947, 993, 1013, 1050, 1087, 1136, 1164, 1193, 1238, 1261, 1287, 1304, 1329, 1369, 1426, 1452, 1478, 1518, 1586, 1600, 2507, 2610, 2867, 2924, 2947, 3341 cm^{-1}. ^{1}H-NMR (400 MHz, CD_3OD) δ: 1.21 (t, J = 7.6 Hz, 3 H, -$CH_2C\underline{H}_3$), 1.56-1.68 (complex signal, 2 H, 11-H_2), 1.76-1.86 [complex signal, 4 H, 10(12)-H_2], 2.55 (q, J = 7.6 Hz, 2 H, -$C\underline{H}_2CH_3$), 2.98-3.12 [complex signal, 4 H, 9(13)-H_2], 3.13 (t, J = 6.4 Hz, 2 H, 8-H_2), 3.51 (t, J = 6.4 Hz, 2 H, 7-H_2), 6.64-6.70 (complex signal, 2 H, Ar), 7.01-7.10 (complex signal, 2 H, Ar). ^{13}C-NMR (100.5 MHz, CD_3OD) δ: 13.8 (CH_3, -$CH_2\underline{C}H_3$), 23.4 (CH_2, C11), 24.8 (CH_2, $\underline{C}H_2CH_3$), 24.9 [CH_2, C10(12)], 40.2 (CH_2, C7), 55.0 [CH_2, C9(13)], 57.4 (CH_2, C8), 111.3 (CH, C6), 118.9 (CH, C4), 128.0 (CH, C5), 129.3 (CH, C3), 130.0 (C, C2), 146.2 (C, C1). HRMS-ESI+ m/z $[M+H]^+$ calcd for $[C_{15}H_{24}N_2+H]^+$: 233.2012, found: 233.2005.

2-isopropyl-*N*-[2-(piperidin-1-yl)ethyl]aniline hydrochloride, 9d. Following general procedure B, 2-isopropylaniline (2.83 mL, 20 mmol) and 1-(2-chloroethyl)piperidine hydrochloride (1.83 g, 10 mmol) gave the product as a brown oil (2.02 g, 82%), that formed its hydrochloride salt as a pale brown solid (1.15 g), mp = 140-141 ºC. IR (ATR) ν: 760, 855, 948, 966, 1007, 1039, 1096, 1172, 1193, 1257, 1270, 1294, 1327, 1356, 1376, 1403, 1445, 1513, 1583, 1599, 2356, 2529, 2614, 2861, 2932, 3328 cm^{-1}. ^{1}H-NMR (400 MHz, CD_3OD) δ: 1.22 [d, J = 6.8 Hz, 6 H, -$CH(C\underline{H}_3)_2$], 1.54-1.66 (complex signal, 2 H, 11-H_2), 1.74-1.84 [complex signal, 4 H, 10(12)-H_2],

2.94-3.05 [complex signal, 5 H, 9(13)-H_2, and -C<u>H</u>$(CH_3)_2$], 3.07 (t, *J* = 6.4 Hz, 2 H, 8-H_2), 3.47 (t, *J* = 6.4 Hz, 2 H, 7-H_2), 6.68 (broad d, *J* = 8.0 Hz, 1 H, 6-H), 6.70 (dt, *J* = 7.2 Hz, *J'* = 1.2 Hz, 1 H, 5-H), 7.05 (dt, *J* = 7.6 Hz, *J'* = 1.6 Hz, 1 H, 4-H), 7.12 (dd, *J* = 7.6 Hz, *J'* = 1.6 Hz, 1 H, 3-H). ^{13}C-NMR (100.5 MHz, CD_3OD) δ: 23.1 [CH_3, -CH(<u>C</u>$H_3)_2$], 23.6 (CH_2, C11), 25.2 [CH_2, C10(12)], 27.9 [CH, -<u>C</u>H$(CH_3)_2$], 40.5 (CH_2, C7), 55.0 [CH_2, C9(13)], 57.5 (CH_2, C8), 111.9 (CH, C6), 119.1 (CH, C4), 126.1 (CH, C5), 127.7 (CH, C3), 134.6 (C, C2), 145.6 (C, C1). HRMS-ESI+ m/z $[M+H]^+$ calcd for $[C_{16}H_{26}N_2+H]^+$: 247.2169, found: 247.2166.

2-*t*-butyl-*N*-[2-(piperidin-1-yl)ethyl]aniline hydrochloride, 9e. Following the general procedure A, 2-*tert*-butylaniline (1.56 mL, 10 mmol), 1-(2-chloroethyl)piperidine hydrochloride (0.92 g, 5 mmol), K_2CO_3 (1.38 g, 10 mmol) and KI (83 mg, 0.5 mmol) in dry DMF (2.5 mL) were mixed to obtain a brown oil (0.99 g). After column chromatography, the product was obtained as a yellow oil (290 mg, 20% yield) that formed its hydrochloride salt as a white solid (234 mg), mp = 101-102 ºC. IR (ATR) ν: 747, 773, 847, 899, 987, 1054, 1108, 1147, 1173, 1194, 1232, 1256, 1287, 1305, 1367, 1387, 1444, 1504, 1576, 1594, 2346, 2537, 2661, 2950, 3379, 3416 cm^{-1}. ^{1}H-NMR (400 MHz, CD_3OD) δ: 1.42 (s, 9 H, C(C<u>H</u>$_3)_3$], 1.56 (m, 1 H, 11-H_{ax}), 1.76-2.00 [complex signal, 5 H, 11-H_{eq} and 10(12)-H_2], 3.05 [td, *J* = 12.4 Hz, *J'* = 3.2 Hz, 2 H, 9(13)-H_{ax}], 3.37 (t, *J* = 6.8 Hz, 2 H, 8-H_2), 3.63 (dm, J = 12.4 Hz, 2 H, 9(13)-H_{eq}), 3.73 (t, *J* = 6.8 Hz, 2 H, 7-H_2), 6.77 (ddd, *J* = *J'* = 7.6 Hz, *J''* = 1.2 Hz, 1 H, 4-H), 6.84 (dd, *J* = 8.0, *J'* = 1.2, 1 H, 6-H), 7.14 (ddd, *J* = 8.0 Hz, *J'* = 7.6 Hz, *J''* = 1.6 Hz, 1 H, 5-H), 7.28 (dd, *J* = 7.6 Hz, *J'* = 1.6 Hz, 1 H, 3-H). ^{13}C-NMR (100.5 MHz, CD_3OD) δ: 22.5 (CH_2, C11), 24.2 [CH_2, C10(12)], 30.7 [CH_3, C(<u>C</u>$H_3)_3$], 35.3 [C, <u>C</u>$(CH_3)_3$], 42.1 (CH_2, C7), 55.0 [CH_2, C9(13)], 56.1 (CH_2, C8), 116.1 (CH, C6), 122.0 (CH, C4), 128.1

(CH, C5*), 128.5 (CH, C3*), 137.6 (C, C2), 143.6 (C, C1). HRMS-ESI+ m/z $[M+H]^+$ calcd for $[C_{17}H_{28}N_2+H]^+$: 261.2325, found: 261.2333.

2-methoxy-*N*-[2-(piperidin-1-yl)ethyl]aniline hydrochloride, 9f.[52] Following the general procedure A, 2-methoxyaniline (0.56 mL, 5 mmol), 1-(2-chloroethyl)piperidine hydrochloride (0.92 g, 5 mmol), K_2CO_3 (2.07 g, 15 mmol) and KI (83 mg, 0.5 mmol) in dry DMF (2.5 mL) were mixed to obtain a brown oil (0.94 g). After column chromatography, the product was obtained as a yellow oil (380 mg, 29% yield) that formed its hydrochloride salt as a yellow solid (291 mg), mp = 174-175 ºC. IR (ATR) ν: 638, 754, 798, 827, 853, 948, 971, 1023, 1039, 1098, 1121, 1163, 1186, 1263, 1289, 1325, 1413, 1439, 1501, 1578, 1612, 2341, 2532, 2651, 2940, 3328 cm^{-1}. ^{1}H-NMR (400 MHz, CD_3OD) δ: 1.55 (m, 1 H, 11-H_{ax}), 1.78-2.06 [complex signal, 5 H, 11-H_{eq} and 10(12)-H_2], 3.06 [m, 2 H, 9(13)-H_{ax}], 3.51 (t, *J* = 6.8 Hz, 2 H, 8-H_2), 3.63 (m, 2 H, 9(13)-H_{eq}), 3.87 (t, *J* = 6.8 Hz, 2 H, 7-H_2), 4.00 (s, 3 H, OCH_3), 7.10 (ddd, *J* = *J'* = 7.6 Hz, *J''* = 1.2 Hz, 1 H, 5-H), 7.24 (dd, *J* = 8.4, *J'* = 1.2, 1 H, 3-H), 7.43 (ddd, *J* = 8.4 Hz, *J'* = 7.6 Hz, *J''* = 1.6 Hz, 1 H, 4-H), 7.51 (dd, *J* = 7.6 Hz, *J'* = 1.6 Hz, 1 H, 6-H). ^{13}C-NMR (100.5 MHz, CD_3OD) δ: 22.5 (CH_2, C11), 24.2 [CH_2, C10(12)], 44.5 (CH_2, C7), 53.8 (CH_2, C8), 55.0 [CH_2, C9(13)], 56.9 (CH_3, OCH_3), 113.8 (CH, C6), 122.6 (CH, C3), 123.0 (CH, C4), 126.2 (C, C1), 130.9 (CH, C5), 153.1 (C, C2). HRMS-ESI+ m/z $[M+H]^+$ calcd for $[C_{14}H_{22}N_2O+H]^+$: 235.1805, found: 235.1814.

4-chloro-*N*-[2-(piperidin-1-yl)ethyl]aniline hydrochloride, 9g.[53] Following general procedure B, 4-chloroaniline (2.55 g, 20 mmol) and 1-(2-chloroethyl)piperidine hydrochloride (1.83 g, 10 mmol) gave a pale yellow oil (1.74 g). After column chromatography (Hexane/Ethyl acetate mixture) the product was obtained as a yellow oil (1.16 g, 73% yield) that formed its hydrochloride salt as a white solid (310 mg), mp= 198-199 ºC. IR (ATR) ν: 651, 704, 809, 829, 861, 957, 971, 1004, 1070, 1091, 1134,

1183, 1200, 1253, 1292, 1310, 1460, 1478, 1488, 1520, 1599, 2542, 2639, 2947, 3261 cm^{-1}. ^{1}H-NMR (400 MHz, CD_3OD) δ: 1.50-1.80 (complex signal, 2 H, 11-H_2), 1.81-1.98 [complex signal, 4 H, 10(12)-H_2], 3.00-3.42 [complex signal, 4 H, 9(13)-H_2], 3.29 (t, *J* = 6.4 Hz, 2 H, 8-H_2), 3.53 (t, *J* = 6.4 Hz, 2 H, 7-H_2), 6.68 [m, 2 H, 2(6)-H], 7.11 [m, 2 H, 3(5)-H]. ^{13}C-NMR (100.5 MHz, CD_3OD) δ: 22.7 (CH_2, C11), 24.1 [CH_2, C10(12)], 39.4 (CH_2, C7), 54.6 [CH_2, C9(13)], 56.8 (CH_2, C8), 115.3 [CH, C2(6)], 123.4 (CH, C4), 130.1 [CH, C3(5)], 147.9 (C, C1).

2-bromo-*N*-[2-(piperidin-1-yl)ethyl]aniline hydrochloride, 9h. Following the general procedure A, 2-bromoaniline (1.13 mL, 10 mmol), 1-(2-chloroethyl)piperidine hydrochloride (0.92 g, 5 mmol), K_2CO_3 (1.38 g, 10 mmol) and KI (83 mg, 0.5 mmol) in dry DMF (2.5 mL) were mixed to obtain a brown oil (1.78 g). After column chromatography, the product was obtained as a yellow oil (134 mg, 8% yield) that formed its hydrochloride salt as a dark yellow solid (139 mg), mp = 161-162 ºC. IR (ATR) ν: 654, 752, 948, 964, 1018, 1090, 1173, 1194, 1222, 1271, 1297, 1336, 1405, 1452, 1504, 1589, 2485, 2614, 2940, 3317 cm^{-1}. ^{1}H-NMR (400 MHz, CD_3OD) δ: 1.47-1.61 (complex signal, 2 H, 11-H_2), 1.78-2.00 [complex signal, 4 H, 10(12)-H_2], 3.03 [td, *J* = 12.0 Hz, *J'* = 3.2 Hz, 2 H, 9(13)-H_{ax}], 3.35 (t, *J* = 6.4 Hz, 2 H, 8-H_2), 3.61 (dm, *J* = 12.0 Hz, 2 H, 9(13)-H_{eq}), 3.69 (t, *J* = 6.4 Hz, 2 H, 7-H_2), 6.65 (ddd, *J* = *J'* = 8.0 Hz, *J''* = 1.6 Hz, 1 H, 5-H), 6.85 (dd, *J* = 8.0, *J'* = 1.2, 1 H, 6-H), 7.24 (ddd, *J* = *J'* = 8.0 Hz, *J''* = 1.2 Hz, 1 H, 4-H), 7.44 (dd, *J* = 8.0 Hz, *J'* = 1.6 Hz, 1 H, 3-H). ^{13}C-NMR (100.5 MHz, CD_3OD) δ: 21.3 (CH_2, C11), 22.9 [CH_2, C10(12)], 38.2 (CH_2, C7), 53.6 [CH_2, C9(13)], 55.3 (CH_2, C8), 109.8 (C, C2), 111.8 (CH, C6), 119.0 (CH, C4), 128.6 (CH, C5), 132.7 (CH, C3), 144.0 (C, C1). HRMS-ESI+ m/z $[M+H]^+$ calcd for $[C_{13}H_{19}BrN_2+H]^+$: 283.0804, found: 283.0815.

***N*-[2-(piperidin-1-yl)ethyl]-3-(trifluromethyl)aniline hydrochloride, 9i**.[44] Following the general procedure A, 3-trifluoromethylaniline (2.5 mL, 20 mmol), 1-(2-chloroethyl)piperidine hydrochloride (1.830 g, 10 mmol), K_2CO_3 (2.76 g, 20 mmol) and KI (166 mg, 1 mmol) in dry DMF (4 mL) were mixed to obtain a brown oil (3.73 g). After column chromatography the product was obtained as a yellow oil (1.04 g, 38% yield) that formed its hydrochloride salt as a white solid (824 mg), mp = 169-170 ºC. IR (ATR) ν: 636, 658, 696, 737, 786, 802, 815, 860, 869, 897, 915, 959, 974, 993, 1000, 1037, 1067, 1116, 1168, 1226, 1247, 1319, 1340, 1455, 1477, 1545, 1617, 2262, 2543, 2639, 2944, 3061, 3251 cm^{-1}. ^{1}H-NMR (400 MHz, CD_3OD) δ: 1.58-1.78 (complex signal, 2 H, 11-H_2), 1.82-1.96 [complex signal, 4 H, 10(12)-H_2], 3.00-3.45 [complex signal, 4 H, 9(13)-H_2], 3.31 (t, *J* = 6.4 Hz, 2 H, 8-H_2), 3.59 (t, *J* = 6.4 Hz, 2 H, 7-H_2), 6.90-6.98 (complex signal, 3 H, Ar), 7.32 (t, *J* = 8.6 Hz, 1 H, 5-Ar). ^{13}C-NMR (100.5 MHz, CD_3OD) δ: 22.7 (CH_2, C11), 24.2 [CH_2, C10(12)], 39.1 (CH_2, C7), 54.7 [CH_2, C9(13)], 56.8 (CH_2, C8), 110.1 (q, *J* = 4 Hz, CH, C2), 114.9 (q, *J* = 4 Hz, CH, C4), 117.0 (m, CH, C5), 125.9 (q, *J* = 270 Hz, C, CF_3), 131.0 (CH, C6), 132.6 (q, *J* = 32 Hz, C, C3), 149.6 (C, C1).

***N*-[2-(piperidin-1-yl)ethyl]-4-(trifluromethyl)aniline hydrochloride, 9j**. Following the general procedure A, 4-trifluoromethylaniline (2.5 mL, 20 mmol), 1-(2-chloroethyl)piperidine hydrochloride (1.83 g, 10 mmol), K_2CO_3 (2.76 g, 20 mmol) and KI (166 mg, 1 mmol) in dry DMF (4 mL) were mixed to obtain a brown oil (3.69 g). After column chromatography, the product was obtained as a yellow oil (437 mg, 16% yield) that formed its hydrochloride salt as a white solid (421 mg), mp= 206-207 ºC. IR (ATR) ν: 634, 808, 836, 953, 970, 1007, 1073, 1096, 1121, 1158, 1195, 1267, 1321, 1461, 1492, 1538, 1615, 2547, 2639, 2930, 3261 cm^{-1}. ^{1}H-NMR (400 MHz, CD_3OD) δ: 1.45-1.1.63 (complex signal, 2 H, 11-H_2), 1.78-2.00 [complex signal, 4 H, 10(12)-H_2],

3.02 [td, J = 12.4 Hz, J' = 3.2 Hz, 2 H, 9(13)-H_{ax}], 3.33 (t, J = 6.4 Hz, 2 H, 8-H_2), 3.59 [m, 2 H, 9(13)-H_{eq}], 3.62 (t, J = 6.4 Hz, 2 H, 7-H_2), 6.79 [d, J = 8.8 Hz, 2 H, 2(6)-H], 7.41 [d, J = 8.8 Hz, 2 H, 3(5)-H]. ^{13}C-NMR (100.5 MHz, CD_3OD) δ: 22.6 (CH_2, C11), 24.1 [CH_2, C10(12)], 38.8 (CH_2, C7), 54.6 [CH_2, C9(13)], 56.6 (CH_2, C8), 113.2 [CH, C2(6)], 120.0 (q, J = 32 Hz, C, C4), 126.5 (q, J = 269 Hz, C, CF_3), 127.6 [q, J = 4 Hz, CH, C3(5)], 150.5 (C, C1).

***N*-[2-(piperidin-1-yl)ethyl]-2-(trifluromethyl)aniline hydrochloride, 9k**. Following the general procedure A, 2-trifluoromethylaniline (2.51 mL, 20 mmol), 1-(2-chloroethyl)piperidine hydrochloride (1.83 g, 10 mmol), K_2CO_3 (2.76 g, 20 mmol) and KI (166 mg, 1 mmol) in dry DMF (4 mL) were mixed to obtain a brown oil (3.65 g). After column chromatography, the product was obtained as a yellowish oil (972 mg, 36% yield) that formed its hydrochloride salt as a white solid (787 mg), mp = 165-166 ºC. IR (ATR) ν: 648, 753, 762 856, 899, 950, 964, 1007, 1030, 1053, 1090, 1107, 1127, 1158, 1224, 1258, 1281, 1304, 1335, 1404, 1452, 1478, 1520, 1583, 1609, 2405, 2496, 2519, 2610, 2947, 3341 cm^{-1}. ^{1}H-NMR (400 MHz, CD_3OD) δ: 1.46-1.60 (complex signal, 1 H, 11-H_{ax}), 1.76-2.00 [complex signal, 5 H, 10(12)-H_2 and 11-H_{eq}], 3.05 [td, J = 12.0 Hz, J' = 2.8 Hz, 2 H, 9(13)-H_{ax}], 3.34 (t, J = 6.6 Hz, 2 H, 8-H_2), 3.62 (dm, J = 11.6 Hz, 2 H, 9(13)-H_{eq}), 3.75 (t, J = 6.4 Hz, 2 H, 7-H_2), 6.81 (t, J = 7.6 Hz, 1 H, 4-H), 6.98 (d, J = 8.4 Hz, 1 H, 6-H), 7.42-7.50 (complex signal, 2 H, 3-H and 5-H). ^{13}C-NMR (100.5 MHz, CD_3OD) δ: 22.6 (CH_2, C11), 24.2 [CH_2, C10(12)], 39.1 (CH_2, C7), 54.9 [CH_2, C9(13)], 56.3 (CH_2, C8), 113.2 (CH, C6), 115.3 (q, J = 29.1 Hz, C, C2), 117.9 (CH, C4), 126.4 (q, J = 271 Hz, C, CF_3), 127.8 (m, CH, C3), 134.7 (CH, C5), 145.8 (C, C1).

3,5-dichloro-*N*-[2-(piperidin-1-yl)ethyl]aniline hydrochloride, 9l. Following the general procedure A, 3,5-dichloroaniline (1.62 g, 10 mmol), 1-(2-chloroethyl)piperidine

hydrochloride (0.92 g, 5 mmol), K_2CO_3 (1.38 g, 10 mmol) and KI (83 mg, 0.5 mmol) in dry DMF (2 mL) were mixed to obtain a dark oil (1.67 g). After column chromatography, the product was obtained as a brown oil (465 mg, 34 % yield) that formed its hydrochloride salt as a brown solid (527 mg), mp = 195-196 ºC. IR (ATR) ν: 677, 771, 799, 854, 895, 930, 953, 973, 1016, 1077, 1102, 1130, 1168, 1246, 1319, 1365, 1383, 1426, 1443, 1469, 1524, 1565, 1590, 2040, 2162, 2546, 2632, 2850, 2951, 3265 cm^{-1}. ^{1}H-NMR (400 MHz, CD_3OD) δ: 1.54 (m, 1 H, 11-H_{ax}), 1.78-1.99 [complex signal, 5 H, 11-H_{eq} and 10(12)-H_2], 3.01 [td, J = 12.0 Hz, J' = 4.0 Hz, 2 H, 9(13)-H_{ax}], 3.32 (t, J = 6.4 Hz, 2 H, 8-H_2), 3.57 (t, J = 6.4 Hz, 2 H, 7-H_2), 3.60 [m, 2 H, 9(13)-H_{eq}], 6.68-6.71 (complex signal, 3 H, Ar-H). ^{13}C-NMR (100.5 MHz, CD_3OD) δ: 22.6 (CH_2, C11), 24.1 [CH_2, C10(12)], 39.1 (CH_2, C7), 54.6 [CH_2, C9(13)], 56.4 (CH_2, C8), 112.4 [CH, C2(6)], 118.2 (CH, C4), 136.7 [C, C3(5)], 150.8 (C, C1). HRMS-ESI+ m/z $[M+H]^+$ calcd for $[C_{13}H_{18}Cl_2N_2+H]^+$: 273.0920, found: 273.0917.

3,5-difluoro-*N*-[2-(piperidin-1-yl)ethyl]aniline hydrochloride, 9m. A mixture of 3,5-difluroroaniline (2.58 g, 20 mmol), 1-(2-chloroethyl)piperidine hydrochloride (1.84 g, 10 mmol), NaH (0.72 g, 30 mmol) and KI (166 mg, 1 mmol) in dry DMF (4 mL) were stirred under N_2 atmosphere at 90 ºC for 24 hours. The mixture was allowed to reach room temperature, poured into ice and extracted with DCM (3 x 10 mL). The combined organics were dried over anh. Na_2SO_4, filtered and concentrated *in vacuo* to obtain a dark oil (2.66 g). After column chromatography, the product was obtained as a yellowish oil (232 mg, 11% yield) that formed its hydrochloride salt as a yellowish solid (250 mg), mp = 173-174 ºC. IR (ATR) ν: 670, 776, 801, 842, 882, 945, 960, 978, 993, 1039, 1084, 1107, 1132, 1180, 1201, 1216, 1239, 1307, 1327, 1362, 1385, 1426, 1443, 1469, 1512, 1542, 1618, 2470, 2546, 2668, 2946, 3032, 3225 cm^{-1}. ^{1}H-NMR (400 MHz, CD_3OD) δ: 1.54 (m, 1 H, 11-H_{ax}), 1.78-1.99 [complex signal, 5 H, 11-H_{eq} and 10(12)-

H_2], 3.02 [td, *J* = 12.0 Hz, *J'* = 3.2 Hz, 2 H, 9(13)-H_{ax}], 3.32 (t, *J* = 6.4 Hz, 2 H, 8-H_2), 3.54-3.62 (complex signal, 2 H, 9(13)-H_{eq}), 3.58 (t, *J* = 6.4 Hz, 2 H, 7-H_2), 6.20 (m, 1 H, 4-H), 6.33 [m, 2 H, 2(6)-H]. ^{13}C-NMR (100.5 MHz, CD_3OD) δ: 22.6 (CH_2, C11), 24.1 [CH_2, C10(12)], 39.3 (CH_2, C7), 54.7 [CH_2, C9(13)], 56.4 (CH_2, C8), 93.5 (t, *J* = 27 Hz, CH, C4), 97.0 [m, CH, C2(6)], 151.3 (m, C, C1), 165.7 [dd, *J* = 243 Hz, *J'* = 16 Hz, C, C3(5)]. HRMS-ESI+ m/z [*M*+H]$^+$ calcd for [$C_{13}H_{18}F_2N_2$+H]$^+$: 241.1511, found: 241.1514.

***N*-[2-(piperidin-1-yl)ethyl]-3,5-bis(trifluoromethyl)aniline hydrochloride, 9n**. Following the general procedure A, 3,5-bis(trifluoromethyl)aniline (1.55 mL, 10 mmol), 1-(2-chloroethyl)piperidine hydrochloride (0.92 g, 5 mmol), K_2CO_3 (1.38 g, 10 mmol) and KI (83 mg, 0.5 mmol) in dry DMF (2 mL) were mixed to obtain a dark oil (2.20 g). After column chromatography, the product was obtained as a brown oil (515 mg, 30% yield) that formed its hydrochloride salt as a brown solid (175 mg), mp = 162-163 ºC. IR (ATR) ν: 680, 700, 730, 854, 882, 968, 991, 1011, 1122, 1165, 1178, 1274, 1317, 1362, 1383, 1405, 1433, 1471, 1562, 1615, 2536, 2622, 2860, 2941, 3093, 3265 cm^{-1}. ^{1}H-NMR (400 MHz, CD_3OD) δ: 1.55 (m, 1 H, 11-H_{ax}), 1.76-2.00 [complex signal, 5 H, 11-H_{eq} and 10(12)-H_2], 3.04 [td, *J* = 12.2 Hz, *J'* = 3.2 Hz, 2 H, 9(13)-H_{ax}], 3.36 (t, *J* = 6.4 Hz, 2 H, 8-H_2), 3.61 [dm, *J* = 12.2 Hz, 2 H, 9(13)-H_{eq}], 3.66 (t, *J* = 6.4 Hz, 2 H, 7-H_2), 7.15 (m, 1 H, 4-H), 7.18 [m, 2 H, 2(6)-H]. ^{13}C-NMR (100.5 MHz, CD_3OD) δ: 22.6 (CH_2, C11), 24.1 [CH_2, C10(12)], 38.8 (CH_2, C7), 54.7 [CH_2, C9(13)], 56.5 (CH_2, C8), 110.7 (sept, *J* = 4 Hz, CH, C4), 113.2 [m, CH, C2(6)], 125.1 (q, *J* = 271.5 Hz, C, CF_3), 133.6 [q, *J* = 32.5 Hz, C, C3(5)], 150.5 (C, C1). HRMS-ESI+ m/z [*M*+H]$^+$ calcd for [$C_{15}H_{18}F_6N_2$+H]$^+$: 341.1447, found: 341.1449.

3-chloro-*N*-[2-(piperidin-1-yl)ethyl]-5-(trifluoromethyl)aniline hydrochloride, 9o. Following the general procedure A, 3-chloro-5-trifluoromethylaniline (1.38 mL, 10

mmol), 1-(2-chloroethyl)piperidine hydrochloride (0.92 g, 5 mmol), K_2CO_3 (1.38 g, 10 mmol) and KI (83 mg, 0.5 mmol) in dry DMF (2 mL) were mixed to obtain a dark oil (2.02 g). After column chromatography, the product was obtained as a brown oil (320 mg, 21% yield) that formed its hydrochloride salt as a brown solid (327 mg), mp = 191-192 ºC. IR (ATR) ν: 690, 703, 824, 837, 900, 971, 988, 1014, 1097, 1120, 1165, 1236, 1259, 1279, 1302, 1347, 1428, 1464, 1595, 1605, 2541, 2632, 2946, 3088, 3270 cm^{-1}. ^{1}H-NMR (400 MHz, CD_3OD) δ: 1.56 (m, 1 H, 11-H_{ax}), 1.72-2.04 [complex signal, 5 H, 11-H_{eq} and 10(12)-H_2], 3.02 [m, 2 H, 9(13)-H_{ax}], 3.33 (t, J = 6.4 Hz, 2 H, 8-H_2), 3.50-3.70 [very broad signal, 2 H, 9(13)-H_{eq}], 3.60 (t, J = 6.4 Hz, 2 H, 7-H_2), 6.88 (complex signal, 2 H, 4-H and 6-H), 6.94 (m, 1 H, 2-H). ^{13}C-NMR (100.5 MHz, CD_3OD) δ: 22.6 (CH_2, C11), 24.1 [CH_2, C10(12)], 38.9 (CH_2, C7), 54.7 [CH_2, C9(13)], 56.5 (CH_2, C8), 109.0 (q, J = 3.8 Hz, CH, C6), 114.4 (q, J = 4.0 Hz, CH, C4), 116.2 (CH, C2), 125.0 (q, J = 272.0 Hz, C, CF_3), 133.9 (q, J = 32.5 Hz, C, C5), 136.9 (C, C3), 150.9 (C, C1). HRMS-ESI+ m/z $[M+H]^+$ calcd for $[C_{14}H_{18}ClF_3N_2+H]^+$: 307.1183, found: 307.1176.

3-chloro-5-fluoro-*N*-[2-(piperidin-1-yl)ethyl]aniline hydrochloride, 9p. Following the general procedure A, 3-chloro-5-fluoroaniline (0.54 mL, 5 mmol), 1-(2-chloroethyl)piperidine hydrochloride (0.46 g, 2.5 mmol), K_2CO_3 (691 mg, 5 mmol) and KI (42 mg, 0.25 mmol) in dry DMF (2 mL) were mixed to obtain a dark oil (1.10 g). After column chromatography, the product was obtained as a yellow oil (210 mg, 33% yield) that formed its hydrochloride salt as a white solid (199 mg), mp = 194-195 ºC. IR (ATR) ν: 670, 776, 804, 849, 885, 938, 963, 981, 1001, 1036, 1079, 1110, 1135, 1170, 1198, 1218, 1246, 1269, 1319, 1360, 1385, 1426, 1451, 1476, 1509, 1534, 1603, 2359, 2546, 2587, 2632, 2951, 3012, 3048, 3255 cm^{-1}. ^{1}H-NMR (400 MHz, CD_3OD) δ: 1.54 (m, 1 H, 11-H_{ax}), 1.78-1.99 [complex signal, 5 H, 11-H_{eq} and 10(12)-H_2], 3.02 [td, J = 12.0 Hz, J' = 3.6 Hz, 2 H, 9(13)-H_{ax}], 3.32 (t, J = 6.2 Hz, 2 H, 8-H_2), 3.52-3.62

[complex signal, 2 H, 9(13)-H_{eq}], 3.58 (t, *J* = 6.2 Hz, 2 H, 7-H_2), 6.44 [complex signal, 2 H, 2-H and 6-H], 6.58 (m, 1 H, 4-H). ^{13}C-NMR (100.5 MHz, CD_3OD) δ: 22.6 (CH_2, C11), 24.1 [CH_2, C10(12)], 39.2 (CH_2, C7), 54.6 [CH_2, C9(13)], 56.4 (CH_2, C8), 99.3 (d, *J* = 26 Hz, CH, C6), 105.8 (d, *J* = 26 Hz, CH, C4), 110.2 (d, *J* = 3 Hz, CH, C2), 136.7 (d, *J* = 14 Hz, C, C3), 151.2 (d, *J* = 12 Hz, C, C1), 165.3 (d, *J* = 244 Hz, C, C5). HRMS-ESI+ m/z $[M+H]^+$ calcd for $[C_{13}H_{18}ClFN_2+H]^+$: 257.1215, found: 257.1218.

3-fluoro-*N*-[2-(piperidin-1-yl)ethyl]-5-(trifluoromethyl)aniline hydrochloride, 9q. Following the general procedure A, 3-fluoro-5-trifluoromethylaniline (0.64 mL, 5 mmol), 1-(2-chloroethyl)piperidine hydrochloride (460 mg, 2.5 mmol), K_2CO_3 (691 mg, 5 mmol) and KI (42 mg, 0.25 mmol) in dry DMF (2 mL) were mixed to obtain a brown oil (1.10 g). After column chromatography, the product was obtained as a yellow oil (71 mg, 10% yield) that formed its hydrochloride salt as a white solid (38 mg), mp = 193-194 ºC. IR (ATR) ν: 698, 720, 806, 829, 857, 887, 917, 948, 963, 988, 1011, 1082, 1100, 1122, 1165, 1203, 1211, 1264, 1307, 1332, 1362, 1378, 1453, 1481, 1529, 1603, 1623, 1651, 2354, 2556, 2637, 2936, 3255 cm^{-1}. ^{1}H-NMR (400 MHz, CD_3OD) δ: 1.54 (m, 1 H, 11-H_{ax}), 1.78-2.00 [complex signal, 5 H, 11-H_{eq} and 10(12)-H_2], 3.02 [td, *J* = 12.4 Hz, *J'* = 3.2 Hz, 2 H, 9(13)-H_{ax}], 3.33 (t, *J* = 6.4 Hz, 2 H, 8-H_2), 3.56-3.64 [complex signal, 2 H, 9(13)-H_{eq}], 3.60 (t, *J* = 6.4 Hz, 2 H, 7-H_2), 6.64 (dm, *J* = 8.4 Hz, 1 H, 4-H), 6.68 (dt, *J* = 11.6, *J'* = 2.4 Hz, 1 H, 2-H), 6.78 (m, 1 H, 6-H). ^{13}C-NMR (125.7 MHz, CD_3OD) δ: 22.6 (CH_2, C11), 24.1 [CH_2, C10(12)], 38.9 (CH_2, C7), 54.7 [CH_2, C9(13)], 56.5 (CH_2, C8), 101.5 (dq, *J* = 25.6 Hz, J'=3.8 Hz, CH, C4), 103.0 (d, *J* = 25.7 Hz, CH, C2), 106.8 (m, CH, C6), 125.0 (dq, *J* = 2.4 Hz, *J'* = 271.3 Hz, C, $\underline{C}F_3$), 134.1 (dq, *J* = 10.6 Hz, *J'* = 32.6 Hz, C, C5), 151.7 (d, *J* = 11.2 Hz, C, C1), 165.4 (d, *J* = 243.5 Hz, C, C3). HRMS-ESI+ m/z $[M+H]^+$ calcd for $[C_{14}H_{18}ClF_4N_2+H]^+$: 291.1479, found: 291.1488.

***N*-[2-(azepan-1-yl)ethyl]-2-(trifluoromethyl)aniline hydrochloride, 10a**. Following the general procedure A, 2-(trifluoromethyl)aniline (1.26 mL, 10 mmol), 1-(2-chloroethyl)azepane hydrochloride (0.99 g, 5 mmol), K_2CO_3 (1.38 g, 10 mmol) and KI (83 mg, 0.5 mmol) in dry DMF (2.5 mL) were mixed to obtain a brown oil (1.86 g). After column chromatography, the product was obtained as an orange oil (351 mg, 22% yield) that formed its hydrochloride salt as a yellow solid (376 mg), mp = 138-139 ºC. IR (ATR) ν: 646, 742, 801, 855, 938, 1031, 1093, 1132, 1165, 1240, 1258, 1292, 1336, 1470, 1522, 1581, 1612, 2625, 2935, 3359 cm^{-1}. ^{1}H-NMR (400 MHz, CD_3OD) δ: 1.76-1.84 [complex signal, 4 H, 11(12)-H_2], 1.86-2.04 [complex signal, 4 H, 10(13)-H_2], 3.30 [m, 2 H, 9(14)-H_a], 3.39 (t, *J* = 6.8 Hz, 2 H, 8-H_2), 3.54 (m, 2 H, 9(13)-H_b), 3.73 (t, *J* = 6.8 Hz, 2 H, 7-H_2), 6.81 (tt, *J* = 7.2 Hz, *J'* = 0.8 Hz, 1 H, Ar), 6.96 (d, J = 8.8 Hz, 1 H, 6-H), 7.42-7.50 (complex signal, 2 H, Ar). ^{13}C-NMR (100.5 MHz, CD_3OD) δ: 24.7 [CH_2, C11(12)], 27.3 [CH_2, C10(13)], 39.4 (CH_2, C7), 56.5 [CH_2, C9(14)], 56.7 (CH_2, C8), 113.3 (CH, C6), 115.7 (q, *J* = 29.5 Hz, C, C2), 118.1 (CH, C4), 126.4 (q, *J* = 260 Hz, C, CF_3), 127.8 (q, *J* = 5.5 Hz, CH, C3), 134.7 (CH, C5), 145.9 (C, C1). HRMS-ESI+ m/z $[M+H]^+$ calcd for $[C_{15}H_{21}F_3N_2+H]^+$: 287.1730, found: 287.1739.

***N*-[2-(azepan-1-yl)ethyl]-2-ethylaniline hydrochloride, 10b**. Following general procedure B, 2-ethylaniline (0.92 mL, 7.5 mmol) and 1-(2-chloroethyl)azepane hydrochloride (0.99 g, 5 mmol) were mixed to obtain a yellow oil (665 mg). After column chromatography (Hexane/Ethyl acetate mixture), the product was obtained as a yellow oil (541 mg, 38% yield) that formed its hydrochloride salt as a white solid (615 mg), mp = 156-157 ºC. IR (ATR) ν: 654, 705, 718, 770, 793, 876, 915, 948, 990, 1015, 1101, 1271, 1315, 1449, 1485, 1594, 2423, 2459, 2583, 2620, 2857, 2930, 3167, 3240 cm^{-1}. ^{1}H-NMR (400 MHz, CD_3OD) δ: 1.33 (t, *J* = 7.6 Hz, 3 H, $CH_2C\underline{H}_3$), 1.66-1.86 [complex signal, 4 H, 10(13)-H_2], 1.92-2.06 [complex signal, 4 H, 11(12)-H_2], 2.83 (q, *J*

= 7.6 Hz, 2 H, C$\underline{H}_2$CH$_3$), 3.30 [m, 2 H, 9(14)-H$_a$], 3.54-3.64 [complex signal, 2 H, 9(14)-H$_b$], 3.69 (t, *J* = 6.8 Hz, 2 H, 8-H$_2$), 3.89 (t, *J* = 6.8 Hz, 2 H, 7-H$_2$), 7.33-7.40 (complex signal, 2 H, Ar), 7.44 (m, 1 H, Ar), 7.49 (m, 1 H, Ar). ^{13}C-NMR (100.5 MHz, CD$_3$OD) δ: 14.9 (CH$_3$, CH$_2\underline{C}$H$_3$), 24.2 (CH$_2$, $\underline{C}$H$_2$CH$_3$), 24.9 [CH$_2$, C11(12)], 27.2 [CH$_2$, C10(13)], 45.8 (CH$_2$, C7), 54.5 (CH$_2$, C8), 56.7 [CH$_2$, C9(14)], 121.9 (CH, Ar), 128.8 (CH, Ar), 129.3 (CH, Ar), 131.4 (C, Ar), 136.1 (C, C2), 137.3 (C, C1). HRMS-ESI+ m/z [*M*+H]$^+$ calcd for [C$_{16}$H$_{26}$N$_2$+H]$^+$: 247.2169, found: 247.2176.

***N*-[2-(azepan-1-yl)ethyl]-2-isopropylaniline hydrochloride, 10c**. Following general procedure B, 2-isopropylaniline (1.42 mL, 10 mmol) and 1-(2-chloroethyl)azepane hydrochloride (0.99 g, 5 mmol) were mixed to obtain a brown oil (1.52 g). After column chromatography (Hexane/Ethyl acetate mixture), the product was obtained as a brown oil (680 mg, 46% yield) that formed its hydrochloride salt as a dark green solid (742 mg), mp = 155-156 ºC. IR (ATR) ν: 618, 757, 873, 917, 951, 1044, 1181, 1312, 1364, 1442, 1452, 1573, 1635, 1997, 2149, 2196, 2361, 2496, 2594, 2863, 2925, 3193, 3312, 3374, 3447, 3509 cm^{-1}. ^{1}H-NMR (400 MHz, CD$_3$OD) δ: 1.33 [d, *J* = 6.8 Hz, 6 H, -CH(C$\underline{H}_3$)$_2$], 1.64-1.90 [complex signal, 4 H, 11(12)-H$_2$], 1.94-2.06 [complex signal, 4 H, 10(13)-H$_2$], 3.23 [sept, *J* = 6.8 Hz, 1 H, -C$\underline{H}$(CH$_3$)$_2$], 3.33 [m, 2 H, 9(14)-H$_a$], 3.60 [m, 2 H, 9(14)-H$_b$], 3.70 (t, *J* = 6.8 Hz, 2 H, 8-H$_2$), 3.86 (t, *J* = 6.8 Hz, 2 H, 7-H$_2$), 7.35 (dt, *J* = 7.8 Hz, *J'* = 1.6 Hz, 1 H), 7.40 (dt, J = 7.8 Hz, J' = 1.2 Hz, 1 H), 7.48 (dd, *J* = 7.8 Hz, *J'* = 1.2 Hz, 1 H), 7.53 (dd, *J* = 7.8 Hz, *J'* = 1.6 Hz, 1 H) (Ar-H). ^{13}C-NMR (100.5 MHz, CD$_3$OD) δ: 24.4 [CH$_3$, -CH($\underline{C}$H$_3$)$_2$], 24.9 [CH$_2$, C11(12)], 27.2 [CH$_2$, C10(12)], 28.7 [CH, -$\underline{C}$H(CH$_3$)$_2$], 46.4 (CH$_2$, C7), 54.5 (CH$_2$, C8), 56.7 [CH$_2$, C9(14)], 122.1 (CH), 128.8 (CH), 129.1 (CH) and 129.7 (CH) (4 CH-Ar), 135.1 (C, C2), 142.3 (C, C1). HRMS-ESI+ m/z [*M*+H]$^+$ calcd for [C$_{17}$H$_{28}$N$_2$+H]$^+$: 261.2325, found: 261.2334.

2-isopropyl-*N*-[3-(piperidin-1-yl)propyl]aniline hydrochloride, 11. Following the general procedure A, 2-isopropylaniline (0.70 mL, 5 mmol), 1-(3-chloropropyl)piperidine hydrochloride (0.49 g, 2.5 mmol), K_2CO_3 (0.69 g, 5 mmol) and KI (42 mg, 0.25 mmol) in dry DMF (2 mL) were mixed to obtain a dark oil (1.65 g). After column chromatography, **11** was obtained as a grey oil (106 mg, 16% yield) that formed its hydrochloride salt as a grey solid (95 mg), mp = 220-221 ºC. IR (ATR) ν: 720, 773, 801, 854, 877, 945, 855, 963, 1014, 1029, 1077, 1092, 1168, 1213, 1228, 1259, 1282, 1302, 1322, 1360, 1383, 1410, 1443, 1466, 1499, 1582, 1595, 2354, 2405, 2501, 2612, 2643, 2668, 2881, 2946 cm^{-1}. ^{1}H-NMR (400 MHz, CD_3OD) δ: 1.35 [d, *J* = 6.8 Hz, 6 H, -CH(C$\underline{H}_3$)$_2$], 1.53 (m, 1 H, 12-H_{ax}), 1.78-2.02 [complex signal, 5 H, 12-H_{eq} and 11(13)-H_2], 2.35 (m, 2 H, 8-H_2), 2.99 [td, *J* = 12.4 Hz, *J'* = 3.2 Hz, 2 H, 10(14)-H_{ax}], 3.18 [sept, *J* = 6.8 Hz, 1 H, -C$\underline{H}$(CH$_3$)$_2$], 3.26 (t, *J* = 8.0 Hz, 2 H, 9-H_2), 3.47 (t, *J* = 8.0 Hz, 2 H, 7-H_2), 3.57 [m, 2 H, 10(14)-H_{eq}], 7.39 (m, 1 H, Ar), 7.49-7.56 (complex signal, 2 H, Ar), 7.60 (dd, *J* = 8.0 Hz, *J'* = 1.6 Hz, 1 H, Ar). ^{13}C-NMR (100.5 MHz, CD_3OD) δ: 22.2 (CH_2, C12), 22.6 (CH_2, C8), 24.2 (CH_3, -CH(C$\underline{H}_3$)$_2$], 24.6 [CH_2, C11(13)], 28.8 [CH, -C$\underline{H}$(CH$_3$)$_2$], 50.6 (CH_2, C7), 54.6 [CH_2, C10(14)], 54.8 (CH_2, C9), 124.4 (CH, C6), 128.9 (CH, C4), 129.6 (CH, C5), 131.6 (CH, C3), 133.3 (C, C2), 143.7 (C, C1). HRMS-ESI+ m/z [*M*+H]$^+$ calcd for [$C_{17}H_{28}N_2$+H]$^+$: 261.2325, found: 261.2330.

2-isopropyl-*N*-[2-(pyrrolidin-1-yl)ethyl]aniline hydrochloride, 12. Following the general procedure A, 2-isopropylaniline (1.41 mL, 10 mmol), 1-(2-chloroethyl)pyrrolidine hydrochloride (0.85 g, 5 mmol), K_2CO_3 (1.38 g, 10 mmol) and KI (83 mg, 0.5 mmol) in dry DMF (2 mL) were mixed to obtain a dark oil (1.88 g). After column chromatography, the product was obtained as a brown oil (307 mg, 26% yield) that formed its hydrochloride salt as a brown solid (380 mg), mp = 160-161 ºC.

IR (ATR) ν: 758, 806, 864, 910, 928, 960, 1008, 1034, 1067, 1082, 1115, 1183, 1218, 1287, 1314, 1362, 1385, 1423, 1451, 1494, 1537, 1585, 1598, 2389, 2475, 2592, 2683, 2860, 2967, 3291 cm^{-1}. ^{1}H-NMR (400 MHz, CD_3OD) δ: 1.33 [d, *J* = 6.8 Hz, 6 H, -CH(C$\underline{H}_3$)$_2$], 2.00-2.28 [complex signal, 4 H, 10(11)-H_2], 3.12-3.28 [complex signal, 2 H, 9(13)-H_a], 3.22 [sept, *J* = 6.8 Hz, 1 H, -C$\underline{H}$(CH$_3$)$_2$], 3.70-3.86 (complex signal, 6 H, 9(13)-H_b, 8-H_2 and 7-H_2), 7.31-7.42 (complex signal, 2 H, 4-H and 5-H), 7.44 (dd, *J* = 8 Hz, *J'* = 1.6 Hz, 1 H, 6-H), 7.53 (m, 1 H, 3-H). ^{13}C-NMR (100.5 MHz, CD_3OD) δ: 24.0 [CH_3, -CH(C$\underline{H}_3$)$_2$], 24.3 [CH_2, C10(11)], 28.7 [CH, -C$\underline{H}$(CH$_3$)$_2$], 47.0 (CH_2, C7), 51.8 (CH_2, C8), 55.6 [CH_2, C9(12)], 121.8 (CH, C6), 128.7 (CH, C4), 129.0 (CH, C5), 129.4 (CH, C3), 135.3 (C, C2), 142.1 (C, C1). HRMS-ESI+ m/z [*M*+H]$^+$ calcd for [$C_{15}H_{24}N_2$+H]$^+$: 233.2012, found: 233.2008.

1-(2-phenoxyethyl)piperidine hydrochloride, 13a.[54] Following general procedure C, from phenol (0.94 g, 10 mmol) and 1-(2-chloroethyl)piperidine hydrochloride (1.83 g, 10 mmol), an orange oil (1.85 g) was obtained. Column chromatography (Hexane/Ethyl acetate mixture) gave the product as a yellow oil (1.43 g, 70% yield) that formed its hydrochloride salt as a yellowish solid (915 mg). The analytical sample was obtained by crystallization with EtOAc/Pentane, mp = 170-171 ºC. IR (ATR) ν: 691, 765, 791, 816, 845, 890, 913, 939, 953, 1002, 1016, 1027, 1087, 1153, 1175, 1227, 1290, 1386, 1412, 1432, 1452, 1472, 1489, 1586, 1595, 2490, 2610, 2856, 2941 cm^{-1}. ^{1}H-NMR (400 MHz, CD_3OD) δ: 1.60-1.80 (complex signal, 2 H, 11-H_2), 1.82-1.98 [complex signal, 4 H, 10(12)-H_2], 3.15-3.50 [complex signal, 4 H, 9(13)-H_2], 3.55 (t, *J* = 4.8 Hz, 2 H, 8-H_2), 4.38 (t, *J* = 4.8 Hz, 2 H, 7-H_2), 6.97-7.06 (complex signal, 3 H, 2(6)-H and 4-H), 7.32 [m, 2 H, 3(5)-H]. ^{13}C-NMR (100.5 MHz, CD_3OD) δ: 22.6 (CH_2, C11), 24.1 [CH_2, C10(12)], 54.9 [CH_2, C9(13)], 57.2 (CH_2, C8), 63.1 (CH_2, C7), 115.7 [CH, C2(6)], 122.9 (CH, C4), 130.7 [CH, C3(5)], 159.2 (C, C1).

1-[2-(4-chlorophenoxy)ethyl]piperidine hydrochloride, 13b. Following general procedure C, from 4-chlorophenol (1.29 g, 10 mmol) and 1-(2-chloroethyl)piperidine hydrochloride (1.83 g, 10 mmol), an orange oil (2.13 g) was obtained. Column chromatography (Hexane/Ethyl acetate mixture) gave the product as a yellow oil (1.40 g, 59% yield) that formed its hydrochloride salt as a white solid (1.40 g), mp = 199-200 ºC. IR (ATR) ν: 668, 802, 816, 828, 953, 967, 1007, 1039, 1070, 1093, 1175, 1244, 1284, 1386, 1429, 1458, 1472, 1489, 1578, 1597, 2513, 2622, 2941 cm^{-1}. ^{1}H-NMR (400 MHz, CD_3OD) δ: 1.50-1.60 (complex signal, 2 H, 11-H_2), 1.81-2.05 [complex signal, 4 H, 10(12)-H_2], 2.85-3.80 [complex signal, 4 H, 9(13)-H_2], 3.56 (t, *J* = 4.8 Hz, 2 H, 8-H_2), 4.37 (t, *J* = 4.8 Hz, 2 H, 7-H_2), 7.01 [m, 2 H, 3(5)-H], 7.31 [m, 2 H, 2(6)-H]. ^{13}C-NMR (100.5 MHz, CD_3OD) δ: 22.6 (CH_2, C11), 24.1 [CH_2, C10(12)], 54.9 [CH_2, C9(13)], 57.1 (CH_2, C8), 63.5 (CH_2, C7), 117.3 [CH, C2(6)], 127.8 (C, C4), 130.6 [CH, C3(5)], 157.9 (C, C1).

1-[2-(2-ethylphenoxy)ethyl]piperidine hydrochloride, 13c.[55] Following general procedure C, from 2-ethylphenol (1.18 mL, 10 mmol) and 1-(2-chloroethyl)piperidine hydrochloride (1.83 g, 10 mmol), an orange oil (2.20 g) was obtained. Column chromatography (Hexane/Ethyl acetate mixture) gave the product as a yellow oil (1.42 g, 61% yield) that formed its hydrochloride salt as a white solid (1.18 g), mp = 136-137 ºC. IR (ATR) ν: 614, 734, 751, 810, 868, 905, 927, 947, 967, 996, 1013, 1053, 1061, 1096, 1127, 1190, 1235, 1295, 1332, 1398, 1426, 1452, 1478, 1495, 1600, 2473, 2507, 2861, 2941 cm^{-1}. ^{1}H-NMR (400 MHz, CD_3OD) δ: 1.20 (t, *J* = 7.6 Hz, 3 H, $CH_2C\underline{H}_3$), 1.56-1.82 (complex signal, 2 H, 11-H_2), 1.84-2.02 [complex signal, 4 H, 10(12)-H_2], 2.68 (q, *J* = 7.6 Hz, 2 H, $C\underline{H}_2CH_3$), 3.00-3.85 [complex signal, 4 H, 9(13)-H_2], 3.60 (t, *J* = 4.8 Hz, 2 H, 8-H_2), 4.40 (t, *J* = 4.8 Hz, 2 H, 7-H_2), 6.92-7.00 (complex signal, 2 H, Ar-H), 7.15-7.22 (complex signal, 2 H, Ar-H). ^{13}C-NMR (100.5 MHz, CD_3OD) δ: 15.0

(CH_3, $CH_2\underline{C}H_3$), 22.5 (CH_2, C11), 24.1 (CH_2, $\underline{C}H_2CH_3$), 24.2 [CH_2, C10(12)], 55.3 [CH_2, C9(13)], 57.5 (CH_2, C8), 64.0 (CH_2, C7), 112.7 (CH, C6), 122.9 (CH, C4), 128.2 (CH, C5), 130.3 (CH, C3), 133.7 (C, C2), 156.8 (C, C1).

1-[2-(2-isopropylphenoxy)ethyl]piperidine hydrochloride, 13d. Following general procedure C, from 2-isopropylphenol (0.67 mL, 5 mmol) and 1-(2-chloroethyl)piperidine hydrochloride (0.91 g, 5 mmol), a yellow oil (1.41 g) was obtained. Column chromatography (Hexane/Ethyl acetate mixture) gave the product as a yellow oil (0.70 g, 57% yield) that formed its hydrochloride salt as a white solid (793 mg), mp = 176-177 ºC. IR (ATR) ν: 744, 822, 855, 930, 969, 1010, 1044, 1080, 1111, 1155, 1196, 1240, 1292, 1343, 1356, 1444, 1493, 1597, 2475, 2604, 2956 cm^{-1}. ^{1}H-NMR (400 MHz, CD_3OD) δ: 1.22 [d, *J* = 6.8 Hz, 6 H, $CH(C\underline{H}_3)_2$], 1.45-2.10 [complex signal, 6 H, 11-H_2 and 10(12)-H_2], 3.16 [m, 2 H, 9(13)-H_{ax}], 3.38 [sept, *J* = 6.8, 1 H, $C\underline{H}(CH_3)_2$], 3.56-3.80 [complex signal, 2H, 9(13)-H_{eq}], 3.61 (t, J = 4.8 Hz, 2 H, 8-H_2), 4.40 (t, *J* = 4.8 Hz, 2 H, 7-H_2), 6.95-7.02 (complex signal, 2 H, 5-H and 6-H), 7.17 (ddd, *J* = 8.8 Hz, *J'* = 7.2 Hz, *J''* = 1.6 Hz, 1 H, 4-H), 7.25 (dd, *J* = 8.0 Hz, *J'* = 1.6 Hz, 1 H, 3-H). ^{13}C-NMR (100.5 MHz, CD_3OD) δ: 22.5 (CH_2, C11), 23.4 [CH_3, $CH(\underline{C}H_3)_2$], 24.2 [CH_2, C10(12)], 27.4 [CH, $\underline{C}H(CH_3)_2$], 55.2 [CH_2, C9(13)], 57.5 (CH_2, C8), 64.1 (CH_2, C7), 112.9 (CH, C6), 123.0 (CH, C4), 127.2 (CH, C5), 127.9 (CH, C3), 138.1 (C, C2), 156.1 (C, C1).

1-[2-(2-ethylphenoxy)ethyl]azepane hydrochloride, 14a.[35] Following general procedure C, from 2-ethylphenol (0.59 mL, 5 mmol) and 1-(2-chloroethyl)azepane hydrochloride (0.99 g, 5 mmol), a yellow oil (1.05 g) was obtained. Column chromatography (Hexane/Ethyl acetate mixture) gave the product as a yellow oil (0.44 g, 35% yield) that form its hydrochloride salt as a white solid (483 mg), mp = 101-102 ºC. IR (ATR) ν: 734, 749, 804, 881, 915, 951, 1023, 1054, 1067, 1126, 1160, 1186,

1232, 1289, 1395, 1449, 1475, 1491, 1594, 2527, 2594, 2863, 2930, 3410 cm^{-1}. ^{1}H-NMR (400 MHz, CD_3OD) δ: 1.20 (t, *J* = 7.6 Hz, 3 H, -$CH_2C\underline{H}_3$), 1.70-1.86 [complex signal, 4 H, 11(12)-H_2], 1.90-2.05 [complex signal, 4 H, 10(13)-H_2], 2.68 (q, *J* = 7.6 Hz, 2 H, -$C\underline{H}_2CH_3$), 3.40-3.60 [complex signal, 4 H, 9(14)-H_2], 3.67 (t, *J* = 5.2 Hz, 2H, 8-H_2), 4.40 (t, *J* = 5.2 Hz, 2 H, 7-H_2), 6.92-7.02 (complex signal, 2 H, H-Ar), 7.15-7.22 (complex signal, 2 H, H-Ar). ^{13}C-NMR (100.5 MHz, CD_3OD) δ: 14.9 (CH_3, -$CH_2\underline{C}H_3$), 24.1 (CH_2, -$\underline{C}H_2CH_3$), 24.6 [CH_2, C11(12)], 27.5 [CH_2, C10(13)], 56.9 [CH_2, C9(14)], 57.7 (CH_2, C8), 64.3 (CH_2, C7), 112.7 (CH, C6), 122.9 (CH, C4), 128.2 (CH, C5), 130.3 (CH, C3), 133.7 (C, C2), 156.8 (C, C1).

1-[2-(2-isopropylphenoxy)ethyl]azepane hydrochloride, 14b.[55] Following general procedure C, from 2-isopropylphenol (0.67 mL, 5 mmol) and 1-(2-chloroethyl)azepane hydrochloride (0.99 g, 5 mmol), a yellow oil (1.34 g) was obtained. Column chromatography (Hexane/Ethyl acetate mixture) gave the product as a yellow oil (0.34 g, 26% yield) that formed its hydrochloride salt as a white solid (316 mg), mp = 168-169 ºC. IR (ATR) ν: 742, 819, 922, 953, 1028, 1080, 1114, 1129, 1152, 1194, 1240, 1287, 1341, 1444, 1478, 1493, 1581, 1597, 2506, 2589, 2863, 2935 cm^{-1}. ^{1}H-NMR (400 MHz, CD_3OD) δ: 1.22 [d, *J* = 7.2 Hz, 6 H, -$CH(C\underline{H}_3)_2$], 1.68-1.86 [complex signal, 4 H, 11(12)-H_2], 1.88-2.04 [complex signal, 4 H, 10(13)-H_2], 3.37 [sept, *J* = 7.2 Hz, 1 H, -$C\underline{H}(CH_3)_2$], 3.43 [m, 2 H, 9(14)-H_a], 3.63 [m, 2 H, 9(14)-H_b], 3.68 (t, J = 5.2 Hz, 2 H, 8-H_2), 4.42 (t, *J* = 5.2 Hz, 2 H, 7-H_2), 6.95-7.04 (complex signal, 2 H, 5-H and 6-H), 7.17 (ddd, *J* = 8.8 Hz, *J'* = 7.6 Hz, *J''* = 1.6 Hz, 1 H, 4-H), 7.25 (dd, *J* = 8.0 Hz, *J'* = 1.6 Hz, 1 H, 3-H). ^{13}C-NMR (100.5 MHz, CD_3OD) δ: 23.4 [CH_3, -$CH(\underline{C}H_3)_2$], 24.6 [CH_2, C10(12)], 27.4 [CH, -$\underline{C}H(CH_3)_2$, and CH_2, C10(13)], 56.9 [CH_2, C9(14)], 57.7 (CH_2, C8), 64.5 (CH_2, C7), 113.0 (CH, C6), 123.1 (CH, C4), 127.2 (CH, C5), 127.9 (CH, C3), 138.2 (C, C2), 156.1 (C, C1).

1-[2-(phenylthio)ethyl]piperidine hydrochloride, 15a.[56] Following general procedure C, from thiophenol (1.0 mL, 10 mmol) and 1-(2-chloroethyl)piperidine hydrochloride (1.83 g, 10 mmol), the product was obtained as a pale yellow oil (1.94 g, 87% yield) that formed its hydrochloride salt as a white solid (821 mg). The analytical sample was obtained by crystallization from MeOH/diethyl ether, mp = 191-192 ºC. IR (ATR) ν: 690, 742, 835, 853, 897, 946, 961, 1021, 1059, 1095, 1147, 1188, 1209, 1325, 1439, 1452, 1480, 1578, 2516, 2620, 2940 cm^{-1}. ^{1}H-NMR (400 MHz, CD_3OD) δ: 1.50-1.78 (complex signal, 2 H, 11-H_2), 1.79-1.98 [complex signal, 4 H, 10(12)-H_2], 2.60-3.80 [complex signal, 8 H, 9(13)-H_2, 7-H_2 and 8-H_2], 7.27 [tt, *J* = 7.4 Hz, *J'* = 1.6 Hz, 1 H, 4-H), 7.36 [tm, *J* = 7.4 Hz, 2 H, 3(5)-H], 7.46 (m, 2 H, 2(6)-H]. ^{13}C-NMR (100.5 MHz, CD_3OD) δ: 22.6 (CH_2, C11), 24.2 [CH_2, C10(12)], 28.5 (CH_2, C7), 54.4 [CH_2, C9(13)], 57.3 (CH_2, C8), 128.4 (CH, C4), 130.5 [CH, C2(6)], 131.4 [CH, C3(5)], 135.1 (C, C1).

1-[2-((4-chlorophenyl)thio)ethyl]piperidine hydrochloride, 15b.[56] Following general procedure C, from 4-chlorothiophenol (1.45 g, 10 mmol) and 1-(2-chloroethyl)piperidine hydrochloride (1.83 g, 10 mmol), the product was obtained as a palid yellow oil (2.31 g, 91% yield) that formed its hydrochloride salt as a white solid (1.003 g), mp = 206-207 ºC. IR (ATR) ν: 748, 813, 833, 853, 947, 962, 1007, 1047, 1067, 1093, 1113, 1153, 1270, 1292, 1327, 1349, 1386, 1429, 1458, 1472, 2525, 2542, 2599, 2633, 2941 cm^{-1}. ^{1}H-NMR (400 MHz, CD_3OD) δ: 1.55-1.75 (complex signal, 2 H, 11-H_2), 1.80-1.94 [complex signal, 4 H, 10(12)-H_2], 3.05-3.40 [complex signal, 8 H, 9(13)-H_2, 7-H_2 and 8-H_2], 7.37 [dd, *J* = 9.2 Hz, *J'* = 2.0 Hz, 2 H, Ar-H], 7.45 [dd, *J* = 9.2 Hz, *J'* = 2.0 Hz, 2 H, Ar-H]. ^{13}C-NMR (100.5 MHz, CD_3OD) δ: 22.8 (CH_2, C11), 24.4 [CH_2, C10(12)], 28.7 (CH_2, C7), 54.5 [CH_2, C9(13)], 57.2 (CH_2, C8), 130.5 [CH, C3(5)], 132.8 [CH, C2(6)], 134.1 (C) and 134.3 (C) (C1 and C4).

1-[2-((2-ethylphenyl)thio)ethyl]piperidine hydrochloride, 15c. Following general procedure C, from 2-ethylthiophenol (1.35 mL, 10 mmol) and 1-(2-chloroethyl)piperidine hydrochloride (1.83 g, 10 mmol), the product was obtained as a palid yellow oil (2.40 g, 96% yield) that formed its hydrochloride salt as a white solid (915 mg), mp = 164-165 ºC. IR (ATR) ν: 679, 742, 768, 793, 853, 902, 947, 964, 987, 1021, 1036, 1056, 1133, 1156, 1184, 1218, 1278, 1398, 1426, 1441, 1458, 1586, 2525, 2565, 2633, 2930, 2976, 3055 cm^{-1}. ^{1}H-NMR (400 MHz, CD_3OD) δ: 1.21 (t, J = 7.6 Hz, 3 H, $CH_2C\underline{H}_3$), 1.50-1.75 (complex signal, 2 H, 11-H_2), 1.76-1.94 [complex signal, 4 H, 10(12)-H_2], 2.81 (q, J = 7.6 Hz, 2 H, $C\underline{H}_2CH_3$), 3.00-3.40 [complex signal, 8 H, 9(13)-H_2, 7-H_2 and 8-H_2], 7.18-7.30 (complex signal, 3 H, Ar), 7.46 (m, 1 H, Ar). ^{13}C-NMR (100.5 MHz, CD_3OD) δ: 15.5 (CH_3, $CH_2\underline{C}H_3$), 22.6 (CH_2, C11), 24.3 [CH_2, C10(12)], 28.0 (CH_2, $\underline{C}H_2CH_3$), 28.3 (CH_2, C7), 54.4 [CH_2, C9(13)], 57.2 (CH_2, C8), 128.1 (CH, C4), 128.6 (CH, C5), 130.3 (CH, C6), 131.1 (CH, C3), 133.5 (C, C2), 146.1 (C, C1).

General Procedure F. Sodium bis-(2-methoxyethoxy)aluminum hydride (65% wt solution in toluene, 1.04 g/mL, 4 mmol) was added dropwise to a cool (5 ºC, ice bath) solution of the required amide (1 mmol) in dry toluene (15 mL). The resulting solution was heated to reflux and stirred for 2 days. The solution was allowed to cool down to room temperature and 30% aqueous KOH was added dropwise until basic pH. The organic phase was separated and the aqueous layer was extracted with dichloromethane (3 x 20 mL). The combined organic extracts were dried over anh. Na_2SO_4, filtered and concentrated under *vacuo* to give the corresponding amine as an oil. The analytical sample of the aniline, as its hydrochloride, was obtained by dissolving this oil in Et_2O and adding an excess of Et_2O/HCl. The resulting suspension was cooled down for 24 h at 0 °C and the precipitated solid was filtered and dried *in vacuo* to afford the

corresponding amine hydrochloride. The analytical sample was obtained by crystallization from methanol.

General procedure G. A solution of amide (3.1 mmol) in dry THF (25 mL) was cooled 0 ºC with an ice bath and BH_3·THF (1M in THF, 12.4 mmol) was added dropwise and stirred at room temperature overnight. Methanol (25 mL) and then water (25 mL) were carefully added. The organic phase was evaporated under *vacuo*. The aqueous phase was extracted with DCM (3 x 25 mL). The combined organic extracts were dried over anh. Na_2SO_4, filtered and concentrated under *vacuo* to give the corresponding amine as an oil. This oil was dissolved in Et_2O and treated with Et_2O/HCl (0.6 N). The resulting suspension was cooled down for 24 h at 0 °C and the precipitated solid was filtered and dried *in vacuo* to afford the corresponding amine hydrochloride. The analytical sample was obtained by crystallization from methanol.

***N*-[(adamant-1-yl)methyl]aniline hydrochloride, 19a**.[57] Following the general procedure F, the reduction of amide **18a** (0.50 g, 1.96 mmol) with sodium bis-(2-methoxyethoxy)aluminum hydride (65% solution in toluene, 2.34 mL, 7.84 mmol), gave the corresponding amine as an oil (0.41 g, 82%). The corresponding purified amine hydrochloride **19a** was obtained after a treatment with Et_2O/HCl (0.6 N) and a crystallization from methanol, mp = >193 ºC (dec). IR (ATR) ν: 2896, 2848, 2659, 2425, 1602, 1581, 1499, 1488, 1431, 1394, 1372, 1185, 1031, 993, 750, 690 cm^{-1}. ^{1}H-NMR, δ_H (400 MHz, DMSO): 1.61-1.70 (complex signal, 12 H, adamantyl-CH_2), 1.97 [broad s, 3 H, 3'(5',7')-H], 2.89 (s, 2 H, CH_2N), 7.15 (m, 1 H, 4-H), 7.30 [m, 2 H, 2(6)-H], 7.37 [m, 2 H, 3(5)-H]. ^{13}C-NMR, δ_C (100.6 MHz, DMSO): 27.6 [CH, C3'(5',7')], 33.0 (C, C1'), 36.2 [CH_2, C4'(6',10')], 39.4 [CH_2, C2'(8',9')], 129.4 (CH, Ar-C). Only an aromatic signal was observed and the CH_2NH signal is a very broad band, difficult to see. MS-DIP (EI), m/e (%); main ions: 241 ($M^{\cdot+}$, 94), 106 (100), 79 (11), 77 (14).

***N*-[(adamant-1-yl)methyl]-4-methylaniline hydrochloride, 19b**.[58] Following the general procedure F, the reduction of amide **18k** (1.00 g, 3.1 mmol) with sodium bis-(2-methoxyethoxy)aluminum hydride (65% solution in toluene, 3.7 mL, 12.4 mmol), gave the corresponding amine as an oil (0.75 g, 78%). The corresponding purified amine hydrochloride **19b** was obtained after a treatment with Et_2O/HCl (0.6 N) and a crystallization from methanol, mp >226 °C (dec). IR (ATR) ν: 2904, 2846, 1595, 1513, 1430, 1369, 1106, 990, 813 cm^{-1}. ^{1}H-NMR, δ_H (400 MHz, DMSO): 1.62-1.71 (complex signal, 12 H, adamantyl-CH_2), 1.98 [broad s, 3 H, 3'(5',7')-H], 2.29 (s, 3 H, Ar-C$\underline{H}_3$), 2.89 (s, 2 H, CH_2N), 7.21 (d, J = 8.0 Hz, 2 H, Ar-H), 7.29 (d, J = 8.0 Hz, 2 H, Ar-H). ^{13}C-NMR, δ_C (100.6 MHz, DMSO): 20.2 (CH_3, Ar-$\underline{C}H_3$), 27.4 [CH, C3'(5',7')], 32.7 (C, C1'), 36.0 [CH_2, C4'(6',10')], 39.2 [CH_2, C2'(8',9')], 62.1 (CH_2, $\underline{C}H_2N$), 120.6 (CH, Ar-C), 129.4 (CH, Ar-C), 134.9 (C, Ar-C), 137.9 (C, Ar-C). MS-DIP (EI), m/e (%); main ions: 255 ($M^{\cdot+}$, 84), 120 (100), 91 (13).

***N*-[(adamant-1-yl)methyl]-2-methylaniline hydrochloride, 19c**. Following the general procedure F, the reduction of amide **18i** (1.00 g, 3.1 mmol) with sodium bis-(2-methoxyethoxy)aluminum hydride (65% solution in toluene, 3.7 mL, 12.4 mmol), gave the corresponding amine as an oil (0.82 g, 85%). The corresponding purified amine hydrochloride **19c** was obtained after a treatment with Et_2O/HCl (0.6 N) and a crystallization from methanol, mp >193 °C (dec). IR (ATR) ν: 2905, 2844, 1580, 1441, 993, 761 cm^{-1}.^{1}H-NMR, δ_H (400 MHz, DMSO): 1.62-1.69 (complex signal, 12 H, adamantyl-CH_2), 1.98 [broad s, 3 H, 3'(5',7')-H], 2.36 (s, 3 H, Ar-C$\underline{H}_3$), 2.87 (s, 2 H, CH_2N), 3.77 (broad s, 1 H, NH), 7.13 (t, J = 7.2 Hz, 1 H, Ar-H), 7.22-7.27 (complex signal, 2 H, Ar-H), 7.38 (d, J = 8.0 Hz, 1 H, Ar-H). ^{13}C-NMR, δ_C (100.6 MHz, DMSO): 7.1 (CH_3, Ar-$\underline{C}H_3$), 27.7 [CH, C3'(5',7')], 33.2 (C, C1'), 36.2 [CH_2, C4'(6',10')], 39.3 [CH_2, C2'(8',9')], 61.5 (CH_2, $\underline{C}H_2N$), 120.3 (CH, Ar-CH), 125.6 (CH, Ar-CH), 127.2

(CH, Ar-CH), 128.9 (C, Ar-C), 131.7 (CH, Ar-CH), 138.8 (C, Ar-CH). MS-DIP (EI), m/e (%); main ions: 255 ($M^{\cdot+}$, 62), 135 (8), 120 (100), 91 (12).

***N*-[(adamant-1-yl)methyl]-2-ethylaniline hydrochloride, 19d**. Following the general procedure F, the reduction of amide **18d** (0.30 g, 1.06 mmol) with sodium bis-(2-methoxyethoxy)aluminum hydride (65% solution in toluene, 1.27 mL, 4.24 mmol), gave the corresponding amine as an oil (0.21 g, 72%). The corresponding purified amine hydrochloride **19d** was obtained after a treatment with Et_2O/HCl (0.6 N) and a crystallization from methanol, mp >178 ºC. IR (ATR) ν: 2900, 2848, 2684, 1583, 1499, 1434, 1372, 1105, 995, 750, 690 cm^{-1}. ^{1}H-NMR, δ_H (400 MHz, CD_3OD): 1.38 (t, J = 7.6 Hz, 3H, $CH_2C\underline{H}_3$), 1.79-1.86 (complex signal, 12 H, adamantyl-CH_2), 2.10 [broad s, 3 H, 3'(5',7')-H], 2.77 (q, J = 7.6 Hz, 2 H, $C\underline{H}_2CH_3$), 3.03 (s, 2 H, CH_2N), 4.86 (broad s, 2 H, NH), 7.38-7.54 (complex signal, 4 H, Ar-H).^{13}C-NMR, δ_C (100.6 MHz, CD_3OD): 14.5 (CH_3, $CH_2\underline{C}H_3$), 23.2 (CH_2, $\underline{C}H_2CH_3$), 29.4 [CH, C3'(5',7')], 34.2 (C, C1'), 37.4 [CH_2, C4'(6',10')], 40.5 [CH_2, C2'(8',9')], 66.8 (CH_2, CH_2N), 128.9 (CH, Ar-C), 131.6 (CH, Ar-C). Only two aromatic signals were observed.

***N*-[(adamant-1-yl)methyl]-2-isopropylaniline hydrochloride, 19e**. Following the general procedure F, **18e** (0.55 g, 1.85 mmol) and sodium bis-(2-methoxyethoxy)aluminum hydride (65% wt solution in toluene, 1.76 mL, 9.00 mmol) in anhydrous toluene (14 mL), gave **19e** as a yellow solid (483 mg, 83%). The pure product was obtained after crystallization from hot EtOAc as a white solid (195 mg, 37% yield), mp = 107-108 ºC. IR (ATR) ν: 733, 811, 925, 958, 986, 1039, 1059, 1100, 1117, 1140, 1249, 1256, 1282, 1309, 1352, 1448, 1507, 1582, 1605, 2329, 2349, 2840, 2901, 2967, 3037, 3448 cm^{-1}. ^{1}H-NMR (400 MHz, $CDCl_3$) δ: 1.29 [d, J = 6.8 Hz, 6 H, -$CH(C\underline{H}_3)_2$], 1.62-1.65 [complex signal, 6 H, 2'(8',9')-H_2], 1.66-1.82 [complex signal, 6 H, 4'(6',10')-H_2], 2.03 [m, 3 H, 3'(5',7')-H], 2.83 (s, 2 H, 7-H_2), 2.88 [sept, J = 6.8 Hz,

1 H, -C<u>H</u>$(CH_3)_2$], 3.72 (broad s, 1 H, NH), 6.66 (broad d, *J* = 8.0 Hz, 1 H, 6-H), 6.70 (td, *J* = 7.6 Hz, *J'* = 1.2 Hz, 1 H, 4-H), 7.08-7.17 (complex signal, 2 H, 3-H and 5-H). ^{13}C-NMR (100.5 MHz, $CDCl_3$) δ: 22.2 [CH_3, -CH(<u>C</u>$H_3)_2$], 27.4 [CH, -<u>C</u>H$(CH_3)_2$], 28.4 [CH, C3'(5',7')], 33.7 (C, C1'), 37.1 [CH_2, C4'(6',10')], 41.0 [CH_2, C2'(8',9')], 56.3 (CH_2, C7), 110.1 (CH, C6), 116.6 (CH, C4), 124.8 (CH, C5), 126.7 (CH, C3), 131.7 (C, C2), 145.6 (C, C1). HRMS-ESI+ m/z $[M+H]^+$ calcd for $[C_{20}H_{29}N+H]^+$: 284.2373, found: 284.2382.

***N*-[(adamant-1-yl)methyl]-4-(benzyloxy)aniline hydrochloride, 19f.** Following the general procedure F, the reduction of amide **18f** (2.00 g, 5.5 mmol) with sodium bis-(2-methoxyethoxy)aluminum hydride (65% solution in toluene, 6.58 mL, 22.0 mmol), gave the corresponding amine as an oil (1.50 g, 79%). The corresponding purified amine hydrochloride **19f** was obtained after a treatment with Et_2O/HCl (0.6 N) and a crystallization from methanol, mp = 199-200 °C. IR (ATR) ν: 2901, 2848, 2494, 2412, 1605, 1577, 1513, 1439, 1250, 1006, 838, 746, 697 cm^{-1}. ^{1}H-NMR, δ_H (400 MHz, DMSO): 1.58-1.70 (complex signal, 12 H, adamantyl-CH_2), 1.97 [broad s, 3 H, 3'(5',7')-H], 2.91 (s, 2 H, CH_2N), 5.12 (s, 2 H, CH_2O), 7.11 (d, *J* = 9.2 Hz, 2 H, Ar-H), 7.33 (m, 1 H, $CH_2C_6H_5$-H_{para}), 7.37 (t, *J* = 6.8 Hz, 2 H, $CH_2C_6H_5$-H_{meta}), 7.42 (d, *J* = 6.8 Hz, 2 H, $CH_2C_6H_5$-H_{ortho}), 7.43 (m, 2 H, Ar-H). ^{13}C-NMR, δ_C (100.6 MHz, DMSO): 27.5 [CH, C3'(5',7')], 32.6 (C, C1'), 36.0 [CH_2, C4'(6',10')], 39.2 [CH_2, C2'(8',9')], 69.6 (CH_2, <u>C</u>H_2O), 115.7 [C, C3(5)], 127.7 (CH, $CH_2C_6H_5$-C_{ortho}), 127.8 (CH, $CH_2C_6H_5$-C_{para}), 128.4 (CH, $CH_2C_6H_5$-C_{meta}), 136.7 (C, $CH_2C_6H_5$-C_{ipso}). No all the C signals were observed. MS-DIP (EI), m/e (%); main ions: 347 ($M^{\cdot+}$, 19), 256 (100), 149 (26), 93 (10), 91 (14).

***N*-[(adamant-1-yl)methyl]-3-(benzyloxy)aniline hydrochloride, 19g**. Following the general procedure F, the reduction of amide **18g** (2.50 g, 6.93 mmol) with sodium bis-

(2-methoxyethoxy)aluminum hydride (65% solution in toluene, 8.29 mL, 27.72 mmol), gave the corresponding amine as an oil (2.23 g, 92%). The corresponding purified amine hydrochloride **19g** was obtained after a treatment with Et_2O/HCl (0.6 N) and a crystallization from methanol, mp = 188-193 °C. IR (ATR) ν: 2899, 2845, 2411, 1611, 1597, 1498, 1425, 1388, 1255, 1145, 1024, 860, 740, 695 cm^{-1}. ^{1}H-NMR, δ_H (400 MHz, DMSO): 1.48-1.69 (complex signal, 12 H, adamantyl-CH_2), 1.95 [broad s, 3 H, 3'(5',7')-H], 2.84 (s, 2 H, CH_2N), 5.08 (s, 2 H, CH_2O), 6.65-6.82 (complex signal, 3 H, 2-H, 4-H and 6-H), 7.20 (t, *J* = 8.0 Hz, 1 H, 5H), 7.31 (t, *J* = 6.8 Hz, 1 H, $CH_2C_6H_5$-H_{para}), 7.37 (t, *J* = 6.8 Hz, 2 H, $CH_2C_6H_5$-H_{meta}), 7.42 (d, *J* = 6.8 Hz, 2 H, $CH_2C_6H_5$-H_{ortho}). ^{13}C-NMR, δ_C (100.6 MHz, DMSO): 27.6 [CH, C3'(5',7')], 33.2 (C, C1'), 36.3 [CH_2, C4'(6',10')], 39.5 [CH_2, C2'(8',9')], 69.2 (CH_2, $\underline{C}H_2O$), 127.5 (C, Ar-C), 127.7 (CH, $CH_2C_6H_5$-C_{ortho}), 127.8 (CH, $CH_2C_6H_5$-C_{para}), 128.6 (CH, $CH_2C_6H_5$-C_{meta}), 130.1 (CH, Ar-C), 136.9 (C, $CH_2C_6H_5$-C_{ipso}), 159.1 (C, C3). No all the C signals were observed. MS-DIP (EI), m/e (%); main ions: 347 ($M^{\cdot+}$, 100), 212 (97), 93 (11), 91 (37).

***N*-[(adamantan-1-yl)methyl]-3-(trifluoromethoxy)aniline hydrochloride, 19h**. Following the general procedure F, the reduction of amide **18h** (0.50 g, 1.47 mmol) with sodium bis-(2-methoxyethoxy)aluminum hydride (65% wt solution in toluene, 2.6 ml, 8.84 mmol), get the corresponding amine as an oil (0.41 g, 87%) . The corresponding purified amine hydrochloride **19h** was obtained after treatment with Et_2O/HCl, mp = 195-196 ºC. IR (ATR) ν: 2902, 1428, 1251, 1213, 116, 864, 791, 681 cm^{-1}. HRMS-ESI$^+$ m/z [*M*+H]$^+$: calcd for [$C_{18}H_{23}F_3NO$+H^+]: 326.17, found: 326.1728.

***N*-[(adamant-1-yl)methyl]-2-(trifluoromethyl)aniline hydrochloride, 19i**. Following the general procedure G, the reduction of amide **18i** (0.30 g, 0.93 mmol) with BH_3·THF (1M in THF, 3.72 mmol), gave the corresponding amine as an oil (0.18 g, 62%). The purified amine hydrochloride **19i** was obtained after a treatment with

Et_2O/HCl (0.6 N) and a crystallization from methanol. mp = 71-72 °C. IR (ATR) ν: 3367, 2906, 2845, 1612, 1585, 1514, 1461, 1292, 1245, 1162, 1095, 1029, 741, 659 cm^{-1}. ^{1}H-NMR, δ_H (400 MHz, DMSO): 1.51 (complex signal, 6 H, 2'(8',9')-CH_2), 1.52-1.69 (complex signal, 6 H, 4'(6',10')-CH_2), 1.94 [broad s, 3 H, 3'(5',7')-H], 2.89 (s, 2 H, $C\underline{H}_2N$), 4.72 (broad signal, 1 H, NH), 6.65 (t, *J* = 7.5 Hz, 1 H, Ar-H), 6.90 (d, *J* = 8.0 Hz, 1 H, Ar-H), 7.37 (complex signal, 2 H, Ar-H). ^{13}C-NMR, δ_C (100.6 MHz, DMSO): 27.7 [CH, C3'(5',7')], 34.2 (C, C1), 36.5 [CH_2, C4'(6',10')], 40.0 [CH_2, C2'(8',9')], 54.0 (CH_2, $\underline{C}H_2N$), 111.0 (C, q, J = 28.6 Hz, 2C), 112.1 (CH, 6C), 114.9 (CH, 4C), 125.3 (C, q, *J* = 272.1 Hz, CF_3), 126.1 (CH, q, *J* = 5.3 Hz, 3C), 133.4 (CH, 5C), 146.3 (C, q, *J* = 1.5 Hz, 1C). MS-DIP (EI), m/e (%); main ions: 309 ($M^{\cdot+}$, 100), 174 (64), 154 (33), 135 (58), 93 (12), 91 (7), 79 (13).

***N*-[(adamant-1-yl)methyl]-3-(trifluoromethyl)aniline hydrochloride, 19j**. Following the general procedure F, the reduction of amide **18j** (1.00 g, 3.1 mmol) with sodium bis-(2-methoxyethoxy)aluminum hydride (65% solution in toluene, 3.7 mL, 12.4 mmol), gave the corresponding amine as an oil (0.99 g, quantitative yield). The corresponding purified amine hydrochloride **19j** was obtained after a treatment with Et_2O/HCl (0.6 N) and a crystallization from methanol, mp = 193-197 °C. IR (ATR) ν: 2916, 2851, 2494, 2417, 1582, 1470, 1435, 1327, 1171, 1123, 1096, 797, 692 cm^{-1}. ^{1}H-NMR, δ_H (400 MHz, DMSO, 50°C): 1.56 (complex signal, 6 H, 2'(8',9')-CH_2), 1.57-1.70 (complex signal, 6 H, 4'(6',10')-CH_2), 1.95 [broad s, 3 H, 3'(5',7')-H], 2.75 (s, 2 H, CH_2N), 4.38 (broad s, 1 H, NH), 6.77 (d, *J* = 7.6 Hz, 1 H, 6-H), 6.90 (dd, *J* = 8.0 Hz, *J'* = 2.0 Hz, 1 H, 4-H), 6.94 (broad s, 1 H, 2-H), 7.24 (t, *J* = 8.0 Hz, 1 H, 5-H). ^{13}C-NMR, δ_C (100.6 MHz, DMSO, 50°C): 27.7 [CH, C3'(5',7')], 33.8 (C, C1'), 36.4 [CH_2, C4'(6',10')], 39.8 [CH_2, C2'(8',9')], 55.2 (CH_2, $\underline{C}H_2N$), 108.2 (CH, C2), 111.2 (CH, C4), 115.3 (CH, C6), 124.3 (C, q, *J* = 273.7 Hz, CF_3), 129.5 (CH, C5), 129.6 (C, q, *J* =

30.7 Hz, C3), 149.7 (C, C1). MS-DIP (EI), m/e (%); main ions: 309 ($M^{\cdot+}$, 80), 290 (9), 174 (82), 135 (100), 93 (19), 79 (21).

***N*-[(adamant-1-yl)methyl]-4-(trifluoromethyl)aniline hydrochloride, 19k**. Following the general procedure G, the reduction of amide **18k** (0.50 g, 1.6 mmol) with $BH_3 \cdot THF$ (1 M in THF, 6.4 mmol), gave the corresponding amine as an oil (0.30 g, 61%). The corresponding purified amine hydrochlororide **19k** was obtained after a treatment with Et_2O/HCl (0.6 N) and a crystallization from methanol, mp = 168-171°C. IR (ATR) ν: 2912, 2849, 2499, 2414, 1617, 1518, 1452, 1414, 1319, 1168, 1129, 1070, 1020, 847, 647 cm^{-1}. ^{1}H-NMR, δ_H (400 MHz, CD_3OD): 1.67 (complex signal, 6 H, 2'(8',9')-CH_2), 1.71-1.81 (m, 6 H, 4'(6',10')-CH_2), 2.02 [broad s, 3 H, 3'(5',7')-H], 2.95 (s, 2 H, C$\underline{H_2}$N), 4.87 (broad signal, 1 H, NH), 7.09 [d, *J* = 8.4 Hz, 2 H, 2(6)-H], 7.53 [d, *J* = 8.4 Hz, 2 H, 3(5)-H].^{13}C-NMR, δ_C (100.6 MHz, CD_3OD): 29.7 [CH, C3'(5',7')], 35.0 (C, C1), 37.9 [CH_2, C4'(6',10')], 41.2 [CH_2, C2'(8',9')], 60.2 (CH_2, $\underline{C}H_2$N), 117.1 [CH, C2(6)], 127.7 [CH, C3(5)], 149.3 (C, C1). The signal from CF_3 was not observed.

***N*-[(adamant-1-yl)methyl]-4-chloroaniline hydrochloride, 19l**.[57] Following the general procedure F, the reduction of amide **18l** (0.25 g, 0.86 mmol) with sodium bis-(2-methoxyethoxy)aluminum hydride (65% solution in toluene, 1.03 mL, 3.44 mmol), gave the corresponding amine as an oil (0.21 g, 91%). The corresponding purified amine hydrochloride **19l** was obtained after a treatment with Et_2O/HCl (0.6 N) and a crystallization from methanol, mp = 186-190 °C. IR (ATR) ν: 2899, 2845, 2660, 1582, 1491, 1415, 1095, 818 cm^{-1}. ^{1}H-NMR, δ_H (400 MHz, DMSO): 1.58-1.69 (complex signal, 12 H, adamantyl-CH_2), 1.95 [broad s, 3 H, 3'(5',7')-H], 2.77 (s, 2 H, CH_2N), 6.94 [broad d, *J* = 7.6 Hz, 2H, 2(6)-H], 7.20 [d, *J* = 8.8 Hz, 2H, 3(5)-H].^{13}C-NMR, δ_C (100.6 MHz, DMSO): 27.7 [CH, C3'(5',7')], 33.6 (C, C1'), 36.4 [CH_2, C4'(6',10')],

39.7 [CH_2, C2'(8',9')], 58.3 (CH_2, $\underline{C}H_2N$), 136.7 (CH, Ar-C). Only an aromatic signal was observed. MS-DIP (EI), m/e (%); main ions: 277 ($M^{\cdot+}$, ^{37}Cl, 36), 275 ($M^{\cdot+}$, ^{35}Cl, 100), 142 (29), 140 (86), 139 (29), 135 (37), 93 (11), 91 (7), 79 (11).

***N*-[(adamantan-1-yl)methyl]-2-bromoaniline hydrochloride, 19m**. Following the general procedure F, the reduction of amide **18m** (0.90 g, 2.69 mmol) with sodium bis(2methoxyethoxy)aluminum hydride (65% wt solution in toluene, 3.21 mL, 10.76 mmol), get the corresponding amine **19m** as an oil (0.74 g, 86%) . The corresponding purified amine hydrochloride was obtained after the working with Et_2O/HCl (0.6 N), mp= 189-190 ºC. IR (ATR) ν: 2909, 2847, 2642, 1566, 1440, 1392, 1060, 989, 851, 757 cm^{-1}. ^{1}H-NMR, δ_H (400 MHz, DMSO): 1.54 [d, *J'*=2.8 Hz, 6 H, 2'(8',9')-H_2], 1.60-1.67 [m, 6 H, 4'(6',10')-H_2], 1.95 [s, 3 H, 3'(5',7')-H], 2.87 (s, 2 H, $C\underline{H}_2N$), 6.5 (dt, *J''* = 7.6 Hz, *J'* = 7.5 Hz, *J* = 1.5 Hz, 1 H, Ar-H), 6.79 (dd, *J'* = 8.3 Hz, *J* = 1.5 Hz, 1 H, Ar-H), 7.10 (ddd, *J''* = 8.6 Hz, *J'* = 7.3 Hz, *J* = 1.5 Hz, 1 H, Ar-H), 7.23 (dd, *J'* = 7.9 Hz, *J* = 1.6 Hz, 1 H, Ar-H). ^{13}C-NMR, δ_C (100.6 MHz, MeOD): 29.3 [CH, C3'(5',7')], 34.2 [CH_2, C4'(6',10')], 37.3 [CH_2, C2'(8',9')], 40.5 (C, C1'), 63.9 (CH_2, $\underline{C}H_2N$), 123.6 (C, C2), 126.6 (CH, C6*), 129.6 (CH, C4*), 129.8 (CH, C3), 131.9 (CH, C5), 136.6 (C, C1).

***N*-[(Adamantan-1-yl)methyl]-2-chloroaniline hydrochloride, 19n**.[57] Following the general procedure F, the reduction of amide **18n** (1.00 g, 3.45 mmol) with sodium bis(2methoxyethoxy)aluminum hydride (65% wt solution in toluene, 4.11 mL, 13.8 mmol), get the corresponding amine **19n** as an oil (0.99 g, 95%) . The corresponding purified amine hydrochloride was obtained after treatment with Et_2O/HCl (0.6 N), mp = 224-225 ºC. IR (ATR) ν: 2895, 2846, 2649, 1580, 1488, 1429, 1394, 1372, 1184, 1106, 992, 749, 717, 690 cm^{-1}. ^{1}H-NMR, δ_H (400 MHz, MeOD): 1.57-1.92 [complex signal, 12 H, adamantyl-H_2], 2.07 [s, 3 H, 3'(5',7')-H], 3.12 (s, 2 H, $C\underline{H}_2N$), 7.22-7.78

(complex signal, 4 H, Ar-H). ^{13}C-NMR, δ_C (100.6 MHz, MeOD): 28.0 [CH, C3'(5',7')], 32.5 (C, C1'), 36.0 [CH_2, C2'(8',9')], 39.2 [CH_2, C4'(6',10')], 65.4 (CH_2, $\underline{C}H_2N$), 122.5 (C, C2), 129.5 (CH, 2 Ar-C), 130.2 (CH, 2 Ar-C), 136.7 (C, C1). HRMS-ESI$^+$ m/z $[M+H]^+$: calcd for $[C_{17}H_{22}ClN+H^+]$: 276.14, found: 276.1521.

***N*-[(adamant-1-yl)methyl]-3-chloroaniline hydrochloride, 19o**.[57] Following the general procedure F, the reduction of amide **18o** (1.00 g, 3.46 mmol) with sodium bis-(2-methoxyethoxy)aluminum hydride (65% wt solution in toluene, 4.14 mL, 13.84 mmol), gave the corresponding amine as an oil (0.79 g, 83%). The corresponding purified amine hydrochloride **19o** was obtained after a treatment with Et_2O/HCl (0.6 N) and a crystallization from methanol, mp = 187-190 °C. IR (ATR) ν: 2901, 2846, 2682, 2416, 1597, 1578, 1481, 1426, 1098, 989, 878, 785, 678 cm^{-1}. ^{1}H-NMR, δ_H (400 MHz, DMSO): 1.53 (broad signal, 6 H, 2'(8',9')-CH_2), 1.63 (m, 6 H, 4'(6',10')-CH_2), 1.94 [broad s, 3 H, 3'(5',7')-H], 2.70 (s, 2 H, $C\underline{H}_2N$), 3.89 (broad signal, 1 H, NH), 6.48 (dd, *J* = 8.0 Hz, *J'* = 1.5 Hz, 1 H, 6-H), 6.59 (dd, *J* = 8.4 Hz, *J'* = 1.5 Hz, 1 H, 4-H), 6.66 (t, *J* = 1.5 Hz, 1 H, 2-H), 7.03 (t, *J* = 8.0 Hz, 1 H, 5-H). ^{13}C-NMR, δ_C (100.6 MHz, DMSO): 27.8 [CH, C3'(5',7')], 34.0 (C, C1), 36.6 [CH_2, C4'(6',10')], 39.9 [CH_2, C2'(8',9')], 55.2 (CH_2, $\underline{C}H_2N$), 110.9 (CH, C6), 111.4 (CH, C2), 114.8 (CH, C4), 130.2 (CH, C5), 133.5 (C, C3), 150.8 (C, C1). MS-DIP (EI), m/e (%); main ions: 275 ($M^{\cdot+}$, 100), 140 (100), 135 (69), 93 (17), 79 (18), 77 (12).

***N*-[(adamantan-1-yl)methyl]-2,6-difluoroaniline hydrochloride, 19p**. Following the general procedure F, the reduction of amide **18p** (1.00 g, 3.43 mmol) with sodium bis-(2-methoxyethoxy)aluminum hydride (65% wt solution in toluene, 6.15 mL, 20.59 mmol), gave the corresponding amine as an oil (0.87 g, 92%) . The corresponding purified amine hydrochloride **19p** was obtained after treatment with Et_2O/HCl (0.6 N), mp = 188-189 ºC. IR (ATR) ν: 2894, 2846, 1509, 1428, 1262, 1096, 956, 795 cm^{-1}. ^{1}H-

NMR, δ_H (400 MHz, MeOD): 1.67 [s, 6 H, 2'(8',9')-H_2], 1.70-1.84 [m, 6 H, 4'(6',10')-H_2], 2.02 [s, 3 H, 3'(5',7')-H], 2.95 (s, 2 H, C$\underline{H_2}$N), 6.96 21 (dddd, *J'''* = 9.1 Hz, *J''* = 8.2 Hz, *J'* = 2.9 Hz, *J* = 1.6, 1 H, Ar-H), 7.08 (ddd, *J''* = 11.4 Hz, *J'* = 8.6 Hz, *J* = 2.8 Hz, 1 H, Ar-H), 7.21 (td, *J* = 9.2 Hz, 1 H, Ar-H). ^{13}C-NMR, δ_C (100.6 MHz, MeOD): 28.2 [CH, C3'(5',7')], 33.3 (C, C1'), 36.3 [CH_2, C2'(8',9')], 39.5 [CH_2, C4'(6',10')], 60.2 (CH_2, $\underline{C}H_2$N), 104.3 (CH, Ar-C_{para}), 111.4 (CH, Ar-C_{meta}), 119.0 (C, Ar-C_{ortho}) 120.8 (C, dd, *J* = 284.7 Hz, Ar-C1). HRMS-ESI$^+$ m/z $[M+H]^+$: calcd for $[C_{17}H_{21}F_2N+H^+]$: 278.16, found: 278.1724.

***N*-[(adamantan-1-yl)methyl)-3,5-difluoroaniline hydrochloride, 19q**. Following the general procedure F, the reduction of amide **18q** (1.00 g, 3.43 mmol) with sodium bis(2-methoxyethoxy)aluminum hydride (65% wt solution in toluene, 6.15 mL, 20.59 mmol), gave the corresponding amine as an oil (0.88 g, 93%) . The corresponding purified amine hydrochloride **19q** was obtained after treatment with Et_2O/HCl (0.6 N), mp = 207-209 ºC. IR (ATR) ν: 2905, 2661, 1616, 1426, 1129, 983, 862, 681 cm^{-1}. ^{1}H-NMR, δ_H (400 MHz, $CDCl_3$): 1.48 [s, 6 H, 2'(8',9')-H_2], 1.56-1.69 [m, 6 H, 4'(6',10')-H_2], 1.94 [s, 3 H, 3'(5',7')-H], 2.68 (d, *J* = 6.0 Hz, 2 H, C$\underline{H_2}$N), 3.84 (s, 1 H, N$\underline{H}$), 5.88-6.16 (m, 3 H, Ar-H). HRMS-ESI$^+$ m/z $[M+H]^+$: calcd for $[C_{17}H_{21}F_2N+H^+]$: 278.16, found: 278.1722.

***N*-[(adamantan-1-yl)methyl]-3,5-dichloroaniline hydrochloride, 19r**. Following the general procedure F, the reduction of amide **18r** (1.00 g, 3.08 mmol) with sodium bis(2-methoxyethoxy) aluminum hydride 65% wt solution in toluene, 3.68 mL, 12.35 mmol), gave the corresponding amine as an oil (0.85 g, 89%) . The corresponding purified amine hydrochloride **19r** was obtained after treatment with Et_2O/HCl (0.6 N), mp = 194-195 ºC. IR (ATR) ν: 2900, 2846, 2657, 1586, 1415, 1106, 914, 862, 802, 674 cm^{-1}. ^{1}H-NMR, δ_H (400 MHz, DMSO): 1.50 [d, *J* = 1.8 Hz, 6 H, 2'(8',9')-H_2], 1.62 [m,

6 H, 4'(6',10')-H_2], 1.92 [s, 3 H, 3'(5',7')-H], 2.69 (s, 2 H, C$\underline{H_2}$N), 3.55 (s, 1 H, N$\underline{H}$), $\underline{6}$.48 (t, *J'* = 2.0 Hz, *J* = 1.8 Hz, 1 H, Ar-H), 6.60 (d, *J* = 1.8 Hz, 2 H, Ar-H). HRMS-ESI$^+$ m/z $[M+H]^+$: calcd for $[C_{17}H_{21}Cl_2N+H^+]$: 310.11, found: 310.1131.

***N*-[(adamantan-1-yl)methyl]-3,5-bis(trifluoromethyl)aniline hydrochloride, 19s**. Following the general procedure F, the reduction of amide **18s** (1.00 g, 2.56 mmol) with sodium bis-(2-methoxyethoxy)aluminum hydride (65% wt solution in toluene, 3.05 mL, 10.24 mmol), gave the corresponding amine as an oil (0.53 g, 55%). The corresponding purified amine hydrochloride **19s** was obtained after treatment with Et_2O/HCl (0.6 N), mp = 170-171 ºC. IR (ATR) ν: 2906, 2641, 1585, 1434, 1369, 1274, 1166, 1129, 886, 681 cm^{-1}. ^{1}H-NMR, δ_H (400 MHz, DMSO): 1.54 [s, 6 H, 2'(8',9')-H_2], 1.63 [m, 6 H, 4'(6',10')-H_2], 1.94 [s, 3 H, 3'(5',7')-H], 2.79 (s, 2 H, C$\underline{H_2}$N), 6.95 (s, 1 H, Ar-H), 7.15 (s, 2 H, Ar-H). ^{13}C-NMR, δ_C (100.6 MHz, MeOD): 29.2 [CH, C3'(5',7')], 35.1 (C, C1'), 37.8 [CH_2, C2'(8',9')], 41.3 [CH_2, C4'(6',10')], 57.4 (CH_2, $\underline{C}H_2$N), 110.1 (CH, Ar-C_{para}), 113.5 (CH, Ar-C_{ortho}), 125.9 (CH, d, *J* = 271.62, $\underline{C}F_3$), 133.1 (C, Ar-C_{meta}), 150.6 (C, C1). HRMS-ESI$^+$ m/z $[M+H]^+$: calcd for $[C_{19}H_{21}F_6N+H^+]$: 378.16, found: 378.1662.

***N*-[(adamant-1-yl)methyl]-3-fluoro-5-(trifluoromethyl)aniline hydrochloride, 19t**. Following the general procedure F, the reduction of amide **18t** (1.00 g, 3.03 mmol) with sodium bis-(2-methoxyethoxy)aluminum hydride (65% solution in toluene, 3.62 mL, 12.12 mmol), gave the corresponding amine as an oil (0.80 g, 83%). The corresponding purified amine hydrochloride **19t** was obtained after a treatment with Et_2O/HCl (0.6 N) and a crystallization from methanol, mp = 146-149 °C. IR (ATR) ν: 2898, 2852, 2488, 2414, 1610, 1581, 1434, 1348, 1180, 1139, 981, 867, 689 cm^{-1}. ^{1}H-NMR, δ_H (400 MHz, DMSO): 1.53-1.69 (complex signal, 12 H, adamantyl-CH_2), 1.94 [broad s, 3 H, 3'(5',7')-H], 2.74 (s, 2 H, CH_2N), 5.65 (broad s, 1 H, NH), 6.52 (broad d, *J* = 8.8 Hz, 1

H, 4-H), 6.64 (dt, *J* = 12.4 Hz, *J* = 2Hz, 1 H, 2-H), 6.80 (broad s, 1 H, 6-H). ^{13}C-NMR, δ_C (100.6 MHz, DMSO): 27.7 [CH, C3'(5',7')], 34.0 (C, C1'), 36.5 [CH_2, C4'(6',10')], 39.8 [CH_2, C2'(8',9')], 54.7 (CH_2, $\underline{C}H_2N$), 97.3 (CH, d, *J* = 25.8 Hz, C4), 100.5 (CH, d, *J* = 26.0 Hz, C2), 104.9 (CH, C6), 131.1 (broad C, C5), 152.4 (C, C1), 163.3 (C, d, *J* = 240.9 Hz, C3). The signal from the CF_3 group is not clearly visible. MS-DIP (EI), m/e (%); main ions: 327 ($M^{\cdot+}$, 62), 309 (13), 192 (26), 135 (100), 93 (16), 91 (7), 79 (15).

***N*-[(adamant-1-yl)methyl]-3-chloro-5-(trifluoromethyl)aniline hydrochloride, 19u**. Following the general procedure F, the reduction of amide **18u** (1.00 g, 2.84 mmol) with sodium bis-(2-methoxyethoxy)aluminum hydride (65% solution in toluene, 3.40 mL, 11.36 mmol), gave the corresponding amine as an oil (0.91 g, 95%). The corresponding purified amine hydrochloride **19u** was obtained after a treatment with Et_2O/HCl (0.6 N) and a crystallization from methanol, mp = 132-138 °C. IR (ATR) ν: 2900, 2852, 2476, 2410, 1577, 1435, 1322, 1176, 1138, 1103, 867, 832, 686 cm^{-1}. ^{1}H-NMR, δ_H (400 MHz, DMSO): 1.53-1.69 (complex signal, 12 H, adamantyl-CH_2), 1.94 [broad s, 3 H, 3'(5',7')-H], 2.74 (s, 2 H, CH_2N), 5.87 (broad s, 1 H, NH), 6.72 (s, 1 H, Ar-H), 6.88 (broad s, 2 H, Ar-H).^{13}C-NMR, δ_C (100.6 MHz, DMSO): 27.7 [CH, C3'(5',7')], 34.0 (C, C1'), 36.5 [CH_2, C4'(6',10')], 39.8 [CH_2, C2'(8',9')], 54.5 (CH_2, $\underline{C}H_2N$), 107.0 (CH, C6), 109.9 (CH, C4), 113.6 (CH, C2), 123.7 (C, q, *J* = 272.7 Hz, CF_3), 131.1 (C, q, *J* = 31.6 Hz, C5), 134.5 (C, C3), 151.6 (C, C1). MS-DIP (EI), m/e (%); main ions: 343 ($M^{\cdot+}$, 63), 208 (25), 135 (100), 93 (15), 91 (7), 79 (14).

***N*-[(adamant-1-yl)methyl]-4-chloro-3-(trifluoromethyl)aniline hydrochloride, 19v**. Following the general procedure F, the reduction of amide **18v** (1.00 g, 3.46 mmol) with sodium bis-(2-methoxyethoxy)aluminum hydride (65% solution in toluene, 4.14 mL, 13.84 mmol), gave the corresponding amine as an oil (1.90 g, quantitative yield). The corresponding purified amine hydrochloride **19v** was obtained after a treatment

with Et_2O/HCl (0.6 N) and a crystallization from methanol, mp = 159-164 °C. IR (ATR) ν: 2908, 2498, 2415, 1483, 1461, 1425, 1317, 1266, 1185, 1134, 1039, 834 cm^{-1}. ^{1}H-NMR, δ_H (400 MHz, DMSO): 1.53 (s, 6 H, 2'(8',9')-CH_2), 1.54-1.68 (complex signal, 6 H, 4'(6',10')-CH_2), 1.93 [broad s, 3 H, 3'(5',7')-H], 2.72 (s, 2 H, CH_2N), 4.75 (broad s, 1 H, NH), 6.83 (dd, *J* = 8.8 Hz, *J'* = 2.8 Hz, 1 H, 6-H), 7.06 (d, *J* = 2.8 Hz, 1 H, 2-H), 7.27 (t, *J* = 9.2 Hz, 1 H, 5-H).^{13}C-NMR, δ_C (100.6 MHz, DMSO): 27.8 [CH, C3'(5',7')], 34.0 (C, C1'), 36.6 [CH_2, C4'(6',10')], 39.9 [CH_2, C2'(8',9')], 54.9 (CH_2, $\underline{C}H_2N$), 110.7 (CH, C2), 114.2 (C, C4), 115.4 (CH, C6), 123.2 (C, q, *J* = 272.8 Hz, CF_3), 126.6 (C, q, *J* = 30.0 Hz, C3), 131.8 (CH, C5), 148.8 (C, C1). MS-DIP (EI), m/e (%); main ions: 343 (M^{+}, 90), 210 (15), 209 (11), 207 (22), 135 (100), 93 (16), 91 (8), 79 (15).

***N*-[(adamantan-1-yl)methyl]-2,3,4,5,6-pentafluoroaniline hydrochloride, 19w**. Following the general procedure F, the reduction of amide **18w** (1.00 g, 2.9 mmol) with sodium bis(2-methoxyethoxy) aluminum hydride (65% wt solution in toluene, 3.68 ml, 12.35 mmol), gave the corresponding amine as an oil (0.65 g, 68%) . The corresponding purified amine hydrochloride **19w** was obtained after treatment with Et_2O/HCl (0.6 N), mp = 185-186 ºC. IR (ATR) ν: 2898, 2846, 2356, 1644, 1493, 1257, 1085, 870, 799 cm^{-1}. ^{1}H-NMR, δ_H (400 MHz, DMSO): 1.50 [s, 6 H, 2'(8',9')-H_2], 1.62 [broad signal, 6 H, 4'(6',10')-H_2], 1.92 [s, 3 H, 3'(5',7')-H], 2.65 (s, 2 H, $C\underline{H}_2N$).

***N*-[(3,5-dimethyladamantan-1-yl)methyl]-3-chloroaniline hydrochloride, 19x**. Following the general procedure F, the reduction of amide **18x** (0.50 g, 1.6 mmol) with sodium bis-(2-methoxyethoxy)aluminum hydride (65% wt solution in toluene, 1.2 mL, 6.3 mmol), gave the corresponding amine as an oil (0.44 g, 92%). The corresponding purified amine hydrochloride **19x** was obtained after treatment with Et_2O/HCl (0.6 N), mp = 157-160 ºC (dec). IR (ATR) ν: 2903, 2834, 2582, 2418, 2356, 1597, 1581, 1477,

1457, 1425, 1375, 1082, 1000, 984, 894, 873, 792, 704, 682 cm^{-1}. ^{1}H-NMR, δ_H (400 MHz, DMSO): 0.79 [s, 6 H, 3(5)-CH_3], 1.09 (m, 2 H, adamantyl-CH_2), 1.17 (m, 4 H, adamantyl-CH_2), 1.28 [m, 4 H, adamantyl-CH_2], 1.37 (m, 2 H, adamantyl-CH_2), 2.02 (m, 1 H, adamantyl-CH), 2.74 (s, 2 H, C$\underline{H}_2$N), 5.27 (broad signal, 1 H, NH), 6.49 (dd, *J* = 8.0 Hz, *J'* = 2.0 Hz, 1 H, 6-H), 6.60 (dd, *J* = 8.0 Hz, *J'* = 2.0 Hz, 1 H, 4-H), 6.67 (t, *J* = 2.0 Hz, 1 H, 2-H), 7.03 (t, *J* = 8.0 Hz, 1 H, 5-H). ^{13}C-NMR, δ_C (100.6 MHz, DMSO): 28.9 (CH, C7'), 30.5 [CH_3, C3(5)-$\underline{C}H_3$], 30.7 [C, C3(5)], 35.7 (CH_2, C4'), 38.5 [CH_2, C2'(9')]*, 42.8 [CH_2, C6'(10')]*, 46.2 (CH_2, C8'), 50.7 (CH_2, $\underline{C}H_2$N), 110.9 (CH, C6), 111.5 (CH, C2), 114.9 (CH, C4), 130.2 (CH, C5), 133.5 (C, C3), 150.7 (C, C1).

3-[(Phenylamino)methyl]adamantan-1-ol hydrochloride, 22a. Following the general procedure F, the reduction of amide **21a** (0.50 g, 1.8 mmol) with sodium bis-(2-methoxyethoxy)aluminum hydride (65% solution in toluene, 2.15 mL, 7.2 mmol), gave the corresponding amine as an oil (0.40 g, 85%). The corresponding purified amine hydrochloride **22a** was obtained after a treatment with Et_2O/HCl (0.6 N) and a crystallization from methanol, mp >183 °C (dec). IR (ATR) ν: 3329, 2903, 2849, 2670, 2430, 1581, 1493, 1429, 1146, 1051, 755, 693 cm^{-1}.^{1}H-NMR, δ_H (400 MHz, DMSO): 1.49-1.54 (complex signal, 12 H, adamantyl-CH_2), 2.12 [broad s, 2 H, 5'(7')-H], 2.93 (s, 2 H, C$\underline{H}_2$N), 7.01-7.35 (complex signal, 5 H, Ar-H).^{13}C-NMR, δ_C (100.6 MHz, DMSO): 29.7 [CH, C5'(7')], 35.1 (CH_2, C6'), 36.5 (C, C1'), 38.5 [CH_2, C8(9)], 44.4 [CH_2, C4(10)], 47.5 (CH_2, C2'), 59.7 (CH_2, $\underline{C}H_2$N), 66.6 (C, C3'), 129.5 (CH, Ar-C). Only an aromatic signal was observed. MS-DIP (EI), m/e (%); main ions: 257 ($M^{\cdot+}$, 50), 151 (6), 107 (20), 106 (100), 93 (12), 77 (11).

3-[((4-Chlorophenyl)amino)methyl]adamantan-1-ol hydrochloride, 22b. Following the general procedure F, the reduction of amide **21b** (0.33 g, 1.08 mmol) with sodium bis-(2-methoxyethoxy)aluminum hydride (65% solution in toluene, 1.30

mL, 4.32 mmol), gave the corresponding amine as an oil (0.24 g, 77%). The corresponding purified amine hydrochloride **22b** was obtained after a treatment with Et_2O/HCl (0.6 N) and a crystallization from methanol, mp >172 °C (dec). IR (ATR) ν: 2913, 2844, 1575, 1489, 1457, 1414, 1339, 1146, 1093, 1052, 902, 823 cm^{-1}.^{1}H-NMR, δ_H (400 MHz, DMSO): 1.43-1.56 (complex signal, 12 H, adamantyl-CH_2), 2.10 [broad s, 2 H, 5'(7')-H], 2.81 (s, 2 H, C$\underline{H}_2$N), 6.61 (broad s, 1 H, NH), 6.88 [d, *J* = 8.5 Hz, 2 H, 2(6)-H], 7.17 [d, *J* = 8.5 Hz, 2 H, 3(5)-H].^{13}C-NMR, δ_C (100.6 MHz, DMSO): 29.8 [CH, C5'(7')], 35.3 (CH_2, C6'), 37.2 (C, C1'), 39.4 [CH_2, C8(9)], 44.6 [CH_2, C4(10)], 47.8 (CH_2, C2'), 56.6 (CH_2, $\underline{C}H_2$N), 66.7 (C, C3'), 128.7 (CH, Ar-C). Only an aromatic signal was observed. MS-DIP (EI), m/e (%); main ions: 293 ($M^{\cdot+}$, ^{37}Cl, 20), 291 ($M^{\cdot+}$, ^{35}Cl, 61), 142 (34), 141 (30), 140 (100), 139 (19), 95 (14), 93 (16).

***N*-[2-(Adamant-1-yl)ethyl]-2-isopropylaniline hydrochloride, 25**. Following the general procedure F, amide **24** (0.370 g, 1.18 mmol) and sodium bis-(2-methoxyethoxy)aluminum hydride (65% wt solution in toluene, 1.15 mL, 5.90 mmol) in anhydrous toluene (9.5 mL), gave **25** as a yellow oil (340 mg, 86%) that formed its hydrochloride salt as a yellow solid after the treatment with HCl/Et_2O (312 mg), mp = 70-71 ºC. IR (ATR) ν: 705, 720, 761, 816, 935, 978, 993, 1024, 1054, 1072, 1097, 1155, 1239, 1271, 1317, 1342, 1362, 1385, 1448, 1494, 1552, 1577, 1739, 2359, 2445, 2653, 2845, 2901, 2951, 3397 cm^{-1}. ^{1}H-NMR (400 MHz, CD_3OD) δ: 1.34 [d, *J* = 6.8 Hz, 6 H, -CH(C$\underline{H}_3$)$_2$], 1.50-1.60 [complex signal, 6 H, 2'(8',9')-H_2 and 8-H_2], 1.64-1.80 [complex signal, 6 H, 4'(6',10')-H_2], 1.96 [m, 3 H, 3'(5',7')-H], 3.07 [sept, *J* = 6.8 Hz, 1 H, -C$\underline{H}$(CH$_3$)$_2$], 3.35 (m, 2 H, 7-H_2), 7.37-7.42 (complex signal, 2 H, 4-H and 6-H), 7.53 (m, 1 H, 5-H), 7.60 (d, 1 H, *J* = 7.6 Hz, 3-H). ^{13}C-NMR (100.5 MHz, $CDCl_3$) δ: 24.5 [CH_3, -CH(C$\underline{H}_3$)$_2$], 28.9 (C, C1'), 29.9 [CH, C3'(5',7') and -C$\underline{H}$(CH$_3$)$_2$], 32.8 (CH_2, C8), 37.8 [CH_2, C4'(6',10')], 40.6 (CH_2, C7), 43.0 [CH_2, C2'(8',9')], 124.5 (CH,

C6), 128.9 (CH, C4), 129.6 (CH, C5), 131.6 (CH, C3), 133.1 (C, C2), 143.6 (C, C1). HRMS-ESI+ m/z $[M+H]^+$ calcd for $[C_{21}H_{31}N+H]^+$: 298.2529, found: 298.2524.

Virological experiments

CPE reduction assays. The procedure to measure anti-influenza virus activity in MDCK (Madin-Darby canine kidney) cells was reported in detail elsewhere.[24] Briefly, MDCK cells, plated in 96-well plates, were infected with influenza virus A/Hong Kong/7/87 (H3N2 subtype); A/PR/8/34 (H1N1 subtype); A/Virginia/ATCC3/2009 (H1N1 subtype) or influenza B/Hong Kong/5/1972. Together with virus, the test compounds were added in serial dilutions. After 72 h incubation at 35 °C, microscopy was done to score the viral cytopathic effect (CPE) and compound cytotoxicity, after which the formazan-based MTS cell viability assay was performed. Similar CPE assays were used to test the compounds against a large panel of DNA and RNA viruses (listed in the Results section) in suitable human cell lines; all details can be found elsewhere.[50] Antiviral activity was expressed as the EC_{50} value, i.e. compound concentration producing 50% inhibition of viral cytopathicity, as determined by CPE or MTS assay. Compound cytotoxicity was expressed as the CC_{50} value, i.e. 50% cytotoxic concentration in the MTS assay; or MCC, i.e. minimum compound concentration causing microscopically detectable alterations of normal cell morphology.

*Selection and characterization of compound **9d**-resistant influenza virus.* MDCK cells were infected with A/PR/8/34 influenza virus as above, and exposed to 0 or 12.5 μM of compound **9d**. Three days later, the supernatants were harvested and inoculated onto fresh MDCK cells with addition of either 0 or 25 μM of **9d**. After this step was repeated with 50 μM of compound, the passage #3 viruses were plaque-purified in MDCK cells covered with 0.8% agarose. Picked clones were expanded in the presence

of **9d** and submitted to HA sequencing. After titration, the viruses underwent antiviral testing in MDCK cells using the CPE reduction assay described above. To estimate the fusion pH, the mutant viruses were expanded once in embryonated hen eggs. These allantoic stocks were used in a hemolysis assay with chicken erythrocytes and different acidic buffers (pH range: 4.6-6.0).[24] The hemolysis pH was calculated as the pH at which 50% hemolysis was observed compared to the value at pH 4.9.

Polykaryon assay for HA-mediated cell fusion

A pCAGEN plasmid [kindly provided by Dr. C. Cepko (Boston, MA) via Addgene (plasmid No. 3211160)[59]] in which we cloned the HA cDNA sequence from A/PR/8/34 (H1), A/duck/Hunan/795/2002 (H5 sequence purchased from Sino Biological Inc.) or A/X31 (H3), was transfected into human HeLa cells as described.[24] Two days later, the HA was activated by 15 min incubation with TPCK-treated trypsin. The cells were then pre-incubated with compound diluted in PBS plus Ca^{2+} and Mg^{2+} (PBS-CM) for 15 min, followed by 5 min exposure to compound diluted in acidified PBS-CM of pH 5.2 for the H1 and H5 HAs or pH 5.0 for the H3 HA (which is 0.2 pH units below the hemolysis pH of the corresponding viruses). After rinsing with PBS-CM, the cells were incubated with medium containing 10% fetal calf serum for 3 h, then fixated with 96% ethanol and stained with Giemsa solution. An inverted microscope at x200 magnification was used to count the number of polykaryons (containing five or more nuclei) in four randomly selected microscopic fields. The EC_{50} value was calculated as the compound concentration producing 50% reduction in the number of polykaryons compared to the condition receiving no compound.

Molecular modeling

Homology modelling and electrostatic surface potential analysis. In the crystallographic structures of HA (H3 and H14 subtypes) bound to TBHQ (PDB entries

3EYM, 3EYK and 3EYJ), the binding site adopts the "open" form, which is characterized by the unfolding of the C-terminal region of the helix A (Supporting Information Figure S2A). This structural feature is also found in the X-ray structures of H3 and H7 HAs complexed to arbidol (PDB entries 5T6N and 5T6S). No similar structural information is available for the binding of fusion inhibitors to H1 HA, for which published X-ray structures are in a "closed" state where residues 56-59 adopt a full helical arrangement (Figure S2B). Accordingly, PDB entry 3EYM,[22] i.e. X31-HA (H3 subtype) co-crystallized with TBHQ, was used as the template to generate 3D models for the HA proteins of A/PR/8/34 (H1; UniprotKB code: I6TAG2), A/Virginia/ATCC3/2009 (H1; ATCC® VR-1736), and A/HongKong/7/1987 (H3; UniprotKB code: Q38TH2). The overall HA amino acid similarity between A/PR/8/34 and A/Virginia/ATCC3/2009 is 81%, and 42% when they are aligned with the A/HongKong/7/1987 protein (Figure S7). However, when the analysis is restricted to the HA2 part, which mainly forms the TBHQ binding site, sequence similarity increases up to 92% between the two H1 strains and to 61% with the H3 subtype. This enabled homology modeling to build a 3D model of H1 HA in the open form.

The 3D structural models were minimized with the staged minimization option on SYBYL (Tripos force field),[60] using the Powell optimization method with Gasteiger-Hückel point charges,[61] a non-bonded cutoff of 8.0 Å, a dielectric constant of 2.0, and a convergence of 0.001 kcal mol^{-1} $Å^{-1}$ or maximum number of 1,500 iterations. This energy minimization was convenient to relax the structure prior to MD simulations, although it did not alter significantly the overall fold of the protein (RMSD < 0.32 Å between the homology modeling and energy-minimized structures). After visual inspection of the optimized structures, linearized Poisson-Boltzmann calculations as implemented in APBS (Adaptive Poisson-Boltzmann solver)[62-63] were performed to

screen the solvent-dependent electrostatic properties of the previously minimized HA models. To this end, a single-point multigrid PB calculation without focusing with a grid spacing of 0.70 Å/point was used. Default parameters of Amber force field were used to set the atomic partial charges and radii of the atoms. A dielectric constant of 2.0 and 78.5 was considered respectively for the biopolymer and the solvent.

Molecular Docking. Surflex-Dock[64] as implemented in Sybyl X2.1 – Tripos, was used to perform molecular docking of compound **9d** (Figure 4) within the TBHQ binding site in the A/PR/8/34, A/Virginia/ATCC3/2009 and A/HK/7/87 homology models. The binding site was defined considering the area covered by a radius of 12 Å around residue $Tyr308_1$ (for A/PR/8/34), $Phe309_1$ (for A/Virginia/ATCC3/2009) and $Phe310_1$ (for A/HK/7/87). Docking-guided conformational exploration of the binding site was performed by molecular fragmentation. A maximum of 20 conformations per fragment were generated. The maximum number of poses per ligand was set to 20 with a minimum RMSD between final poses of 0.50 Å.

Molecular Dynamics simulations. Amber12[65] was used to perform MD simulations on the selected ligand–protein complexes previously generated by docking analysis. In this context, the general Amber force field (GAFF)[66] was used to parameterize the ligand, and the partial charges were derived at the B3LYP/6-31G(d) level,[67] after preliminary optimization of the molecular structure, by using the restrained electrostatic potential (RESP)[68] fitting method implemented in Gaussian09 and Antechamber.

MD simulations were carried out to analyse the conformational flexibility of compound **9d** within the protein environment formed by A/PR/8/34 and A/Virginia/ATCC3/2009 HA models. Accordingly, the two **9d**-A/PR/8/34 and **9d**-A/Virginia/ATCC3/2009 complexes were solvated with a truncated octahedral (TIP3P)[69] water box with a layer of 18 Å and neutralized by adding Na^+ ions.

Complexes were subjected to three-stages of energy minimization that involved firstly all hydrogen atoms, then water molecules, and finally all the system with a maximum number of minimization cycles of 10000 for the latter stage. Before MD simulation, a preliminary heating of the system from 0 to 300 K was accomplished in six steps, the first being performed at constant volume and the rest at constant pressure. The SHAKE algorithm[70] was applied to constrain bonds involving hydrogen atoms. Periodic boundary conditions at constant volume were imposed on the system during the MD simulations. Cut-off for the non-bonded interactions was set to 10 Å. The electrostatic interactions beyond the cut-off within the periodic box were computed by applying the Particle Mesh Ewald (PME) method.[71] Langevin dynamics with a collision frequency of 1.0 was applied for temperature regulation during the heating. Finally, 50 ns of MD simulation at constant volume and temperature (300 K) were run using the weak-coupling algorithm[72] (with a time constant of 10.0 ps) to stabilize the temperature during the simulation. Time step for saving of trajectory was set to 2 ps. A total of 50,000 snapshots were collected for each complex.

NMR experiments

Recombinant H5 HA was prepared as previously described.[73] Briefly, the extracellular domain of H5 HA, extended with a C-terminal foldon domain added for stability and polyhistidine sequence added for subsequent purification, was expressed by baculovirus infection of Sf9 insect cells and purified by Ni^{+} affinity and size exclusion chromatography. Compounds were prepared as 100 mM stock solutions in d_6-DMSO. The experimental conditions were 100 μM compound and 1 μM H5 HA in 20 mM PO_4/pH 7.5, 150 mM NaCl, and 100% ^2H_2O. STD experiments were performed on a Bruker 900 MHz Avance spectrometer equipped with a cryoprobe at 25˚C as previously described,[23,47,73] with a relaxation delay of 2.5 s, saturation time of 1 s, and

256 scans with "on" resonance saturation at -1.5 ppm (i.e. protein ^{1}H saturation) and "off" resonance saturation at 30 ppm (i.e. control ^{1}H saturation outside the spectral range of protein and ligand). Spectra were processed by NMRPipe with a relaxation delay a 5 Hz line broadening and analyzed by NMRDraw.[74] Relative % STD was calculated as described previously.[75] Briefly, % STD = 100 × STD_{obs}/STD_{max}. STD signal was calculated based on the equation: $STD = \Delta I/I_{off}$, where $\Delta I = I_{off} - I_{on}$ and I_{off} and I_{on} are the resonance intensities after the "off" and "on" presaturation of the protein target. Errors in STD experiments were estimated as $\Delta I/I_{ref}[(N_{\Delta I}/\Delta I)^2 + (N_{Iref}/I_{ref})^2]^{0.5}$ where $N_{\Delta I}$ and N_{Iref} are the noise levels calculated by NMRDraw in the appropriate spectrum.

ASSOCIATED CONTENT

Supporting Information.

The Supporting Information is available free of charge on the ACS Publications website at DOI:

Descriptions of the synthesis and characterization of amides **18a-x**, **21** and **24**, elemental analysis data of the new compounds. Tables S1 to S4 and Figures S1 to S7.

Molecular formula string and some data (CSV)

AUTHOR INFORMATION

Corresponding Authors

*Phone: +32 16322098. E-mail: lieve.naesens@kuleuven.be

*Phone: +34 934024533. E-mail: svazquez@ub.edu.

[I]These authors contributed equally to this work.

ACKNOWLEDGEMENTS

We thank financial support from *Ministerio de Economía y Competitividad* and FEDER (Project SAF2014-57094-R to F. J. L. and S. V.) and the *Generalitat de Catalunya* (grants 2014-SGR-00052 and 2014-SGR-1189) and the *Consorci de Serveis Universitaris de Catalunya* for computational resources. R. L. thanks the *Generalitat de Catalunya* and the Spanish *Ministerio de Educación Cultura y Deporte* for PhD Grants (FI and FPU programs). M. B.-X. and S. C. thank the Institute of Biomedicine of the Universitat de Barcelona (IBUB) and the Universitat de Barcelona, respectively, for PhD grants. F. J. L. acknowledges the support from ICREA Academia. L. N. acknowledges technical assistance from W. van Dam and Talitha Boogaerts.

ABBREVIATIONS

ATR, Attenuated Total Reflectance; CPE, cytopathic effect; HA, hemagglutinin; MDCK, Madin-Darby Canine Kidney; MTS, 3-(4,5-dimethylthiazol-2-yl)-5-(3-carboxymethoxyphenyl)-2-(4-sulfophenyl)-2*H*-tetrazolium; STD, saturation transfer difference.

REFERENCES

(1) http://www.who.int/influenza/en/ [Accessed on Sep 24, 2017].

(2) Taubenberger J. K.; Morens, D. M. 1918 Influenza: the mother of all pandemics. *Emerg. Infect. Dis.* **2006**, *12*, 15-22.

(3) Dawood, F. S.; Iuliano, A. D.; Reed, C.; Meltzer, M. I.; Shay, D. K.; Cheng, P.-Y.; Bandaranayake, D.; Breiman, R. F.; Brooks, W. A.; Buchy, P.; Feikin, D. R.; Fowler, K. B.; Gordon, A.; Hien, N. T.; Horby, P.; Huang, Q. S.; Katz, M. A.; Krishnan, A.; Lal, R.; Montgomery, J. M.; Mølbak, K.; Pebody, R.; Presanis, A. M.; Razuri, H.; Steens, A.; Tinoco, Y. O.; Wallinga, J.; Yu, H.; Vong, S.; Bresee, J.; Widdowson, M.-A. Estimated global mortality associated with the first 12 months of 2009 pandemic influenza A H1N1 virus circulation: a modelling study. *Lancet Infect. Dis.* **2012**, *12*, 687-695.

(4) Laborda, P.; Wang, S.-Y.; Voglmeir, J. Influenza neuraminidase inhibitors: synthetic approaches, derivatives and biological activity. *Molecules* **2016**, *21*, 1513.

(5) Wang, J.; Li, F.; Ma, C. Recent progress in designing inhibitors that target the drug-resistant M2 proton channels from the influenza A viruses. *Biopolymers (Pept. Sci.)*, **2015**, *104*, 291-309.

(6) Samson, M.; Pizzorno, A.; Abed, Y.; Boivin, G. Influenza virus resistance to neuraminidase inhibitors. *Antiviral Res.* **2013**, *98*, 174-185.

(7) Das K, Aramini J, Ma L, Krug R, Arnold E, Structures of influenza A proteins and insights into antiviral drug targets. *Nat. Struct. Mol. Biol.,* **2010**, *17*, 530-538.

(8) Hayden, F. G.; Newer influenza antivirals, biotherapeutics and combinations. *Influenza Other Respir. Viruses* **2013**, *7(S1)*, 63-75.

(9) Vanderlinden, E.; Naesens, L. Emerging antiviral strategies to interfere with influenza virus entry. *Med. Res. Rev.* **2014**, *34*, 301-339.

(10) Naesens, L.; Stevaert, A.; Vanderlinden, E. Antiviral therapies on the horizon for influenza. *Curr. Opin. Pharmacol.* **2016**, *30*, 106-115.

(11) Li, F.; Ma, C.; Wang, J. Inhibitors targeting the influenza virus hemagglutinin. *Curr. Med. Chem.* **2015**, *22*, 1361-1382.

(12) Stevaert, A.; Naesens, L. The influenza virus polymerase complex: an update on its structure, functions, and significance for antiviral drug design. *Med. Res. Rev.* **2016**, *36*, 1127-1173.

(13) Engel, D. A. The influenza virus NS1 protein as a therapeutic target. *Antiviral Res.* **2013**, *99*, 409-416.

(14) Skehel, J. J.; Wiley, D. C. Receptor binding and membrane fusion in virus entry: the influenza hemagglutinin. *Ann. Rev. Biochem.* **2000,** *69*, 531-569.

(15) Hamilton, B. S.; Whittaker, G. R.; Daniel, S. Influenza virus-mediated membrane fusion: determinants of hemagglutinin fusogenic activity and experimental approaches for assessing virus fusion. *Viruses* **2012**, *4*, 1144-1168.

(16) Sparrow, E.; Friede, M.; Sheikh, M.; Torvaldsen, S.; Newall, A. T. Passive immunization for influenza through antibody therapies, a review of the pipeline, challenges and potential applications. *Vaccine* **2016**, *34*, 5442-5448.

(17) Lee, P. S.; Wilson, I. A. Structural characterization of viral epitopes recognized by broadly cross-reactive antibodies. *Curr. Top. Microbiol. Immunol.* **2015**, *386*, 323-341.

(18) Blaising, J.; Polyak, S. J.; Pécheur, E. I. Arbidol as a broad-spectrum antiviral: an update. *Antiviral Res.* **2014**, *107*, 84-94.

(19) Leneva, I. A.; Russell, R. J.; Boriskin, Y. S.; Hay, A. J. Characteristics of arbidol-resistant mutants of influenza virus: implications for the mechanism of anti-influenza action of arbidol. *Antiviral Res.* **2009**, *81*, 132-140.

(20) Kadam, R. U.; Wilson, I. A. Structural basis of influenza virus fusion inhibition by the antiviral drug arbidol. *Proc. Natl. Acad. Sci. U. S. A.* **2017**, *114*, 206-214.

(21) Bodian, D.; Yamasaki, R.; Buswell, R.; Stearns, J.; White, J.; Kuntz, I. Inhibition of the fusion-inducing conformational change of influenza hemagglutinin by benzoquinones and hydroquinones. *Biochemistry* **1993**, 32, 2967-2978.

(22) Russell R. J.; Kerry, P. S.; Stevens, D. J.; Steinhauer, D. A.; Martin, S. R.; Gamblin, S. J.; Skehel, J. J. Structure of influenza hemagglutinin in complex with an inhibitor of membrane fusion. *Proc. Natl. Acad. Sci. U. S. A.* **2008**, *105*, 17736-17741.

(23) Antanasijevic, A.; Hafeman, N. J.; Tundup, S.; Kingsley, C.; Mishra, R. K.; Rong, L.; Manicassamy, B.; Wardrop, D.; Caffrey, M. Stabilization and improvement of a promising influenza antiviral: making a PAIN PAINless. *ACS Infect. Dis.* **2016**, *2*, 608-615.

(24) Vanderlinden E.; Göktas F.; Cesur Z.; Froeyen M.; Reed M. L.; Russell, C. J.; Cesur, N.; Naesens L. Novel inhibitors of influenza virus fusion: structure-activity relationship and interaction with the viral hemagglutinin. *J. Virol.* **2010**, *84*, 4277-4288.

(25) Luo, G.; Colonno, R.; Krystal, M. Characterization of a hemagglutinin-specific inhibitor of influenza A virus. *Virology* **1996**, *226*, 66-76.

(26) Luo, G.; Torri, A.; Harte, W. E.; Danetz, S.; Cianci, C.; Tiley, L.; Say, S.; Mullaney, D.; Yu, K.-L.; Ouellet, C.; Dextraze, P.; Meanwell, N.; Colonno, R.; Kyrstal, M. Molecular mechanism underlying the action of a novel fusion inhibitor of influenza A virus. *J. Virol.* **1997**, *71*, 4062-4070.

(27) Deshpande, M. S.; Wei, J.; Luo, G.; Cianci, C.; Danetz, S.; Torri, A. ; Tiley, L. ; Krystal, M. ; Yu, K.-L.; Huang, S.; Gao, Q.; Meanwell, N. A. An approach to the identification of potent inhibitors of influenza virus fusion using parallel synthesis methodology. *Bioorg. Med. Chem. Lett.* **2001**, *11*, 2393-2396.

(28) Cianci, C.; Yu, K.-L.; Dischino, D. D.; Harte, W. ; Deshpande, M. ; Luo, G. ; Colonno, R. J. ; Meanwell, N. A. ; Krystal, M. J. pH-Dependent changes in photoaffinity labelling patterns of the H1 influenza virus hemagglutinin by using an inhibitor of viral fusion. *Virology* **1999**, *73*, 1785-1794.

(29) Plotch, S. J.; O'Hara, B.; Morin, J.; Palant, O.; LaRocque, J.; Bloom, J. D.; Lang, Jr., S. A.; DiGrandi, M. J.; Bradley, M.; Nilakantan, R.; Gluzman, Y. Inhibition of influenza A virus replication by compounds interfering with the fusogenic function of the viral hemagglutinin. *J. Virology* **1999**, *73*, 140-151.

(30) Liu, S.; Li, R.; Zhang, R.; Chan, C. C. S.; Xi, B.; Zhu, Z.; Yang, J.; Poon, V. K. M. ; Zhou, J.; Münch, J.; Kirchhoff, F.; Pleschka, S.; Haarmann, T.; Dietrich, U.; Pan, C.; Du, L.; Jiang, S.; Zheng, B. CL-385319 inhibits H5N1 avian influenza A virus infection by blocking viral entry. *Eur. J. Pharm.* **2011**, *660*, 460-467.

(31) Li, R.; Song, D.; Zhu, Z.; Xu, H.; Liu, S. An induced pocket for the binding of potent fusion inhibitor CL-385319 with H5N1 influenza virus hemagglutinin. *PLoS One* **2012**, *7*, e41956.

(32) Tang, G.; Lin, X.; Qiu, Z.; Li, W.; Zhu, L.; Wang, L.; Li, S.; Li, H.; Lin, W.; Yang, M.; Guo, T.; Chen, L.; Lee, D.; Wu, J. ; Yang, W. Design and synthesis of benzenesulfonamide derivatives as potent anti-influenza hemagglutinin inhibitors. *ACS Med. Chem. Lett.* **2011**, *2*, 603-607.

(33) Zhu, L.; Li, Y.; Li, S.; Li, H.; Qiu, Z.; Lee, C.; Lu, H.; Lin, X.; Zhao, R.; Chen, L.; Wu, J.; Tang, G.; Yang, W. Inhibition of influenza A virus (H1N1) fusion by benzenesulfonamide derivatives targeting viral hemagglutinin. *PLos One,* **2011**, *6*, e29120.

(34) White, K. M.; De Jesus, P.; Chen, Z.; Abreu, Jr., P.; Barile, E.; Mak, P. A.; Anderson, P.; Nguyen, Q. T.; Inoue, A.; Stertz, S.; Koenig, R.; Pellecchia, M.; Palese, P.; Kuhen, K.; García-Sastre, A.; Chanda, S. K.; Shaw, M. L. Potent anti-influenza compound blocks fusion through stabilization of the prefusion conformation of the hemagglutinin protein. *ACS Infect. Dis.* **2015**, *1*, 98-109.

(35) Basu, A.; Antanasijevic, A.; Wang, M.; Li, B.; Mills, D. M.; Ames, J. A.; Nash, P. J.; Williams, J. D.; Peet, N. P.; Moir, D. T.; Prichard, M. N.; Keith, K. A.; Barnard, D. L.; Caffrey, M.; Rong, L.; Bowlin, T. L. New small molecule entry

inhibitors targeting hemagglutinin-mediated influenza A virus fusion. *J. Virology* **2014**, *88*, 1447-1460.

(36) Basu, A.; Komazin-Meredith, G.; McCarthy, C.; Antanasijevic, A.; Cardinale, S. C.; Mishra, R. K.; Barnard, D. L.; Caffrey, M.; Rong, L.; Bowlin, T. L. Molecular mechanism underlying the action of the influenza A virus fusion inhibitor MBX2546. *ACS Infect. Dis.* **2017**, *3*, 330-335.

(37) Wanka, L.; Iqbal, K.; Schreiner, P. R. The lipophilic bullet hits the targets: medicinal chemistry of adamantane derivatives. *Chem. Rev.* **2013**, *113*, 3516-604.

(38) Duque, M. D.; Ma, C.; Torres, E.; Wang, J.; Naesens, L.; Juárez-Jiménez, J.; Camps, P.; Luque, F. J.; DeGrado, W. F.; Lamb, R. A.; Pinto, L. H.; Vázquez, S. Exploring the size limit of templates for inhibitors of the M2 ion channel of influenza A virus. *J. Med. Chem.* **2011**, *54*, 2646–2657.

(39) Torres, E.; Duque, M. D.; Vanderlinden, E.; Ma, C.; Pinto, L. H.; Camps, P.; Froeyen, M.; Vázquez, S.; Naesens, L. Role of the viral hemagglutinin in the anti-influenza virus activity of newly synthesized polycyclic amine compounds. *Antiviral Res.* **2013**, *99*, 281-291.

(40) Rey-Carrizo, M.; Torres, E.; Ma, C.; Barniol-Xicota, M.; Wang, J.; Wu, Y.; Naesens, L.; DeGrado, W. F.; Lamb, R. A.; Pinto, L. H.; Vazquez, S. Azatetracyclo[5.2.1.$1^{5,8}$.$0^{1,5}$]undecane derivatives: from wild-type inhibitors of the M2 ion channel of influenza A virus to derivatives with potent activity against the V27A mutant. *J. Med. Chem.* **2013**, *56*, 9265–9274.

(41) Rey-Carrizo, M.; Barniol-Xicota, M.; Ma, C.; Frigolé-Vivas, M.; Torres, E.; Naesens, L.; Llabrés, S.; Juárez-Jiménez, J.; Luque, F. J.; DeGrado, W. F.; Lamb,

R. A.; Pinto, L. H.; Vázquez, S. Easily accessible polycyclic amines that inhibit the wild-type and amantadine-resistant mutants of the M2 channel of influenza A virus. *J. Med. Chem.* **2014**, *57*, 5738–5747.

(42) Rey-Carrizo, M.; Gazzarrini, S.; Llabrés, S.; Frigolé-Vivas, M.; Juárez-Jiménez, J.; Font-Bardia, M.; Naesens, L.; Moroni, A.; Luque, F. J.; Vázquez, S. New polycyclic dual inhibitors of the wild type and the V27A mutant M2 channel of the influenza A virus with unexpected binding mode. *Eur. J. Med. Chem.* **2015**, *96*, 318-329.

(43) Barniol-Xicota, M.; Gazzarrini, S.; Torres, E.; Hu, Y.; Wang, J.; Naesens, L.; Moroni, A.; Vázquez, S. Slow but steady wins the race: dissimilarities among new dual inhibitors of the wild-type and the V27A mutant M2 channels of influenza A virus. *J. Med. Chem.* **2017**, *60*, 3727-3738.

(44) Boido, V.; Sparatore, F. *N*-Lupinilarilammine e *N*-amminoalchil-*m*-triflurometilaniline d'interesse farmacologico e microbiologico. *Farmaco Sci.* **1974**, *29*, 526-533.

(45) Wanka, L.; Cabrele, C.; Vanejews, M.; Schreiner, P. R. γ-Aminoadamantanecarboxylic acids through direct C-H bond amidations. *Eur. J. Org. Chem.* **2007**, 1474–1490.

(46) Nayak, D. P.; Reichl, U. Neuraminidase activity assays for monitoring MDCK cell culture derived influenza virus. *J. Virol. Methods* **2004**, *122*, 9-15.

(47) Antanasijevic, A.; Cheng, H.; Wardrop, D.; Rong, L.; Caffrey, M. Inhibition of influenza H7 hemagglutinin-mediated entry. *PLoS One* **2013**, *8*, e76363.

(48) Meyers, B.; Peters, S. NMR spectroscopy techniques for screening and identifying ligand binding to protein receptors. *Angew. Chem. Int. Ed.* **2003**, *42*, 864-890.

(49) Guan, S.; Wang, T.; Kuai, Z.; Qian, M.; Tian, X.; Zhang, X.; Yu, Y.; Wang, S.; Zhang, H.; Li, H.; Kong, W.; Shan, Y. Exploration of binding and inhibition mechanism of a small molecule inhibitor of influenza virus H1N1 hemagglutinin by molecular dynamics simulation. *Sci. Rep.* **2017**, *7*, 3786.

(50) Rogolino, D.; Carcelli, M.; Bacchi, A.; Compari, C.; Contardi, L.; Fisicaro, E.; Gatti, A.; Sechi, M.; Stevaert, A.; Naesens, L. A versatile salicyl hydrazonic ligand and its metal complexes as antiviral agents. *J. Inorg. Biochem.* **2015**, *150*, 9-17.

(51) Wright, W. R.; Brabander, H. J.; Hardy, Jr., R. A. Synthetic analgesics. II. Basic anilides and carbanilates. *J. Org. Chem.* **1961**, *26*, 476-485.

(52) Sawa, Y.; Kawakami, Y.; Imai, S.; Kawarazaki, T. Synthesis of *N*-(2-picolyl)-*N*-phenyl-*N*-(2-piperidinoethyl)amine (TAT-3), its derivatives, and its organic acid salts. *Takeda Kenkyushoho* **1970**, *29*, 275-282.

(53) Van Gilse, J.; Paerels, G. B. Algicidal Composition and Method of Preventing or Controlling Algae with Said Composition. U.S. Patent 4,286,983, Sep 1, 1981.

(54) Protiva, M. Antihistamine substances. VIII. Ethers and thioethers derived from β-(1-piperidino)ethanol and β-piperidinoethyl mercaptan. The degradation of several quaternary bases. *Collect. Czech. Chem. Commun.* **1949**, *14*, 354-366.

(55) Basu, A.; Mills, D. M.; Williams, J. D.; Peet, N. P.; Moir, D. T.; Bowlin, T. L. Aminoalkyl Phenol Ether Inhibitors of Influenza A Virus. PCT WO 2013/074965 A1, May 23, 2013.

(56) Sousa, J. A.; Weinstein, J. Photoisomerization of 2-(2,4-dinitrobenzyl)pyridine and 2-(2-nitro-4-cyanobenzyl)pyridine. *J. Org. Chem.* **1962**, *27*, 3155-3159.

(57) Averin, A. D.; Ulanovskaya, M. A.; Bryak, A. K.; Savel'ev, E. N.; Orlinson, B. S.; Novakov, I. A.; Beletskaya, I. P. Arylation of adamantanamines: II. Palladium-catalyzed amination of dihalobenzenes with adamantylalkanamines. *Russ. J. Org. Chem.* **2010**, *46*, 1790-1811.

(58) Kadutskii, A. P.; Kozlov, N. G. Potential synthetic adaptogens 1. Synthesis and studies of new N-[(adamantan-1-yl)methyl]aniline derivatives based on adamantane-1-carbaldehyde. *Russ. Chem. Bull.* **2016**, *65*, 1336.

(59) Matsuda, T.; Cepko, C. L. Electroporation and RNA interference in the rodent retina in vivo and in vitro. *Proc. Natl. Acad. Sci. U. S. A.* **2004**, *101*, 16-22.

(60) Clark, M.; Cramer, R. D.; Van Opdenbosch, N. Validation of the general purpose Tripos 5.2 force field. *J. Comput. Chem*. **1989**, *10*, 982-1012.

(61) Fletcher, R.; Powell, M. J. A rapidly convergent descent method for minimization. *Comput. J.* **1963**, *6*, 163-168.

(62) Baker, N. A.; Sept, D.; Joseph, S.; Holst, M. J.; McCammon, J. A. Electrostatics of nanosystems: application to microtubules and the ribosome. *Proc. Natl. Acad. Sci. U. S. A.* **2001**, *98*, 10037-10041.

(63) Dolinsky, T. J.; Czodrowski, P.; Li, H.; Nielsen, J. E.; Jensen, J. H.; Klebe, G.; Baker, N. A. PDB2PQR: Expanding and upgrading automated preparation of biomolecular structures for molecular simulations. *Nucleic Acids Res*. **2007**, *35*, W522-W525.

(64) Spitzer, R.; Jain, A. N. Surflex-Dock: Docking benchmarks and real-world application. *J. Comput. Aided Mol. Des*. **2012**, *26*, 687-699.

(65) Case, D. A.; Darden, T. A.; Cheatham, T. E.; Simmerling, C. L.; Wang, J.; Duke, R. E.; Luo, R.; Walker, R. C.; Zhang, W.; Merz, K. M.; Roberts, B.; Hayik, S.; Roitberg, A.; Seabra, G.; Swails, J.; Goetz, A. W.; Kolossváry, I.; Wong, K. F.; Paesani, F.; Vanicek, J.; Wolf, R. M.; Liu, J.; Wu, X.; Brozell, S. R.; Steinbrecher, T.; Gohlke, H.; Cai, Q.; Ye, X.; Wang, J.; Hsieh, M. J.; Cui, G.; Roe, D. R.; Mathews, D. H.; Seetin, M. G.; Salomon-Ferrer, R.; Sagui, C.; Babin, V.; Luchko, T.; Gusarov, S.; Kovalenko, A.; Kollman, P. A. AMBER 12, 2012.

(66) Wang, J.; Wolf, R. M.; Caldwell, J. W.; Kollman, P. A.; Case, D. A. Development and testing of a general Amber force field. *J. Comput. Chem.* **2004**, *25*, 1157-1174.

(67) Gaussian 09, Revision E.01, Frisch, M. J.; Trucks, G. W.; Schlegel, H. B.; Scuseria, G. E.; Robb, M. A.; Cheeseman, J. R.; Scalmani, G.; Barone, V.; Mennucci, B.; Petersson, G. A.; Nakatsuji, H.; Caricato, M.; Li, X.; Hratchian, H. P.; Izmaylov, A. F.; Bloino, J.; Zheng, G.; Sonnenberg, J. L.; Hada, M.; Ehara, M.; Toyota, K.; Fukuda, R.; Hasegawa, J.; Ishida, M.; Nakajima, T.; Honda, Y.; Kitao, O.; Nakai, H.; Vreven, T.; Montgomery, J. A., Jr.; Peralta, J. E.; Ogliaro, F.; Bearpark, M.; Heyd, J. J.; Brothers, E.; Kudin, K. N.; Staroverov, V. N.; Kobayashi, R.; Normand, J.; Raghavachari, K.; Rendell, A.; Burant, J. C.; Iyengar,

S. S.; Tomasi, J.; Cossi, M.; Rega, N.; Millam, J. M.; Klene, M.; Knox, J. E.; Cross, J. B.; Bakken, V.; Adamo, C.; Jaramillo, J.; Gomperts, R.; Stratmann, R. E.; Yazyev, O.; Austin, A. J.; Cammi, R.; Pomelli, C.; Ochterski, J. W.; Martin, R. L.; Morokuma, K.; Zakrzewski, V. G.; Voth, G. A.; Salvador, P.; Dannenberg, J. J.; Dapprich, S.; Daniels, A. D.; Farkas, Ö.; Foresman, J. B.; Ortiz, J. V.; Cioslowski, J.; Fox, D. J. Gaussian, Inc., Wallingford CT, 2009.

(68) Wang, J.; Cieplak, P.; Kollman, P. A. How well does a restrained electrostatic potential (RESP) model perform in calculating conformational energies of organic and biological molecules? *J. Comput. Chem.* **2000**, *21*, 1049-1074.

(69) Jorgensen, W. L.; Chandrasekhar, J.; Madura, J. D.; Impey, R. W.; Klein, M. L. Comparison of simple potential functions for simulating liquid water. *J. Chem. Phys*. **1983**, *79*, 926.

(70) Ryckaert, J.-P.; Ciccotti, G.; Berendsen, H. J. C. Numerical integration of the cartesian equations of motion of a system with constraints: molecular dynamics of n-alkanes. *J. Comput. Phys.* **1977**, *23*, 327-341.

(71) Darden, T.; York, D.; Pedersen, L. An N·log(N) method for Ewald sums in Llrge systems. *J. Chem. Phys*. **1993**, *98*, 10089.

(72) Berendsen, H. J., Postma, J. V., van Gunsteren, W. F., DiNola, A. R. H. J., & Haak, J. R. Molecular dynamics with coupling to an external bath. *J. Chem. Phys*. **1984**, *81*, 3684-3690.

(73) Antanasijevic, A.; Kingsley, C.; Basu, A.; Bowlin, T.L.; Rong, L.; Caffrey, M. Application of virus-like particles (VLP) to characterize the interactions between inhibitors and viral membrane proteins. *J. Biomolec. NMR* **2016**, *64*, 255-65.

(74) Delaglio, F.; Grzesiek, S.; Vuister, G. W.; Zhu, G.; Pfeifer, J.; Bax, A. NMRPipe: a multidimensional spectral processing system based on UNIX pipes. *J. Biomol. NMR* **1995**, *6*, 277-293.

(75) McCullough, C.; Wang, M.; Rong, L; Caffrey, M. NMR characterization of influenza hemagglutinin receptor interactions. *PLoS One* **2012**, *7*, e33958.

Table of Contents Graphic